The American Journal of Human Genetics, Volume *99*

Supplemental Data

Trans-ethnic Meta-analysis and Functional Annotation Illuminates the Genetic Architecture of Fasting Glucose and Insulin

Ching-Ti Liu, Sridharan Raghavan, Nisa Maruthur, Edmond Kato Kabagambe, Jaeyoung Hong, Maggie C.Y. Ng, Marie-France Hivert, Yingchang Lu, Ping An, Amy R. Bentley, Anne M. Drolet, Kyle J. Gaulton, Xiuqing Guo, Loren L. Armstrong, Marguerite R. Irvin, Man Li, Leonard Lipovich, Denis V. Rybin, Kent D. Taylor, Charles Agyemang, Nicholette D. Palmer, Brian E. Cade, Wei-Min Chen, Marco Dauriz, Joseph A.C. Delaney, Todd L. Edwards, Daniel S. Evans, Michele K. Evans, Leslie A. Lange, Aaron Leong, Jingmin Liu, Yongmei Liu, Uma Nayak, Sanjay R. Patel, Bianca C. Porneala, Laura J. Rasmussen-Torvik, Marieke B. Snijder, Sarah C. Stallings, Toshiko Tanaka, Lisa R. Yanek, Wei Zhao, Diane M. Becker, Lawrence F. Bielak, Mary L. Biggs, Erwin P. Bottinger, Donald W. Bowden, Guanjie Chen, Adolfo Correa, David J. Couper, Dana C. Crawford, Mary Cushman, John D. Eicher, Myriam Fornage, Nora Franceschini, Yi-Ping Fu, Mark O. Goodarzi, Omri Gottesman, Kazuo Hara, Tamara B. Harris, Richard A. Jensen, Andrew D. Johnson, Min A. Jhun, Andrew J. Karter, Margaux F. Keller, Abel N. Kho, Jorge R. Kizer, Ronald M. Krauss, Carl D. Langefeld, Xiaohui Li, Jingling Liang, Simin Liu, William L. Lowe, Jr.,, Thomas H. Mosley, Kari E. North, Jennifer A. Pacheco, Patricia A. Peyser, Alan L. Patrick, Kenneth M. Rice, Elizabeth Selvin, Mario Sims, Jennifer A. Smith, Salman M. Tajuddin, Dhananjay Vaidya, Mary P. Wren, Jie Yao, Xiaofeng Zhu, Julie T. Ziegler, Joseph M. Zmuda, Alan B. Zonderman, Aeilko H. Zwinderman, AAAG Consortium, CARe Consortium, COGENT-BP Consortium, eMERGE Consortium, MEDIA Consortium, Adebowale Adeyemo, Eric Boerwinkle, Luigi Ferrucci, M. Geoffrey Hayes, Sharon L.R. Kardia, Iva Miljkovic, James S. Pankow, Charles N. Rotimi, Michele M. Sale, Lynne E. Wagenknecht, Donna K. Arnett, Yii-Der Ida Chen, Michael A. Nalls, MAGIC Consortium, Michael A. Province, W.H. Linda Kao, David S. Siscovick, Bruce M. Psaty, James G. Wilson, Ruth J.F. Loos, Josée Dupuis, Stephen S. Rich, Jose C. Florez, Jerome I. Rotter, Andrew P. Morris, and James B. Meigs

Supplemental Materials

Table of Brief Contents

Table of contents

Figure S1 Schematic study diagram

Figure S2 Venn diagram of trans-ethnic analysis and transferability results

Figure S3 Trans-ethnic fine-mapping of 22 loci (13 FG, 8 FI, and 1 both FG and FI) with greater than 20% reduction in the 99% credible set.

FG loci

Figure S3A. *FOXA2* locus
Figure S3B. *GCK* locus
Figure S3C. *CRY2* locus
Figure S3D. *KL* locus
Figure S3E. *ADCY5* locus
Figure S3F. *GCKR* locus
Figure S3G. *PROX1* locus
Figure S3H. *DPYSL5* locus
Figure S3I. *IGF2BP2* locus
Figure S3J. *CDKN2B* locus
Figure S3K. *ADRA2A* locus
Figure S3L. *TCF7L2* locus
Figure S3M. *FADS1* locus
Figure S3N. *DGKB-TMEM195* locus

FI loci

Figure S3O. *ARL15* locus
Figure S3P. *PPP1R3B* locus
Figure S3Q. *COBLL1-GRB14* locus
Figure S3R. *IRS1* locus
Figure S3S. *GCKR* locus
Figure S3T. *FAM13A* locus
Figure S3U. *ANKRD55-MAP3K1* locus
Figure S3V. *UHRF1BP1* locus
Figure S3W. *PPARG* locus

Figure S4 Plots of regional association and RegulomeDB and Islet Regulome Browser information at 14 FG and 9 FI loci with substantially narrowed credible sets after trans-ethnic analysis

FG loci

Figure S4A. *TCF7L2* locus
Figure S4B. *ADRA2* locus
Figure S4C. *DGKB-TMEM195* locus
Figure S4D. *FADS1* locus
Figure S4E. *PROX1* locus
Figure S4F. *GCK* locus
Figure S4G. *ADCY5* locus
Figure S4H. *GCKR* locus
Figure S4I. *CDKN2B* locus
Figure S4J. *FOXA2* locus
Figure S4K. *CRY2* locus
Figure S4L. *DPYSL5* locus
Figure S4M. *IGF2BP2* locus
Figure S4N. *KL* locus

FI loci

Figure 4SO. *ARL15* locus
Figure 4SP. *COBLL1-GRB14* locus
Figure 4SQ. *IRS1* locus
Figure 4SR. *UHRF1BP1* locus
Figure 4SS. *FAM13A* locus
Figure 4ST. *PPARG* locus
Figure 4SU. *GCKR* locus
Figure 4SV. *PPP1R3B* locus
Figure 4SW. *ANKRD55-MAP3K1* locus

Figure S5 Concordance of effect size and Comparison of EA trait-raising allele Frequency in EA and AA

Figures S5A Effect size comparison for EA FG SNPs
Figures S5B Effect size comparison for EA FI SNPs
Figures S5C Allele frequency comparison for EA FG SNPs
Figures S5D Allele frequency comparison for EA FI SNPs

Figure S6 Genome-wide association plots and quantile-quantile (QQ) plots for FG and FI

Figures S6A Miami plots of association with FG
Figures S6B the QQ plots for FG
Figures S6C Miami plots of association with FI
Figures S6D the QQ plots for FI
Figures S6E genome-wide association plots of trans-ethnic meta-analysis results for FG
Figures S6F genome-wide association plots of trans-ethnic meta-analysis results for FI

Figure S7 Conditional analysis at *PELO*/rs6450057

Figures S7A the comparison for unconditional association results with HapMap 2 CEU LD information
Figures S7B the comparison for conditional association results with HapMap 2 CEU LD information
Figures S7C the comparison for unconditional association results with HapMap 2 YRI LD information
Figures S7D the comparison for conditional association results with HapMap 2 YRI LD information

Supplemental Figure Legends

Supplemental Tables and Legends

Supplemental References

Participating consortia and investigators

The data used in the current report were derived from published results from The Meta-Analyses of Glucose and Insulin-related traits Consortium (**MAGIC**)[1] and from unpublished meta-analyses from the African American Glucose and Insulin genetic Epidemiology (**AAGILE**) consortium. Only non-diabetic individuals were included in the trans-ethnic meta-analysis that combined data from MAGIC and AAGILE consortium. All data on participants of European ancestry (EA) were obtained from MAGIC (n = 51,750) while all data on participants of African ancestry (AA) were obtained from the AAGILE Consortium (n = 20,209). Cohorts that contributed data to the MAGIC consortium and names of the steering committee members are listed on the consortium website: http://www.magicinvestigators.org/.

The AAGILE consortium includes AA individuals from 16 cohorts. Key characteristics for each discovery and replication study sample are shown in **Table S1**. Investigators from AAGILE consortium are listed in the author list while those from the MAGIC consortium are shown below.

MAGIC investigator [1]

Manning AK, Hivert MF, Scott RA, Grimsby JL, Bouatia-Naji N, Chen H, Rybin D, Liu CT, Bielak LF, Prokopenko I, Amin N, Barnes D, Cadby G, Hottenga JJ, Ingelsson E, Jackson AU, Johnson T, Kanoni S, Ladenvall C, Lagou V, Lahti J, Lecoeur C, Liu Y, Martinez-Larrad MT, Montasser ME, Navarro P, Perry JR, Rasmussen-Torvik LJ, Salo P, Sattar N, Shungin D, Strawbridge RJ, Tanaka T, van Duijn CM, An P, de Andrade M, Andrews JS, Aspelund T, Atalay M, Aulchenko Y, Balkau B, Bandinelli S, Beckmann JS, Beilby JP, Bellis C, Bergman RN, Blangero J, Boban M, Boehnke M, Boerwinkle E, Bonnycastle LL, Boomsma DI, Borecki IB, Böttcher Y, Bouchard C, Brunner E, Budimir D, Campbell H, Carlson O, Chines PS, Clarke R, Collins FS, Corbatón-Anchuelo A, Couper D, de Faire U, Dedoussis GV, Deloukas P, Dimitriou M, Egan JM, Eiriksdottir G, Erdos MR, Eriksson JG, Eury E, Ferrucci L, Ford I, Forouhi NG, Fox CS, Franzosi MG, Franks PW, Frayling TM, Froguel P, Galan P, de Geus E, Gigante B, Glazer NL, Goel A, Groop L, Gudnason V, Hallmans G, Hamsten A, Hansson O, Harris TB, Hayward C, Heath S, Hercberg S, Hicks AA, Hingorani A, Hofman A, Hui J, Hung J, Jarvelin MR, Jhun MA, Johnson PC, Jukema JW, Jula A, Kao WH, Kaprio J, Kardia SL, Keinanen-Kiukaanniemi S, Kivimaki M, Kolcic I, Kovacs P, Kumari M, Kuusisto J, Kyvik KO, Laakso M, Lakka T, Lannfelt L, Lathrop GM, Launer LJ, Leander K, Li G, Lind L, Lindstrom J, Lobbens S, Loos RJ, Luan J, Lyssenko V, Mägi R, Magnusson PK, Marmot M, Meneton P, Mohlke KL, Mooser V, Morken MA, Miljkovic I, Narisu N, O'Connell J, Ong KK, Oostra BA, Palmer LJ, Palotie A, Pankow JS, Peden JF, Pedersen NL, Pehlic M, Peltonen L, Penninx B, Pericic M, Perola M, Perusse L, Peyser PA, Polasek O, Pramstaller PP, Province MA, Räikkönen K, Rauramaa R, Rehnberg E, Rice K, Rotter JI, Rudan I, Ruokonen A, Saaristo T, Sabater-Lleal M, Salomaa V, Savage DB, Saxena R, Schwarz P, Seedorf U, Sennblad B, Serrano-Rios M, Shuldiner AR, Sijbrands EJ, Siscovick DS, Smit JH, Small KS, Smith NL, Smith AV, Stančáková A, Stirrups K, Stumvoll M, Sun YV, Swift AJ, Tönjes A, Tuomilehto J, Trompet S, Uitterlinden AG, Uusitupa M, Vikström M, Vitart V, Vohl MC, Voight BF, Vollenweider P, Waeber G, Waterworth DM, Watkins H, Wheeler E, Widen E, Wild SH, Willems SM, Willemsen G, Wilson JF, Witteman JC, Wright AF, Yaghootkar H, Zelenika D, Zemunik T, Zgaga L; DIAbetes Genetics Replication And Meta-analysis (DIAGRAM) Consortium; Multiple Tissue Human Expression Resource (MUTHER) Consortium, Wareham NJ, McCarthy MI, Barroso I, Watanabe RM, Florez JC, Dupuis J, Meigs JB, Langenberg C.

Sources of data for pleiotropy studies

Consortia that contributed results for associations between fasting glucose or fasting insulin SNPs and insulin-related traits (i.e., hypertension, systolic and diastolic blood pressure, triglycerides, high density lipoprotein cholesterol, low density lipoprotein cholesterol, body mass index and waist-to-hip ratio-adjusted for BMI) are shown below:

1. **Continental Origins and Genetic Epidemiology Network (COGENT) consortium[2]**

   The COGENT consortium provided association results for hypertension and for systolic and diastolic blood pressure.

2. **Electronic Medical Records and Genomics Network (eMERGE)[3]**

   The eMERGE consortium provided triglyceride data from BioVU at Vanderbilt University Medical Center (https://victr.vanderbilt.edu/pub/biovu/) and triglyceride and blood pressure (hypertension and systolic and diastolic blood pressure) data from Mt. Sinai School of Medicine.

3. **The National, Heart, Lung and Blood Institute's Candidate gene Association Resource (CARe)[4]**

   The CARe consortium contributed association results for high density lipoprotein cholesterol and low density lipoprotein cholesterol.

4. **MEta-analysis of type 2 DIabetes in African Americans (MEDIA) Consortium[5]**

   The MEDIA consortium provided association results for type 2 diabetes.

5. **African Ancestry Anthropometry Genetics (AAAG) Consortium[6,7]**

   The AAAG consortium provided association results for body mass index and waist-hip-ratios.

Author contributions

The contributions of authors are summarized below:

Assembling and steering the consortium: AA, APM, BMP, CNR, CTL, DJC, DKA, DS, DWB, EB, EPB, IM, JBM, JCF, JD, JGW, JIR, JSP, LEW, LF, MAN, MAP, MMS, RJFL, SSR, YIC

Genotyping and data imputation: AA, EPB, GC, JAS, JIR, JY, KDT, LJRT, MAP, MF, MMS, MOG, RJFL, SLRK, TT, XG, YIC, YL

Phenotyping of the study participants: ANK, DS, EPB, JAP, JIR, JK, JMZ, MAP, MLB, PAP, RJFL, RK, SLRK, YIC, YL

Statistical analyses: AA, ABZ, AC, ADJ, AHZ, AJK, ALP, AMD, ARB, BEC, BP, CA, CDL, CTL, DC, DV, DS, DSE, DVR, DWB, EKK, EPB, ES, GC, JACD, JD, JDE, JH, JL, JL, JTZ, JY, KEN, KJG, KMR, LAL, LFB, LL, LLA, LRY, MAJ, MAP, MBS, MC, MCYN, MFK, MGH, MKE, ML, MPW, MRI, MS, NA, NF, NM, OG, PA, PAP, RAJ, RK, SL, SR, SRP, SS, ST, TBH, THM, TLE, TT, UN, WLL, WMC, WMC, WZ, XG, XL, XZ, YL, YL, YPF

SNP annotation: AMD, KJG, LL, JH, SR, KH

Drafting of the manuscript: AMD, APM, ASL, CTL, DS, DMB, DV, EKK, EPB, ES, JBM, JCF, JD, JGW, JH, JIR, KDT, KH, KJG, LL, LRY, MCYN, MD, MFH, MGH, ML, MOG, MMS, NM, PA, RJFL, RK, SR, SSR, WHLK, WMC, XG, XL, YIC, YL

Enhancing the manuscript for intellectual content: All authors

Approval of the final version: All authors

SNP annotation

Following trans-ethnic meta-analysis of data from **MAGIC** (EA participants) and the **AAGILE** consortium (AA participants), we identified 14 fasting glucose (FG) and 9 fasting insulin (FI) loci (**Table S5**) in which the number of SNPs in a locus or the size of the genomic region likely to harbor the causative SNP was reduced by at least 20%. For each of the SNPs in the narrowed region, referred to as the 99% credible set, we used HaploReg V2 to annotate their biological relevance. HaploReg provides useful annotation information for the SNP of interest as well as those within a user-specified LD. The fully operational web version is available at http://www.broadinstitute.org/mammals/haploreg/haploreg.php. HaploReg reports any evidence for regulatory chromatin marks, DNAse I hypersensitivity sites (DHSI), transcription factor binding sites (TFBS), transcription factor binding motifs, or expression quantitative trait loci (eQTL) overlapping with each SNP of interest and thus gives mechanistic insights into how non-coding SNPs may lead to a given disease condition. Ward and Kellis provide more detailed information on HaploReg and its usage.[8]

After HaploReg we performed additional annotation manually using annotation resources in the public domain (i.e., RegulomeDB, ENCODE, Islet Regulome and FANTOM) to further characterize potential regulatory functions of the variants in the credible sets. Use of HaploReg together with manual annotation revealed whether a given SNP lies in a location with a histone mark suggestive of regulatory activity, a DHSI, TFBS, or if the SNP is in a gene expressed in a diabetes-relevant tissue, e.g., the liver or pancreas. In the case of histone marks we also evaluated whether the histone mark corresponds to an enhancer or promoter. Finally, we catalogued other traits with significant associations reported within the credible set from the NHGRI GWAS Catalog. Below we provide detailed information on the potential biological relevance of SNPs in each of the 14 FG and 9 FI loci that we annotated; the index SNP in EA indicated in parentheses.

1. **FOXA2 (rs6048205)**
   a. Credible set interval in hg18: chr20:22505099-22508971
   b. Credible set interval in hg19: chr20:22557099-22560971
   c. The region contains the 5' end of TCONS_00028636 (lincRNA)
      i. Displays especially high expression in liver cell lines
      ii. Is accompanied by moderate to high transcription levels (RNA-seq) only in HepG2 cell lines
      iii. The EST BG655894 indicates expression in pancreatic Islets
   d. There are five broad and weak H3K4Me1 peaks in the region
      i. Especially prominent in Embryonic stem cells
   e. There are 51 TFBSs in the region, all but 2 are expressed in liver cell lines
   f. The lead SNP is 20bp telomeric (p arm) to a DHSI (19/125) which is found in pancreatic islet cell lines
   g. The lead SNP sits inside 10 TFBSs
      i. They are all found in liver cell lines
      ii. Includes FOXA1 and FOXA2
   h. The RNA-seq information from the TFBSs in the region as well as the expression profile of the lincRNA indicate that the locus plays a role in the liver. The lead SNPs position in several binding sites may lead to a disruption in the binding of TFBSs.

2. **GCK (rs4607517)**

This credible set contained a single SNP; annotation overlap for the SNP can be found in Supplemental Table 5.

3. CRY2 (rs11605924)

a. Credible set interval in hg18: chr11:45820718-45835568
b. Credible set interval in hg19: chr11:45864142-45878992
c. Contains 5' end of CRY2
d. There is one NHGRI SNP
    i. rs11605924 – fasting glucose traits
e. There are 7 moderate to weak HK4Me1 peaks in the region
f. There are 3 weak and 1 strong H3K4Me3 peaks in the region
g. There are 2 weak and 2 strong H3K27Ac peaks in the region
h. The lead SNP is 1kbp upstream of a weak H3K4Me1 peak
    i. DHSI (27) found in liver cell lines
    ii. 9 TFBSs
i. 5.6kbp upstream of weak H3K4Me1 and H3K27Ac peaks
    i. DHSI (57) found in muscle and pancreatic islets
    ii. 3TFBSs
j. 1kbp downstream of a weak H3K4Me1 peak
    i. DHSI (3) and (32)
k. 3.8kbp downstream of dual H3K4me1, H3K4Me3, and H3K27Ac peaks
    i. DHSI (111) and (125)
    ii. 101 TFBSs
l. 6.5kbp telomeric (p arm) to the SNP is a strong H3K4Me3 peak
m. 8kbp telomeric to the SNP are weak H3K4Me1, H3K27Ac, H3M4Me3 peaks
    i. DHSI (125)
    ii. 49 TFBSs
n. The lead SNP lies in the promoter region of CRY2, which explains its proximity to several H3K4Me1 peaks. Because CRY2 impacts metabolism, a polymorphism in the gene's promoters may alter the function.

4. KL (rs576674)

a. Credible set interval in hg18: chr13:32209005-32701555
b. Credible set interval in hg19: chr13:33311005-33803555
c. Four genes in the region
    i. 3' end of PDS5B
    ii. KL
    iii. STARD13
    iv. TCONS_00021632 (lincRNA)
d. Four NHGRI GWAS SNPs
    i. rs2555603 – BMI
    ii. (not related) rs2555603 – aneurysm
    iii. (not related) rs642899 –behavioral disinhibition
    iv. (not related) rs990324 – total ventricular volume
e. There are 29 H3K4Me1 peaks throughout the region
f. There are two H3K4Me3 peaks (weak)
g. 15 H3K27Ac peaks throughout the region
h. The lead SNP lies within a FOXA2 binding site found in liver cell lines
    i. This is clustered near three other binding sites, all found in liver cell lines

i. 10.5kbp telomeric (q arm) to a moderate H3K4Me1 peak and weak H3K4Me3 and H3K27Ac peaks
    i. DHSI (66) found in muscle and pancreatic cells
    ii. 6 TFBSs
j. 4.6kbp upstream of a DHSI (26) in pancreatic islets
    i. 12 TFBSs
k. The lead SNP is in an intergenic region, and may serve as a bidirectional, distant regulator to both TCONS_00021632 and KL. The SNP may impact the binding of FOXA2 to its TFBS, and exert its effects primarily in the liver.

5. ADCY5 (rs11708067)

This credible set contained a single SNP; annotation overlap for the SNP can be found in Supplemental Table 5.

6. GCKR (rs780094)

This credible set contained a single SNP; annotation overlap for the SNP can be found in Supplemental Table 5.

7. PROX1 (rs340874)

a. Credible set interval in hg18: chr1: 212212012-212230298
b. Credible set interval in hg19: chr1:214145389-214163675
c. Contains the 5'UTRs of PROX-AS1 and PROX1
d. Exonic to the mRNA AK096113, overlaps PROX-AS1. Found in liver cell lines
e. The 5'UTR of PROX-AS1 overlaps the mRNA AK096113, which comes from human liver cells
f. There are 2 NHGRI SNPs in the region
    i. rs2075423 – Type 2 Diabetes
    ii. rs340874 – Fasting glucose traits
g. There are 4 H3K4Me1 peaks throughout the region
h. There is one weak and one strong H3K4Me3 peaks
i. There are two H3K27Ac peaks
j. The 5'UTR of PROX1 is overlaps with a level of moderate transcription according to RNA-seq, especially strong in HepG2 cell lines (2.2kbp telomeric to (p arm) lead SNP)
    i. There are also moderate H3K4Me1 and H3K27Ac peaks and a strong H3K4Me3 peak
    ii. There is a DHSI (116/125) with 36 TFBSs (31 present in liver cells)
        1. TFBSs include FOXA1 and FOXA2
k. 12.5kbp downstream, there is a large H3K4Me1 peak, with a DHSI (25/125) found in HSMM cells and one TFBS
l. 8.2kbp downstream, there are strong H3K4Me1 dual peaks and small H3K37Ac peaks. There is a DHSI (27/125) and 9 TFBSs
m. The lead SNP lies within an area of mild H3K4Me1 expression and several different DHSI and 41 TFBSs (31 expressed in liver cells)
    i. The SNP is within two TFBSs: EZH2 and CTBP2
n. The histone modifications are consistent with the location of the SNP within the promoter region of PROX1 and PROX1-AS1. This area may play an important role in the liver, as indicated by the tissue specificity of TFBSs, RNA-seq, and human mRNA.

8. **DPYSL5 (rs1371614)**
    a. Credible set interval in hg18: chr2: 26957635-27251700
    b. Credible set interval in hg19: chr2:27104131-27398196
    c. Contains 12 different genes
        i. DPYSL5
        ii. MAPRE3
        iii. TMEM214
        iv. OST4
        v. KHK
        vi. EMILIN1
        vii. AGBL5
        viii. CGREF1
        ix. ABHD1
        x. PREB
        xi. C2orf53
        xii. TCF23
    d. The 3'UTR of DYPSL5 contains high transcription levels, according to RNA-seq
    e. Two NHGRI SNPs
        i. rs1371614 – Fasting glucose traits
        ii. (not related) rs7588926 – Response to cytadine analogues
    f. There are 23 H3K4Me1 peaks throughout the region
    g. There are 12 H3K4Me3 peaks throughout the region
    h. There are 14 H3K27Ac peaks throughout the region
    i. The lead SNP lies with a DHSI (3) and 2 TFBSs, FOXA1 and FOXA2, both found in liver cell lines
    j. 4kbp downstream of a small H3K4Me1 peak
        i. DHSI (26) found in liver, muscle, and pancreatic cell lines
        ii. 23 TFBSs, all found in liver cell lines
    k. 13kbp upstream of an area of weak H3K4Me1 modification
        i. DHSI (113) and 13 TFBSs
    l. This is a larger transethnic region, with explains the large amount of genes with associated histone modifications. The SNP may impact the binding of FOXA1 and FOXA2, specifically in liver cells, which would affect liver metabolism.

9. **IGF2BP2 (rs7651090)**
    a. Credible set interval in hg18: chr3: 186750043-187067565
    b. Credible set interval in hg19: chr3:185267349-185584871
    c. Five genes in the region
        i. LIPH
        ii. SENP2
        iii. IGF2BP2
            1. Human mRNA BC021290 indicates expression in pancreas
        iv. C3Orf65
        v. TCONS_00006340 (lincRNA)
    d. Five NHGRI GWAS SNPs
        i. (not related) rs720390 – height
        ii. rs1374910 – Type 2 Diabetes
        iii. rs6769511 – Type 2 Diabetes

iv. rs1470579 – Type 2 Diabetes
v. rs4402960 – Type 2 Diabetes

e. There are 24 H3K4Me1 peaks throughout the region
f. There are 3 H3K4Me3 peaks throughout the region
g. There are 15 H3K27Ac peaks throughout the region
h. The lead SNP is intronic to IGF2BP2
i. 1.3kbp downstream of large H3K4Me1 and H3K27Ac peaks
    i. DHSI (93) and 28 TFBSs
j. 12kbp downstream of a DHSI (87)
    i. 29 TFBSs
k. 4.7kbp upstream of a moderate H3K4Me1 peak
    i. DHSI (12)
l. 13kbp upstream of an area of moderate H3K4Me1
    i. DHSI (60) found in muscle and pancreatic cells
    ii. 5 TFBSs
m. The large Type 2 Diabetes SNP cloud indicates the importance of the region in that disease. The lead SNP is intronic to IGF2BP2, and 27 kbp from the nearest exon. Its role may be with the nearby putative promoter, located 1.3 kbp away. Further validation could show if this promoter is associated with IGF2BP2, or the downstream lincRNA TCONS_00006340.

10. CDKN2B (rs10811661)

a. Credible set interval in hg18: chr9: 22118180-22124094
b. Credible set interval in hg19: chr9:22128180-22134094
c. No genes within the region
d. 4 NHGRI GWAS SNPs
    i. rs7020996 – Type 2 diabetes
    ii. rs2383208 – Type 2 Diabetes
    iii. rs10965250 – Type 2 Diabetes
    iv. rs10811661 – Type 2 Diabetes
e. There are three moderate, broad H3M4Me1 peak, especially prominent in blood vessel cells
    i. 4kbp, 4.6kbp, and 5.4kbp telomeric (p arm) to the lead SNP
f. 4.5kbp telomeric to the SNP, there is a DHSI (36/125) which is in HSMM and pancreatic islet cells. There are three TFBSs nearby, including FOXA2
g. The entire region is intergenic and contains a large Type 2 Diabetes SNP cloud. This indicates the importance of the enhancer region, which overlaps a DHSI site with tissue specificity in diabetes-relevant tissues.

11. ADRA2A (rs10885122)

a. Credible set interval in hg18: chr10: 112960941-113029657
b. Credible set interval in hg19: chr10:112970951-113039667
c. No genes in region
d. Only histone modification is a very small H3K4Me1 peak between 113,005,278-113,007,774 only in HSMM cells
e. There is a DHSI (8/125) in HSMM and PanIsletD.
f. There are 9 TFBSs in the region, and 7 are present in liver cell lines
g. **When using lift over, the lead SNP lies just outside the credible region** (113042093)

h. This trans-ethnic region contains little biological information, being both intergenic and having little regulatory information. However, the information that is available shows tissue specificity to diabetes-relevant tissues, and may impact a genomic element not currently reported.

12. TCF7L2 (rs7903146)

a. Credible set interval in hg18: chr10: 114742493-114778805
b. Credible set interval in hg19: chr10:114752503-114788815
c. The entire region is intronic to TCF7L2
    i. Human mRNA FJ010174 indicates expression in pancreatic, hepatic, renal, muscle and adipose cells
d. There are five NHGRI GWAS SNPs
    i. rs12243326 – 2 hour glucose challenge
    ii. (not related) rs7904519 – Breast cancer
    iii. rs7903146 – Type 2 diabetes
    iv. rs4506565 – fasting glucose traits/Type 2 Diabetes
    v. rs7901695 – Type 2 diabetes
e. There are 5 H3K4Me1 peaks (two strong, three weak)
    i. The weak peaks are located 2.3kbp, 3.8kbp, and 5kbp downstream from the lead SNP
f. 8.8kbp downstream, there is a DHSI (8/125) preset in liver cell lines with 21 TFBSs, all present in liver cell lines
    i. This coincides with a very strong peak of conservation
g. The large Type 2 Diabetes SNP cloud, along with the tissue specificity information from the human mRNA, confirms the region's importance in diabetes. The SNP may play a role in the promoter regions and impact the transcription of TCF7L2, which is important in maintaining blood glucose levels. (http://www.ncbi.nlm.nih.gov/gene/6934)

13. FADS1 (rs174550)

a. Credible set interval in hg18: chr11: 61307932-61366326
b. Credible set interval in hg19: chr11:61551356-61609750
c. There are five genes in the region
    i. MYRF
    ii. FEN1
        1. EST CA868349 indicating expression in pancreas
    iii. TMEM258
    iv. FADS1
    v. FADS2
        1. EST BP237803 indicating expression in liver
d. There are 20 NHGRI GWAS SNPs
    i. rs174541 – metabolite levels
    ii. rs4246215 – platelet counts, phospholipid levels
    iii. rs174538 – blood metabolite levels
    iv. rs102275 – blood cholesterol/metabolite levels, metabolic syndrome
    v. (not related) rs174537 – colorectal cancer
    vi. rs174556 – blood metabolite levels
    vii. rs174555 – blood fatty acid levels

viii. rs174550 – fasting glucose related traits
ix. rs174548 – blood metabolite levels
x. rs174547 – metabolic traits
xi. rs174546 – metabolic syndrome, cholesterol
xii. rs174578 – blood metabolite levels
xiii. rs2727271 – blood metabolite levels
xiv. rs2727270 – fatty acid levels
xv. (not related) rs174583 – response to statins
xvi. (not related) rs174577 – P wave duration
xvii. rs174574 – phospholipid levels
xviii. rs1535 – metabolic syndromw
xix. (not related) rs174570 – glycated hemoglobin levels
xx. rs968567 – blood metabolite levels

e. Seven H3K27Ac peaks
   i. Two are associated with H3K4Me1 peaks
f. There are three H3KeMe3 peaks, all associated with H3K27Ac peaks
g. There are eleven H3K4Me1 peaks, seven are associated with H3K27Ac peaks
h. The lead SNP is intronic to FADS1
i. The lead SNP is inside of a H3K4Me1 peak
j. 12kbp upstream are strong H3K4Me3 and H3K27Ac peaks
   i. associated with several DHSI (55,117,124,125,14). The 14/125 DHSI is in both hepatocytes and pancreatic cells. There are over 150 associated TFBSs
   ii. On either side of this region are H3K4Me1 peaks
k. 3.9kbp upstream of H3K4Me1 and K3K17Ac peaks
   i. DHSI (12) found in pancreatic islet cells
   ii. 42 TFBSs
l. 11kbp telomeric (q arm) to H3K4Me3 and H3K27Ac peaks
   i. DHSI (125) and (116)
   ii. 87 TFBSs
m. This region contains an expansive SNP cloud, which strengthens the case for the importance of the region in Type 2 Diabetes. Furthermore, several of the genes in the region are associated with metabolism and cholesterol, including FADS1 and FADS2. The location of the lead SNP within a promoter region may impact the transcription of these elements.

14. DGKB-TMEM195 (rs2191349)

a. Credible set interval in hg18: chr7: 14888532-15032137
b. Credible set interval in hg19: chr7:14922007-15065612
c. Contains the 5’ end of DGKB
d. Contains 3 NHGRI SNPs
   i. rs10244051 – metabolic traits
   ii. rs2191349 – fasting glucose related traits
   iii. rs6947830 – metabolic syndrome
e. There are three small H3K4Me1 peaks
   i. 8.7kbp telomeric (p arm) there is a DHSI (104) with HSMM, HepG2, and PanIslets cell lines. There are 16 TFBSs
f. This transethnic region is mostly intergenic, with few biological elements. However, the presence of a SNP cloud indicates the importance of this region to Type 2 diabetes. The

SNP cloud is clustered around a small H3K4Me1 peak, which may be involved in distant regulation.

15. ARL15 (rs4865796)

a. Credible set interval in hg18: chr5: 53059217-53557802
b. Credible set interval in hg19: chr5:53023460-53522045
c. There are two genes in the region
    i. TCONS_l2_00022897 (lincRNA)
    ii. 3' end of ARL15
        1. EST AV660016 indicating expression in liver
d. There are 5 NHGRI SNPs in the region
    i. rs4311394 – adiponectin levels
    ii. rs6450176 – adiponectin levels/cholesterol
    iii. (not related) rs273218 – migraine
    iv. rs702634 – Type 2 diabetes
    v. (not related) rs255758 – rheumatoid arthritis
e. There are 14 H3K4Me1 peaks
        i. There is one small peak located 1.5kbp downstream of the SNP
        ii. 7kbp upstream there is a small peak, associated with a DHSI (42) present in HepG2 Cells and 7 TFBSs
f. There are 3 H3K17Ac peaks, each corresponding to a H3K4Me1 peak
g. There are numerous DHSI and TFBS throughout the region, as well as low-levels of transcription according to RNA-seq
h. The lead SNP is located near a promoter region intronic to ARL15. While this may regulate the gene, which is shown to have tissue specificity to the liver and play a role in glucose levels via adiponectin (PMID: 20011104), it may also impact regulation of the downstream lncRNA TCONS_l2_00022897.

16. PPP1R3B (rs4841132)

This credible set contained a single SNP (rs1461729); annotation overlap for the SNP can be found in Supplemental Table 5.

17. COBLL1-GRB14 (rs7607980)

a. Credible set interval in hg18: chr2: 165214970-165266498
b. Credible set interval in hg19: chr2:165506724-165558252
c. There are two genes in the region
    i. 3' end of COBLL1
        1. EST CB270545 indicates expression in adipose tissue
    ii. TCONS_00004484 (lncRNA)
        1. Increased expression in liver and adrenal tissue.
d. Five NHGRI GWAS SNPs
        i. rs10195252: Triglycerides
        ii. rs13389219: Waist hip ratio
        iii. (not related) rs6717858: sexual dimorphism is anthropometric traits

iv. rs12328675: cholesterol
v. rs7607980: fasting insulin traits

e. Between 165,536,302-165,558,065 (coinciding with COBLL1), there is moderate to high transcription according to RNA-seq
   i. This is especially prominent in HepG2 cells
f. 1.3kbp downstream, there is a DHSI (5/125) present in HepG2 cells, with 25 TFBSs (17 present in liver cells)
g. 3.1kbp upstream, there is a DHSI (32) present in HSMM, PANC-1, and HepG2, associated with 7 TFBSs (all in liver cells)
h. There is a moderate H3K4Me1 peak and small H3K27Ac peak in the region
i. This trans-ethnic region shows several instances of tissue specificity in liver tissue, including information from TFBSs, DHSI, and lncRNA expression profiles. The lead SNP is exonic to COBLL1, which plays a role in cholesterol levels (PubMed: 17903299). This variant may impact the function of this gene.

18. IRS1 (rs2943634)

a. Credible set interval in hg18: chr2: 226735108-226872748
b. Credible set interval in hg19: chr2:227026864-227164504
c. There are three genes in the region
   i. TCONS_l2_00015614 (lncRNA) – especially prominent in thyroid
   ii. TCONS_00003502 (lncRNA)
   iii. TCONS_00004599 (lncRNA)
d. There are seven NHGRI GWAS SNPs
   i. rs2972146 – triglycerides/HDL cholesterol
   ii. rs2943641 – Type 2 Diabetes
   iii. rs2943650 – adiposity
   iv. rs1515110 – adiponectin levels
   v. rs2972146 – triglycerides/HDL cholesterol
   vi. (not related) rs2943636 - sexual dimorphism is anthropometric traits
   vii. rs2943634 – fasting insulin traits
e. There are five H3K4Me1 peaks
   i. 12.7kbp centromeric (q arm) – especially prominent in HSMM cell lines
   ii. 10kbp telomeric – especially prominent in HSMM cell lines
f. There are three H3K27Ac peaks, each coinciding with a H3K4Me1 peak
   i. 12.7kbp centromeric (q arm) – especially prominent in HSMM cell lines
   ii. 10kbp telomeric – especially prominent in HSMM cell lines
g. 12.7kbp centromeric is a DHSI (21) with 9 TFBS (all in liver cells)
h. 10kbp telomeric are two DHSIs with 27 TFBSs
i. This region contains only non-coding SNPs, highlighting their importance in metabolic disorders. The SNP cloud resides in an intergenic area of the region, with relatively few genomic features. However, the genomic features that are present display tissue specificity to Type 2 Diabetes relevant tissues. Further validation could uncover if this area serves as a distant regulator to another genomic area involved in Type 2 Diabetes.

19. GCKR (rs780094)

This credible set contained a single SNP; annotation overlap for the SNP can be found in Supplemental Table 5.

20. ANKRD55-MAP3K1 (rs459193)

a. Credible set interval in hg18: chr5: 55595454-56092481
b. Credible set interval in hg19: chr5:55559697-56056724
c. There are five genes in the region
    i. TCONS_00009667 (lncRNA)
    ii. TCONS_00010339 (lncRNA) – especially prominent in kidney and adrenal
    iii. TCONS_00009669 (lncRNA) – especially prominent in kidney and adrenal
    iv. TCONS_00010343 (lncRNA) – especially prominent in kidney and adrenal
        1. 3' end located less than 1kbp from lead SNP
    v. TCONS_00010346 (lncRNA)
d. There are 11 NHGRI GWAS SNPs
    i. rs9686661 – triglycerides
    ii. (not related) rs11743303 - sexual dimorphism is anthropometric traits
    iii. rs6867983 – waist circumference/triglycerides
    iv. rs30360 – fasting insulin/insulin resistance
    v. (not related) rs456867 – urate levels
    vi. (not related) rs1020388 – Celiac's disease
    vii. (not related) rs889312 – breast cancer
    viii. (not related) rs16886181 – breast cancer
    ix. (not related) rs16886165 – breast cancer
    x. (not related) rs16886034 – breast cancer
    xi. (not related) rs16886113 – breast cancer
e. There are approximately 28 H3K4Me1 peaks
f. The region has 1 H3K4Me3 peak
g. There are seven H3K27Ac peaks, each coinciding with a H3K4Me1 peak
h. 6kbp centromeric (q arm) is an area of high conservation and transcription according to RNA-seq. While there is no gene, histone mod, or TFBS corresponding to this region, there are 41 ESTs
i. 9kb centromeric there is a H3K4Me1 peak. There is a DHSI (41) with 10 TFBSs
    i. The DHSI is present in HSMMtube and PanIsletD cell lines
j. 3.1kbp centromeric is a DHSI (6) present in HepG2 cells. There are 6 TFBSs, all present in liver cell lines
k. 5.5 kbp telomeric is a H3K4Me1 peak. There is a DHSI (48) with 11 TFBSs.
    i. The DHSI is present in HSMM and HepG2 cell lines
l. 15 kbp telomeric is a broad H3K4Me1 peak. This encompasses several DHSI and TFBSs
m. This region contains numerous lncRNA and regulatory elements, further emphasizing their importance. The tissue specificity of these elements in Type 2 Diabetes tissues, such as liver and muscle tissue, indicates that these features may be playing a role in the metabolic disorder. Further validation could be done to identify the specific targets of these areas.

21. FAM13A (rs3822072)

a. Credible set interval in hg18: chr4: 89840095-90083469
b. Credible set interval in hg19: chr4:89621072-89864446
c. Contains two genes
    i. 3' end of HERC3
    ii. FAM13A
        1. The entire region of the gene shows transcription levels particularly prominent in HepG2 cell lines
d. There are two NHGRI GWAS SNPs
    i. (not related) rs2609255 – lung disease

ii. rs3822072 – HDL cholesterol
e. The region has 15 H3K4Me1 peaks
f. There are 2 H3K4Me3 peaks (each coinciding with an Me3 peak)
g. There are 6 H3K27Ac peaks (each coinciding with an Me3 peak)
h. The lead SNP is intronic to FAM13A, is within a DHSI (4) and a TFBS (GATA3)
i. 3.3kbp upstream there are peaks for each form of histone modification.
   i. DHSI (119) and approximately 70 TFBSs
j. 9kbp downstream is a DHSI (17) with 11 TFBSs, all present in liver cells
k. The lead SNP in this region resides in the promoter region of the short isoform FAM13A, and may impact its rate of transcription. The tissue-specificity of the RNA-seq and TFBSs to the liver indicates where this effect may occur.

22. UHRF1BP1 (rs4646949)

a. Credible set interval in hg18: chr6: 34872900-35090036
b. Credible set interval in hg19: chr6:34764922-34982058
c. Contains three genes
   i. 3' end of UHRF1BP1
   ii. TAF11
   iii. 5' end of ANKS1A
d. There are 6 NHGRI GWAS SNPs
   i. (not related) rs3734266 – lupus
   ii. (not related) rs2140418 – alcoholism
   iii. (not related) rs1535001 – lupus
   iv. (not related) rs847845 – lung cancer
   v. (not related) rs12205331 – CAD
   vi. rs4646949 – fasting insulin traits
e. There are 18 H3K4Me1 peaks
f. There is one H3K4Me3 peak
g. There are eight H3K27Ac peaks
h. The lead SNP is inside an area of high transcription according to RNA-seq and in between the short isoform of UHRF1BP1 and TAF11, but intronic to the long isoform of UHRF1BP1
i. 1kbp telomeric (p arm) is a small H3K4Me1 peak
   i. DHSI (1) with 6TFBSs
j. 12kbp telomeric are strong H3K4Me1 and H3K27Ac peaks
   i. DHSI (33) In HSMM and PanIsletD cell lines
   ii. 33 TFBSs, with 32 in blood tissue
k. 10kbp centromeric are strong H3K4Me3 and H3K27Ac peaks, and a moderate H3K3Me1 peak
   i. There are several DHSIs (35,20,125,110)
   ii. Over 100 TFBSs
l. The lead SNP resides near the 3' end of two different genes, which explains its high rate of transcription. However, the small H3K4Me1 peak where the lead SNP resides may be a distant regulator of the downstream target ANKS1A, which has been previously identified in an obesity and Type 2 diabetes study (PMCID: PMC3364960).

23. PPARG (rs17036328)

a. Credible set interval in hg18: chr3: 12311507-12371955
b. Credible set interval in hg19: chr3:12336507-12396955
c. The entire region is intronic to PPARG
d. There are 2 NHGRI GWAS SNPs

    i. (not related) rs11128603 - PAI-1 levels
    ii. rs1801282 – Fasting glucose and Type 2 Diabetes
e. The region has only one strong H3K4Me1 peak, and six other weak peaks
f. There are 3 weak H3K27Ac peaks, each coinciding with a Me1 peak
g. The lead SNP is 3kbp downstream of the strong H3K4Me1 peak and a weak Me3 peak
    i. There is a DHSI (67) found in muscle and pancreatic cell lines
    ii. There are 17 TFBSs
h. 1.7kbp Upstream of a DHSI (51) found in muscle and pancreatic cell lines. There are 27 TFBSs
i. 4.4 kbp upstream of a DHSI (40) found in HepG2 and HSMM cell lines
    i. There are 24 TFBSs
j. While the region is intronic to the long isoform of PPARG, the lead SNP is 2.7kbp upstream of the 5' end of the short isoform. The nearby promotor signals, DHSI, and TFBSs may be involved in the regulation of this isoform. Genetic variations impacting PPARG may increase the risk for Type 2 Diabetes (PubMed: 15797964, PubMed 15592662, PubMed: 12882888).

Acknowledgements

ARIC (DJC, EB, ES, JSP, KEN, ML, NM, THM): We thank the staff and participants of the ARIC Study for their important contributions. The Atherosclerosis Risk in Communities Study is carried out as a collaborative study supported by National Heart, Lung, and Blood Institute contracts HHSN268201100005C, HHSN268201100006C, HHSN268201100007C, HHSN268201100008C, HHSN268201100009C, HHSN268201100010C, HHSN268201100011C, and HHSN268201100012C, and grants R01HL087641, R01HL59367 and R01HL086694; National Human Genome Research Institute contract U01HG004402; and National Institutes of Health contract HHSN268200625226C. KEN is supported by grants R01DK089256 and 13GRNT16490017. Infrastructure was partly supported by Grant Number UL1RR025005, a component of the National Institutes of Health and NIH Roadmap for Medical Research. Dr. Selvin was supported by NIH/NIDDK grants K24DK106414 and 2R01DK089174.

BioMe (EPB, KH, RJFL, YL): The Mount Sinai BioMe Biobank Program is supported by the Andrea and Charles Bronfman Philanthropies.

BLSA (LF, TT): The BLSA was supported in part by the Intramural Research Program of the National Institutes of Health, National Institute on Aging.

CARDIA (DSS, EKK, LJRT, MF): The Coronary Artery Risk Development in Young Adults (CARDIA) Study is funded by contracts from the National Heart, Lung, and Blood Institute to the University of Alabama at Birmingham (HHSN268201300025C and HHSN268201300026C), Northwestern University (HHSN268201300027C), University of Minnesota (HHSN268201300028C), Kaiser Foundation Research Institute (HHSN268201300029C), and The Johns Hopkins University School of Medicine (HHSN268200900041C). CARDIA also receives partial support from the National Institute on Aging Intramural Research Program. The National Human Genome Research Institute supported genotyping of CARDIA participants through grants U01-HG-004729, U01-HG-004446, and U01-HG-004424.

CFS (BEC, SRP): This research was conducted in part using data and resources from the Cleveland Family Study (HL46380, HL113338), Case Western Reserve University (M01 RR00080) and the Broad Institute and supported by the National Heart Lung Blood Institute and the National Institutes of Health. Dr. Cade is supported by HL07901.

CHS (BMP, DSS, JIR, JK, JZ, KR, MOG, MLB, RAJ, YIC): This research was supported by contracts HHSN268201200036C, HHSN268200800007C, HL087562, HL103612, HL105756, HL120393, N01HC55222, N01HC85079, N01HC85080, N01HC85081, N01HC85082, N01HC85083, N01HC85086, and grant U01HL080295 from the National Heart, Lung, and Blood Institute (NHLBI), with additional contribution from the National Institute of Neurological Disorders and Stroke (NINDS). Additional support was provided by R01AG023629 from the National Institute on Aging (NIA). A full list of principal CHS investigators and institutions can be found at CHS-NHLBI.org. The content is solely the responsibility of the authors and does not necessarily represent the official views of the National Institutes of Health.

COGENT (JL, NF, XZ): COGENT investigators are supported by NIH grants 5R21HL123677-02 (NF), HG003054(XZ), and 5T32HL007567(XZ).

Family Heart Study (PA, MAP): This research was supported by NIH grants RO1-HL-087700 and RO1-HL-088215 from NHLBI.

Framingham Heart Study (AL, BP, CTL, DR, JBM, JCF, JD, JH, SR): The authors acknowledge the Framingham Heart Study participants and staff. This work was supported by NIH grants R01DK078616 (AL, BP, CTL, JBM, JCF, JD, SR) and K24DK080140 (AL, BP, SR, JBM). JCF is supported by an MGH Research Scholars Award. AL is supported by a Canadian Diabetes Association postdoctoral research fellowship

Framingham OMNI (ADJ, JDE, YF): This research was conducted in part using data and resources from the Framingham Heart Study of the National Heart Lung and Blood Institute of the National Institutes of Health and Boston University School of Medicine. This work was partially supported by the National Heart, Lung and Blood Institute's Framingham Heart Study (Contract No. N01-HC-25195). A portion of this research utilized the Linux Cluster for Genetic Analysis (LinGA-II) funded by the Robert Dawson Evans Endowment of the Department of Medicine at Boston University School of Medicine and Boston Medical Center. Genotyping of the Framingham Heart Study OMNI cohort was supported by National Heart, Lung and Blood Institute Division of Intramural Research program funds.

GeneSTAR (DMB, DV, LRY): GeneSTAR was supported by NIH grants through the National Heart, Lung, and Blood Institute (HL58625-01A1, HL59684, HL071025-01A1, U01HL72518, and HL087698) and the National Institute of Nursing Research (NR0224103) and by M01-RR000052 to the Johns Hopkins General Clinical Research Center.

GENOA (WZ, LFB, MAJ, JAS, PAP, SLRK): Support for GENOA was provided by the National Heart, Lung and Blood Institute (HL119443, HL054464, HL054457, HL054481, and HL087660) of the National Institutes of Health. Genotyping was performed at the Mayo Clinic by Stephan T. Turner, MD, Mariza de Andrade PhD, Julie Cunningham, PhD. We thank Eric Boerwinkle, PhD and Megan L. Grove from the Human Genetics Center and Institute of Molecular Medicine and Division of Epidemiology, University of Texas Health Science Center, Houston, Texas, USA for their help with genotyping. We would also like to thank the families that participated in the GENOA study.

HANDLS (ABZ, MAN, MFK, MKE, ST): This research was supported by the Intramural Research Program of the NIH, National Institute on Aging and the National Center on Minority Health and Health Disparities (project # Z01-AG000513 and human subjects protocol # 09-AG-N248). Data analyses for the HANDLS study utilized the high-performance computational capabilities of the Biowulf Linux cluster at the National Institutes of Health, Bethesda, Md. (http://biowulf.nih.gov).

Health ABC (DSE, MAN, TBH, YL): This research was supported by NIA contracts N01AG62101, N01AG62103, and N01AG62106. The genome-wide association study was funded by NIA grant 1R01AG032098- 01A1 to Wake Forest University Health Sciences, and genotyping services were provided by the Center for Inherited Disease Research (CIDR). CIDR

is fully funded through a federal contract from the National Institutes of Health to The Johns Hopkins University, contract number HHSN268200782096C. This study utilized the high-performance computational capabilities of the Biowulf Linux cluster at the National Institutes of Health, Bethesda, Md. (http://biowulf.nih.gov). This research was supported in part by the Intramural Research Program of the NIH, National Institute on Aging.

HELIUS (AHZ, CA, MBS): The HELIUS study is conducted by the Academic Medical Center Amsterdam and the Public Health Service of Amsterdam; both organisations provided core support for HELIUS. The HELIUS study is also funded by the Dutch Heart Foundation, the Netherlands Organization for Health Research and Development (ZonMw), and the European Union (FP-7).

HUFS/AADM (AA, ARB, CNR, GC): The contents of this paper are solely the responsibility of the authors and do not necessarily represent the official view of the National Institutes of Health. The study was supported by National Institutes of Health grants S06GM008016-320107 to C. Rotimi and S06GM008016-380111 to A. Adeyemo, both from the NIGMS/MBRS/SCORE Program. Participant enrollment for HUFS was carried out at the Howard University General Clinical Research Center, which is supported by grant 2M01RR010284 from the National Center for Research Resources, a component of the National Institutes of Health. This research was supported in part by the Intramural Research Program of the National Human Genome Research Institute in the Center for Research in Genomics and Global Health (CRGGH—Z01HG200362). CRGGH is also supported by National Institute of Diabetes and Digestive and Kidney Diseases (NIDDK), Center for Information Technology, and the Office of the Director at the National Institutes of Health. Support for participant recruitment and initial genetic studies of the AADM study was provided by NIH grant No. 3T37TW00041-03S2 from the Office of Research on Minority Health. Support for the Africa America Diabetes Mellitus (AADM) study is also provided by the National Institute on Minority Health and Health Disparities, NIDDK and NHGRI.

HyperGEN (DKA, MRI): HyperGEN: Genetics of Left Ventricular Hypertrophy, ancillary to the Family Blood Pressure Program, http://clinicaltrials.gov/ct/show/NCT00005267. Funding sources included National Heart, Lung, and Blood Institute grant R01 HL55673 and cooperative agreements (U01) with the National Heart, Lung, and Blood Institute: HL54471, HL54515 (UT); HL54472, HL54496

IRAS/IRASFS (AJK, CDL, JIR, JTZ, KT, LEW, MG, MPW, NDP, SSR, XG, YDIC): Computing resources for analysis of IRAS and IRASFS data were provided, in part, by the Wake Forest School of Medicine Center for Public Health Genomics. This study and investigators were supported by the following grants/contracts from the National Institutes of Health: DK081350 (Palmer), HL047887 (IRAS), HL047889 (IRAS), HL047890 (IRAS), HL47902 (IRAS), HL060944 (IRASFS), HL061019 (IRASFS), HL060919 (IRASFS).

JHS (AC, JGW, LAL, MS): The Jackson Heart Study is supported by contracts HHSN268201300046C, HHSN268201300047C, HHSN268201300048C, HHSN268201300049C, HHSN268201300050C from the National Heart, Lung, and Blood

Institute and the National Institute on Minority Health and Health Disparities. The authors thank the participants and data collection staff of the Jackson Heart Study.

MEDIA (CNR, DWB, MCYN, SL): We thank all the study participants for their valuable contributions to the parent studies (ARIC, CARDIA, CFS, CHS, FamHS, FIND, GeneSTAR, GENOA, HANDLS, Health ABC, HUFS, JHS, MESA, MESA Family, SIGNET-REGARDS, WFSM and WHI) of the discovery stage of the MEDIA consortium. We thank the contributions of investigators and staff of the parent studies for data collection, genotyping, data analysis and sharing of association results to the MEDIA consortium. The work at the coordinating center (Wake Forest) of the MEDIA consortium was supported by NIH grant R01 DK066358 (DWB).

MESA and MESA Family (JIR, JSP, JY, KT, MG, SSR, XG, YDIC): This research was supported by a research grant and contract NIDDK DK 078616 from the NIH on Common Genetic Variants and Quantitative Diabetic Traits (MAGIC). MESA, MESA Family, and the MESA SHARe project are conducted and supported by the National Heart, Lung, and Blood Institute (NHLBI) in collaboration with MESA investigators. Support is provided by grants and contracts N01-HC-95159, N01-HC-95160, N01-HC-95161, N01-HC-95162, N01-HC-95163, N01-HC-95164, N01-HC-95165, N01-HC-95166, N01-HC-95167, N01-HC-95168, N01-HC-95169 and by grants UL1-TR-000040 and UL1-RR-025005 from NCRR. Funding for MESA SHARe genotyping was provided by NHLBI Contract N02-HL-6-4278. The provision of genotyping data was supported in part by the National Center for Advancing Translational Sciences, CTSI grant UL1TR000124, and the National Institute of Diabetes and Digestive and Kidney Disease Diabetes Research Center (DRC) grant DK063491 to the Southern California Diabetes Endocrinology Research Center.

NUgene (ANK, LLA, JAP, MGH): This work was funded in part by U01HG004609 and U01HG006388 as part of the eMERGE Network. The Northwestern University Enterprise Data Warehouse was funded in part by a grant from the National Center for Research Resources, UL1RR025741.

PARC (JIR, KT, MG, MOG, RMK, XG, XL, YDIC): This research was supported by the National Institutes of Health: grant U19HL069757 from the National Heart, Lung, and Blood Institute; grants R01DK79888 and P30DK063491 from the National Institute of Diabetes and Digestive and Kidney Diseases; and grant UL1TR000124 from the National Center for Advancing Translational Sciences.

REGARDS (MC, WMC): The authors thank the other investigators, the staff, and the participants of the REGARDS study for their valuable contributions. A full list of participating REGARDS investigators and institutions can be found at http://www.regardsstudy.org. This study was supported by a cooperative agreement U01 NS041588 from the National Institute of Neurological Disorders and Stroke (NINDS).

SIGNET (MC, MS, WMC): The Sea Islands Genetics Network (SIGNET) was supported by R01 DK084350 (MM Sale), and consists of data from the REasons for Geographic And Racial Differences in Stroke (REGARDS) cohort, (U01 NS041588; G Howard), Project SuGAR (Sea

Islands Genetic African American Registry) (W.M. Keck Foundation; WT Garvey), a South Carolina Center of Biomedical Research Excellence (COBRE) in Oral Health Project P20 RR017696 (PI: Kirkwood; Sub-award: JK Fernandes), and the Systemic Lupus Erythematosus in Gullah Health (SLEIGH) study (PI: GS Gilkeson; K23 AR052364, DL Kamen; UL1 RR029882, KT Brady), DK084350.

Tobago Health Study (ALP, IM, JMZ): Tobago Health Study was supported, in part, by funding or in-kind services from the Division of Health and Social Services and Tobago House of Assembly, and by grants from the National Institute of Arthritis and Musculoskeletal and Skin Diseases (R01AR049747) and the National Institute of Diabetes and Digestive and Kidney Diseases (K01-DK083029 and R01-DK097084).

Vanderbilt University BioVU and eMERGE (DCC, EKK, SCS, TLE): The dataset used in the analyses described were obtained from Vanderbilt University Medical Center's BioVU which is supported by institutional funding and by the Vanderbilt CTSA grant ULTR000445 from NCATS/NIH. Genome-wide genotyping was funded by NIH grants RC2GM092618 from NIGMS/OD and U01HG004603 from NHGRI/NIGMS. The eMERGE Network was initiated and funded by NHGRI through the following grants: U01HG006378 (Vanderbilt University); and U01HG006385 (Vanderbilt University serving as the Coordinating Center). TLE was also supported by 5R21HL121429.

WHI (JL): We thank the WHI investigators, staff, and study participants for their outstanding dedication and commitment.

Miscellaneous (APM): Andrew P Morris is a Wellcome Trust Senior Fellow in Basic Biomedical Science under award WT098017

Conflict of Interest and Disclaimer

Conflicts of Interest

BMP serves on the DSMB of a clinical trial for the device manufacturer Zoll LifeCor and on the Steering Committee for the Yale Open Data Access Project funded by Johnson & Johnson. DV is a consultant for Consumable Science, Inc. JRK holds the ownership of stock in Pfizer, Inc, and Gilead Sciences, Inc.

Disclaimer

The views expressed in this manuscript are those of the authors and do not necessarily represent the views of the National Heart, Lung, and Blood Institute; the National Institutes of Health; or the U.S. Department of Health and Human Services.

Supplemental Figures

Table of Contents for Supplemental Figures and Legends

Figure S4X. *FOXA2* locus
Figure S4Y. *CRY2* locus
Figure S4Z. *DPYSL5* locus
Figure S4AA. *IGF2BP2* locus
Figure S4BB. *KL* locus

FI loci

Figure 4SX. *ARL15* locus
Figure 4SY. *COBLL1-GRB14* locus
Figure 4SZ. *IRS1* locus
Figure 4SAA. *UHRF1BP1* locus
Figure 4SBB. *FAM13A* locus
Figure 4SCC. *PPARG* locus
Figure 4SDD. *GCKR* locus
Figure 4SEE. *PPP1R3B* locus
Figure 4SFF. *ANKRD55-MAP3K1* locus

Figure S5 Concordance of effect size and Comparison of EA trait-raising allele Frequency in EA and AA

Figures S5A Effect size comparison for EA FG SNPs
Figures S5B Effect size comparison for EA FI SNPs
Figures S5C Allele frequency comparison for EA FG SNPs
Figures S5D Allele frequency comparison for EA FI SNPs

Figure S6 Genome-wide association plots and quantile-quantile (QQ) plots for FG and FI

Figures S6A Miami plots of association with FG
Figures S6B the QQ plots for FG
Figures S6C Miami plots of association with FI
Figures S6D the QQ plots for FI
Figures S6E genome-wide association plots of trans-ethnic meta-analysis results for FG
Figures S6F genome-wide association plots of trans-ethnic meta-analysis results for FI

Figure S7 Conditional analysis at *PELO*/rs6450057

Figures S7A the comparison for unconditional association results with HapMap 2 CEU LD information
Figures S7B the comparison for conditional association results with HapMap 2 CEU LD information
Figures S7C the comparison for unconditional association results with HapMap 2 YRI LD information
Figures S7D the comparison for conditional association results with HapMap 2 YRI LD information

Supplemental Figure Legends

Figure S1.

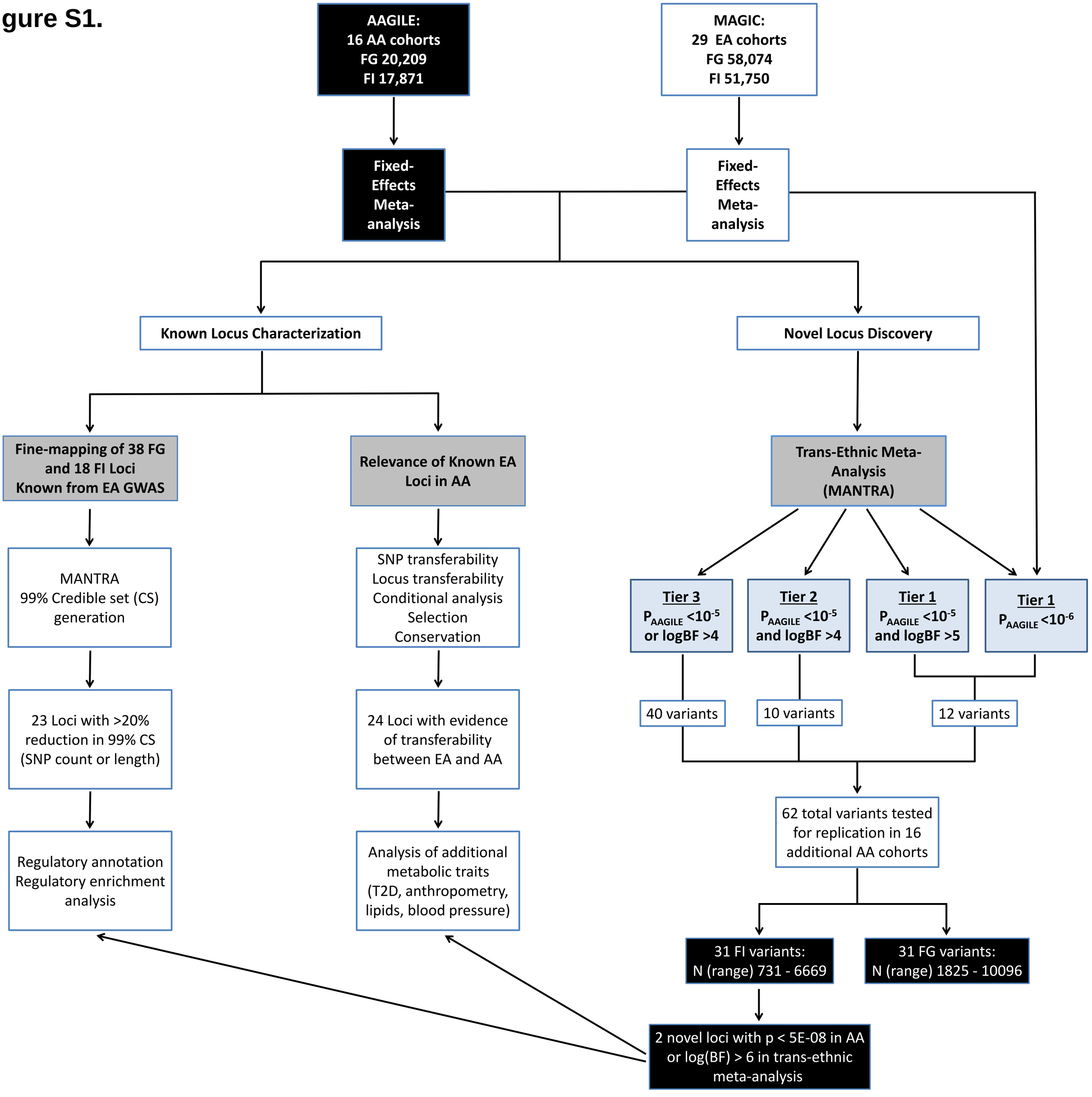
AAGILE:
16 AA cohorts
FG 20,209
FI 17,871
MAGIC:
29 EA cohorts
FG 58,074
FI 51,750
Fixed-Effects Meta-analysis
Fixed-Effects Meta-analysis
Known Locus Characterization
Novel Locus Discovery
Fine-mapping of 38 FG and 18 FI Loci Known from EA GWAS
Relevance of Known EA Loci in AA
Trans-Ethnic Meta-Analysis (MANTRA)
MANTRA
99% Credible set (CS) generation
SNP transferability
Locus transferability
Conditional analysis
Selection
Conservation
Tier 3
P_AAGILE <10^-5 or logBF >4
Tier 2
P_AAGILE <10^-5 and logBF >4
Tier 1
P_AAGILE <10^-5 and logBF >5
Tier 1
P_AAGILE <10^-6
23 Loci with >20% reduction in 99% CS (SNP count or length)
24 Loci with evidence of transferability between EA and AA
40 variants
10 variants
12 variants
Regulatory annotation
Regulatory enrichment analysis
Analysis of additional metabolic traits (T2D, anthropometry, lipids, blood pressure)
62 total variants tested for replication in 16 additional AA cohorts
31 FI variants:
N (range) 731 - 6669
31 FG variants:
N (range) 1825 - 10096
2 novel loci with p < 5E-08 in AA or log(BF) > 6 in trans-ethnic meta-analysis

Figure S2.

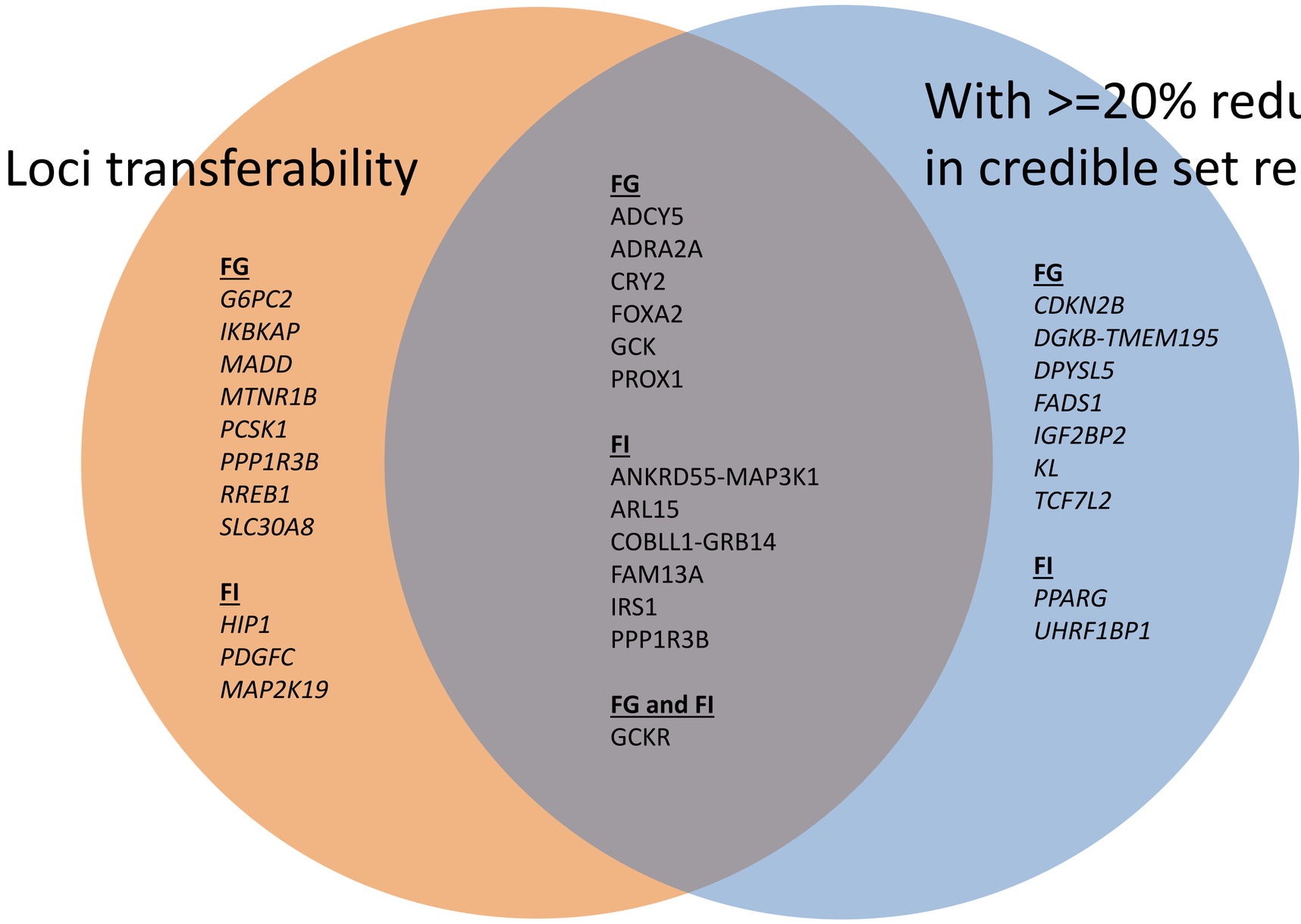
Loci transferability
With >=20% reduction in credible set reduction
FG
G6PC2
IKBKAP
MADD
MTNR1B
PCSK1
PPP1R3B
RREB1
SLC30A8
FI
HIP1
PDGFC
MAP2K19
FG
ADCY5
ADRA2A
CRY2
FOXA2
GCK
PROX1
FI
ANKRD55-MAP3K1
ARL15
COBLL1-GRB14
FAM13A
IRS1
PPP1R3B
FG and FI
GCKR
FG
CDKN2B
DGKB-TMEM195
DPYSL5
FADS1
IGF2BP2
KL
TCF7L2
FI
PPARG
UHRF1BP1

Figure S3A

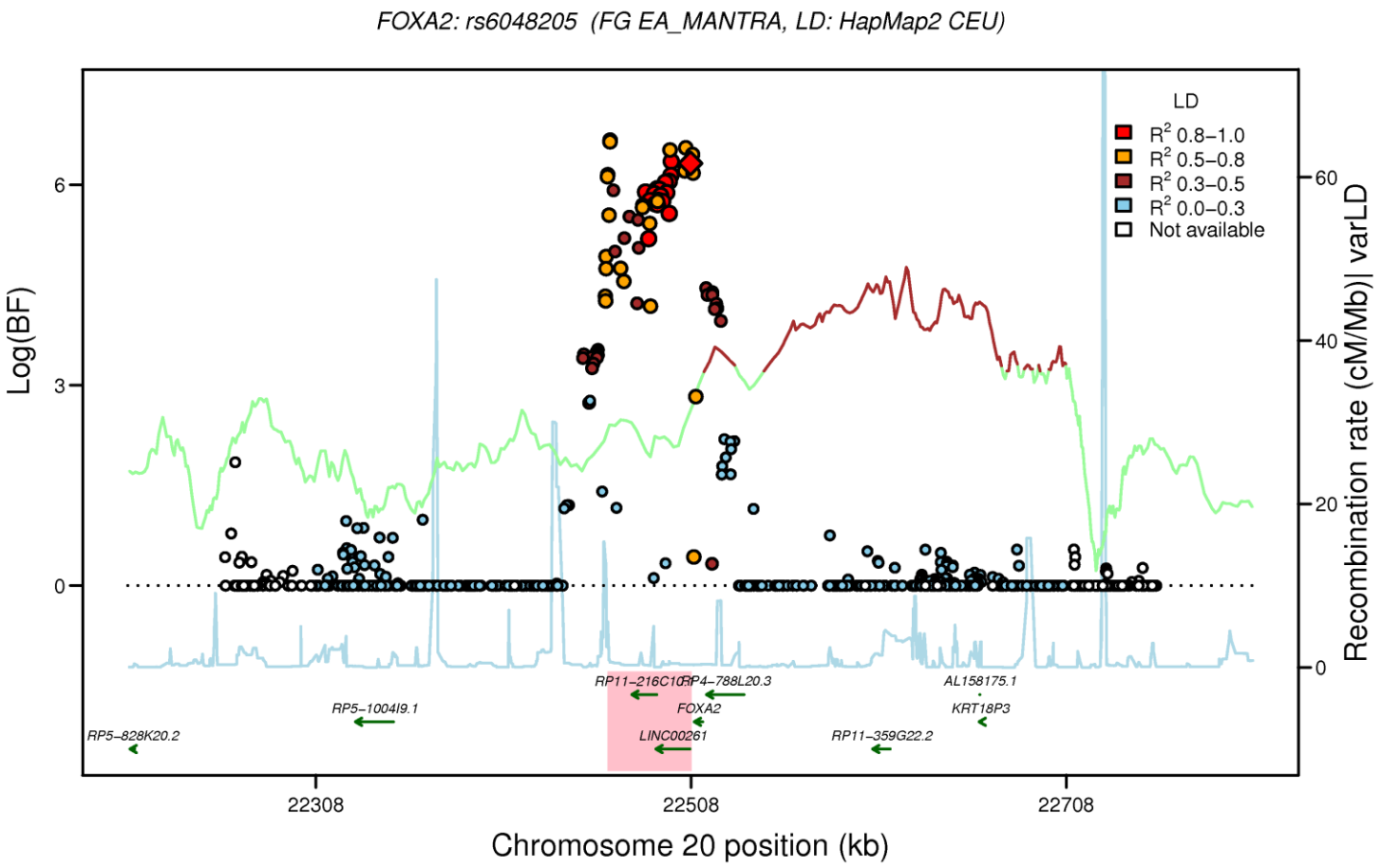
FOXA2: rs6048205 (FG EA_MANTRA, LD: HapMap2 CEU)
LD
R2 0.8–1.0
R2 0.5–0.8
R2 0.3–0.5
R2 0.0–0.3
Not available
Log(BF)
Recombination rate (cM/Mb)| varLD
RP11–216C10.3
RP4–788L20.3
AL158175.1
RP5–1004I9.1
FOXA2
KRT18P3
RP5–828K20.2
LINC00261
RP11–359G22.2
Chromosome 20 position (kb)

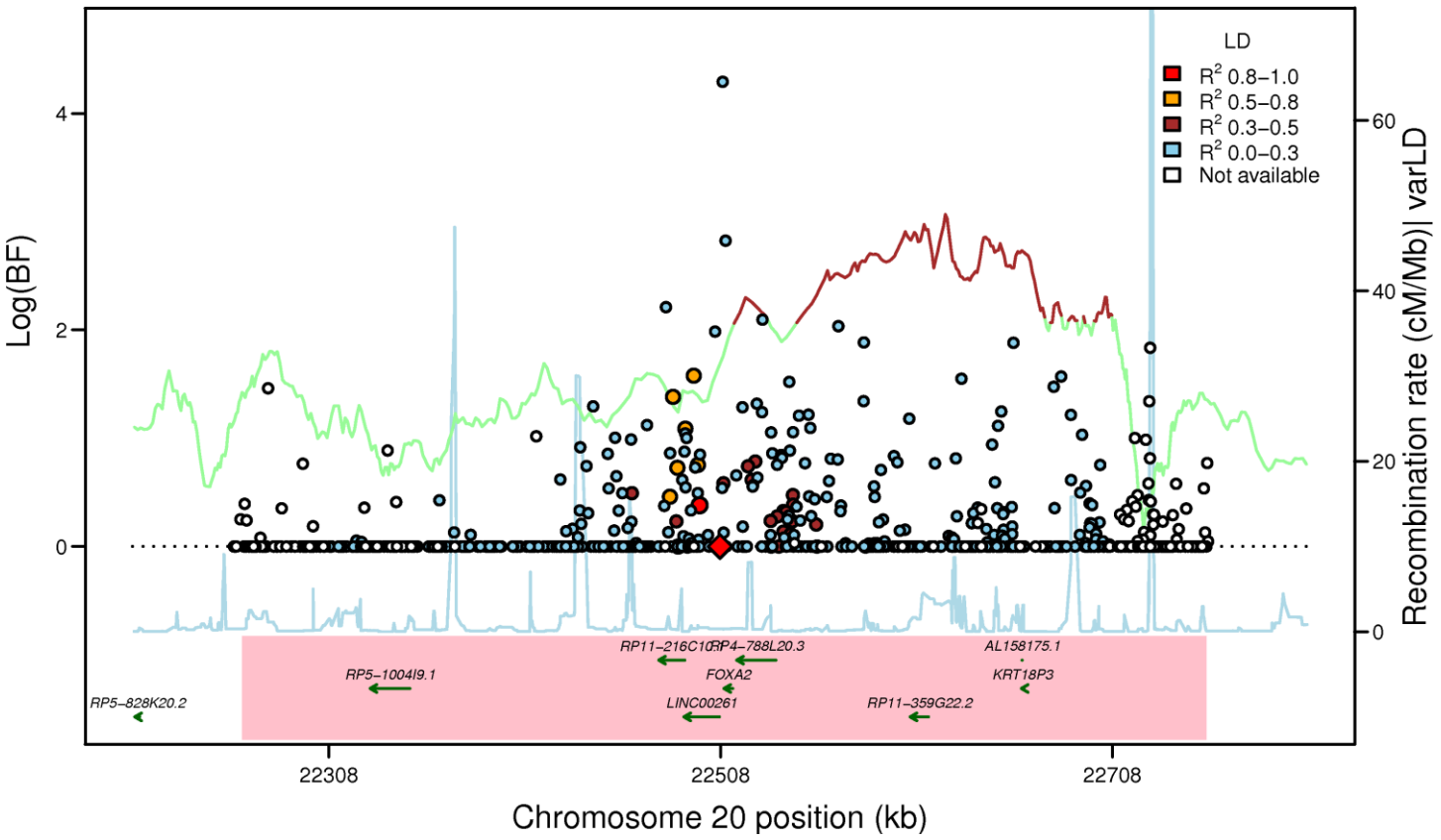
FOXA2: rs6048205 (FG AA_MANTRA, LD: HapMap2 YRI)
LD
R2 0.8–1.0
R2 0.5–0.8
R2 0.3–0.5
R2 0.0–0.3
Not available
Log(BF)
Recombination rate (cM/Mb)| varLD
RP11–216C10.3
RP4–788L20.3
AL158175.1
RP5–1004I9.1
FOXA2
KRT18P3
RP5–828K20.2
LINC00261
RP11–359G22.2
Chromosome 20 position (kb)

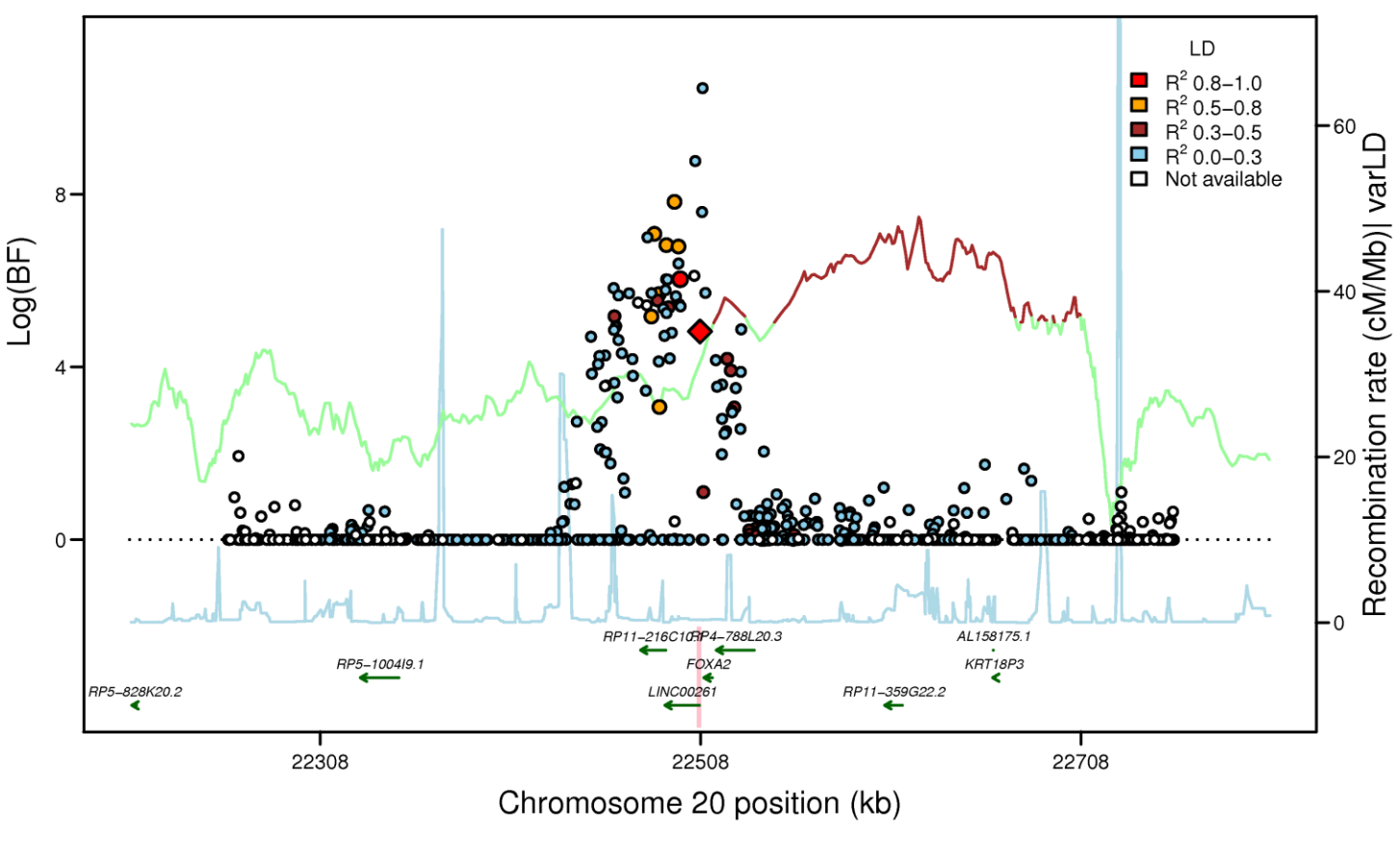
FOXA2: rs6048205 (FG TE_MANTRA, LD: HapMap2 YRI)
LD
R2 0.8–1.0
R2 0.5–0.8
R2 0.3–0.5
R2 0.0–0.3
Not available
Log(BF)
Recombination rate (cM/Mb)| varLD
RP11–216C10.3
RP4–788L20.3
AL158175.1
RP5–1004I9.1
FOXA2
KRT18P3
RP5–828K20.2
LINC00261
RP11–359G22.2
Chromosome 20 position (kb)

Figure S3B

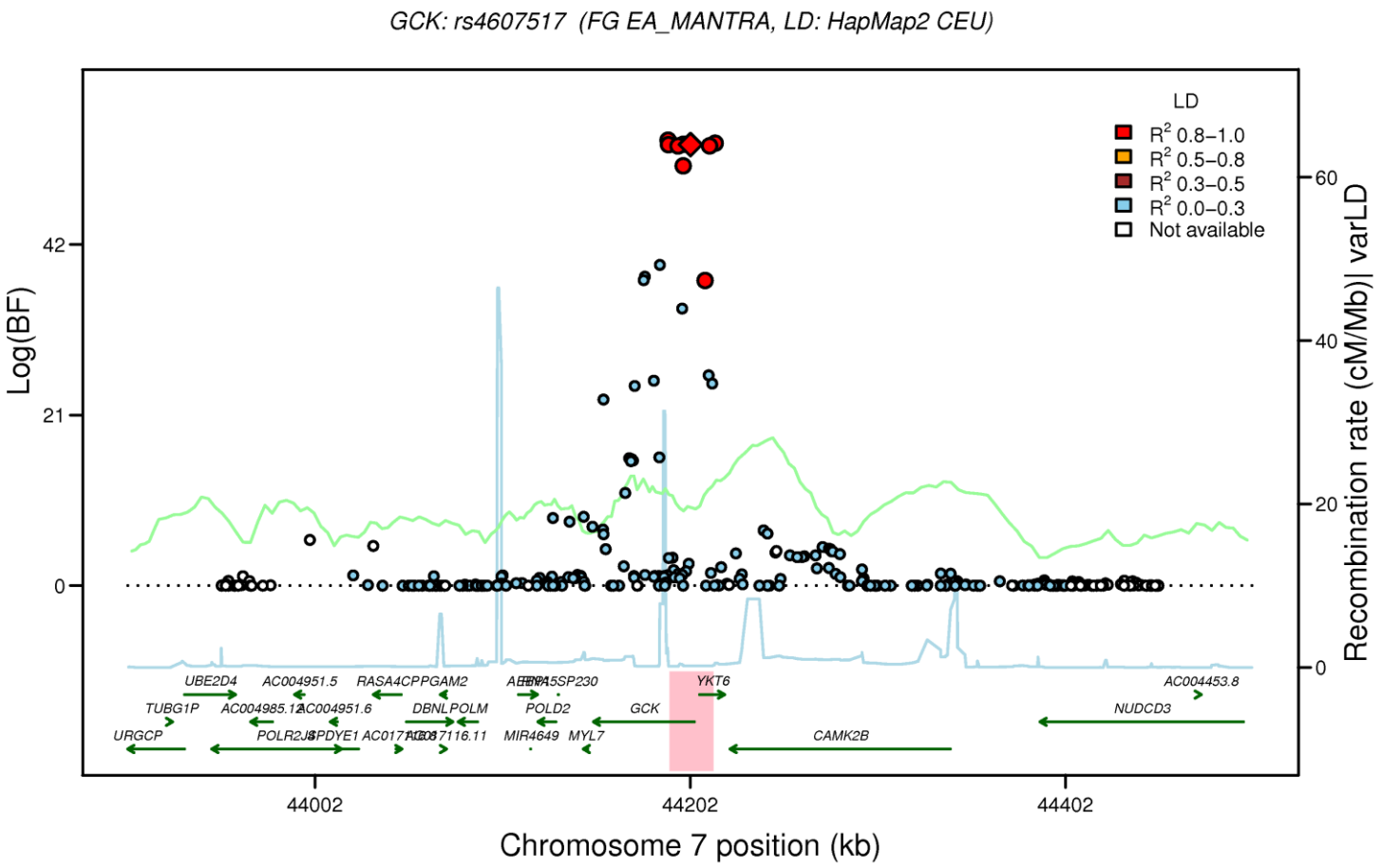
GCK: rs4607517 (FG EA_MANTRA, LD: HapMap2 CEU)
LD
R2 0.8–1.0
R2 0.5–0.8
R2 0.3–0.5
R2 0.0–0.3
Not available
Log(BF)
42
21
0
Recombination rate (cM/Mb)| varLD
60
40
20
0
UBE2D4
AC004951.5
RASA4CP
PGAM2
YKT6
AC004453.8
TUBG1P
AC004985.12
AC004951.6
DBNL
POLM
POLD2
GCK
NUDCD3
URGCP
POLR2J3
SPDYE1
MIR4649
MYL7
CAMK2B
44002
44202
44402
Chromosome 7 position (kb)

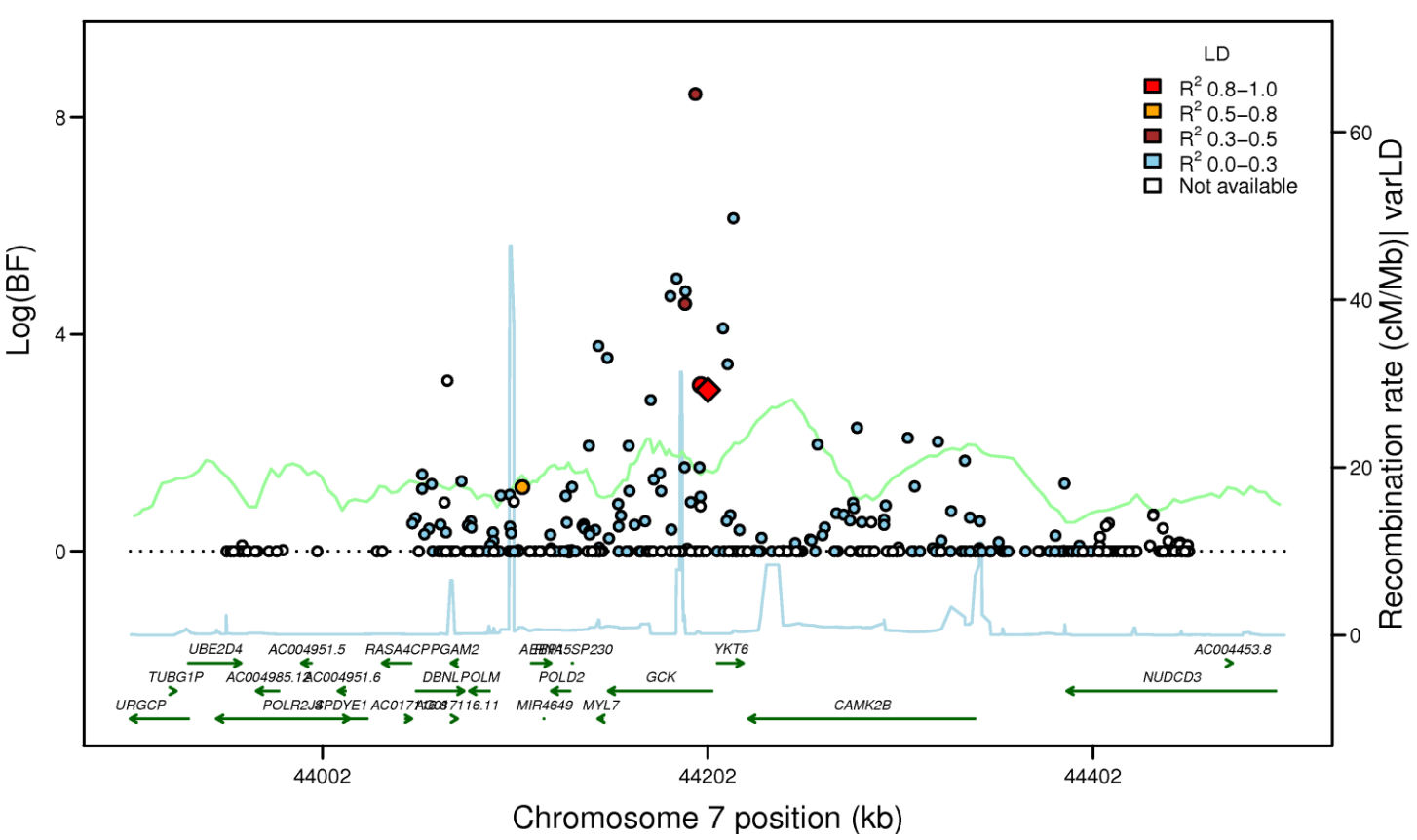
GCK: rs4607517 (FG AA_MANTRA, LD: HapMap2 YRI)
LD
R2 0.8–1.0
R2 0.5–0.8
R2 0.3–0.5
R2 0.0–0.3
Not available
Log(BF)
8
4
0
Recombination rate (cM/Mb)| varLD
60
40
20
0
UBE2D4
AC004951.5
RASA4CP
PGAM2
YKT6
AC004453.8
TUBG1P
AC004985.12
AC004951.6
DBNL
POLM
POLD2
GCK
NUDCD3
URGCP
POLR2J3
SPDYE1
MIR4649
MYL7
CAMK2B
44002
44202
44402
Chromosome 7 position (kb)

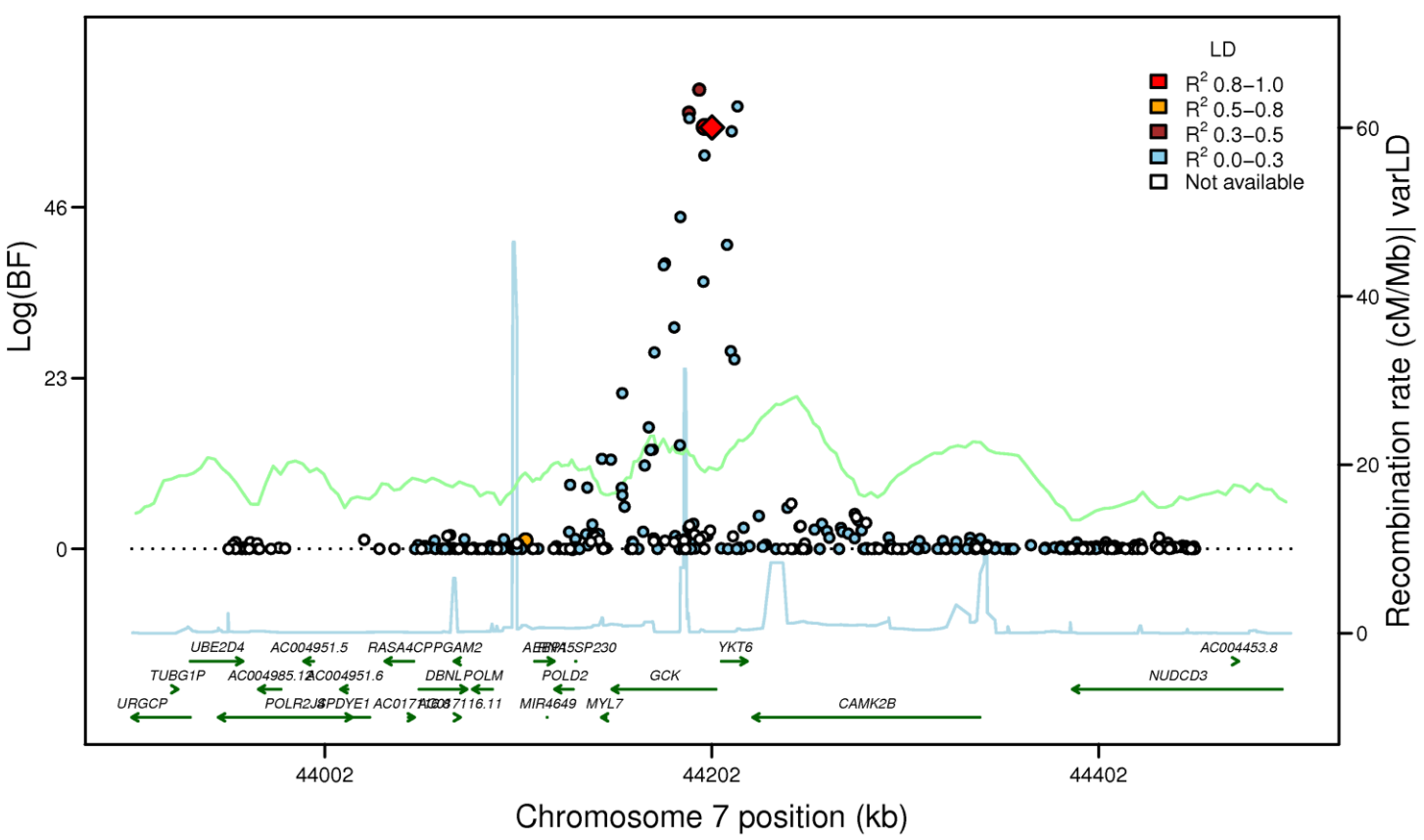
GCK: rs4607517 (FG TE_MANTRA, LD: HapMap2 YRI)
LD
R2 0.8–1.0
R2 0.5–0.8
R2 0.3–0.5
R2 0.0–0.3
Not available
Log(BF)
46
23
0
Recombination rate (cM/Mb)| varLD
60
40
20
0
UBE2D4
AC004951.5
RASA4CP
PGAM2
YKT6
AC004453.8
TUBG1P
AC004985.12
AC004951.6
DBNL
POLM
POLD2
GCK
NUDCD3
URGCP
POLR2J3
SPDYE1
MIR4649
MYL7
CAMK2B
44002
44202
44402
Chromosome 7 position (kb)

Figure S3C

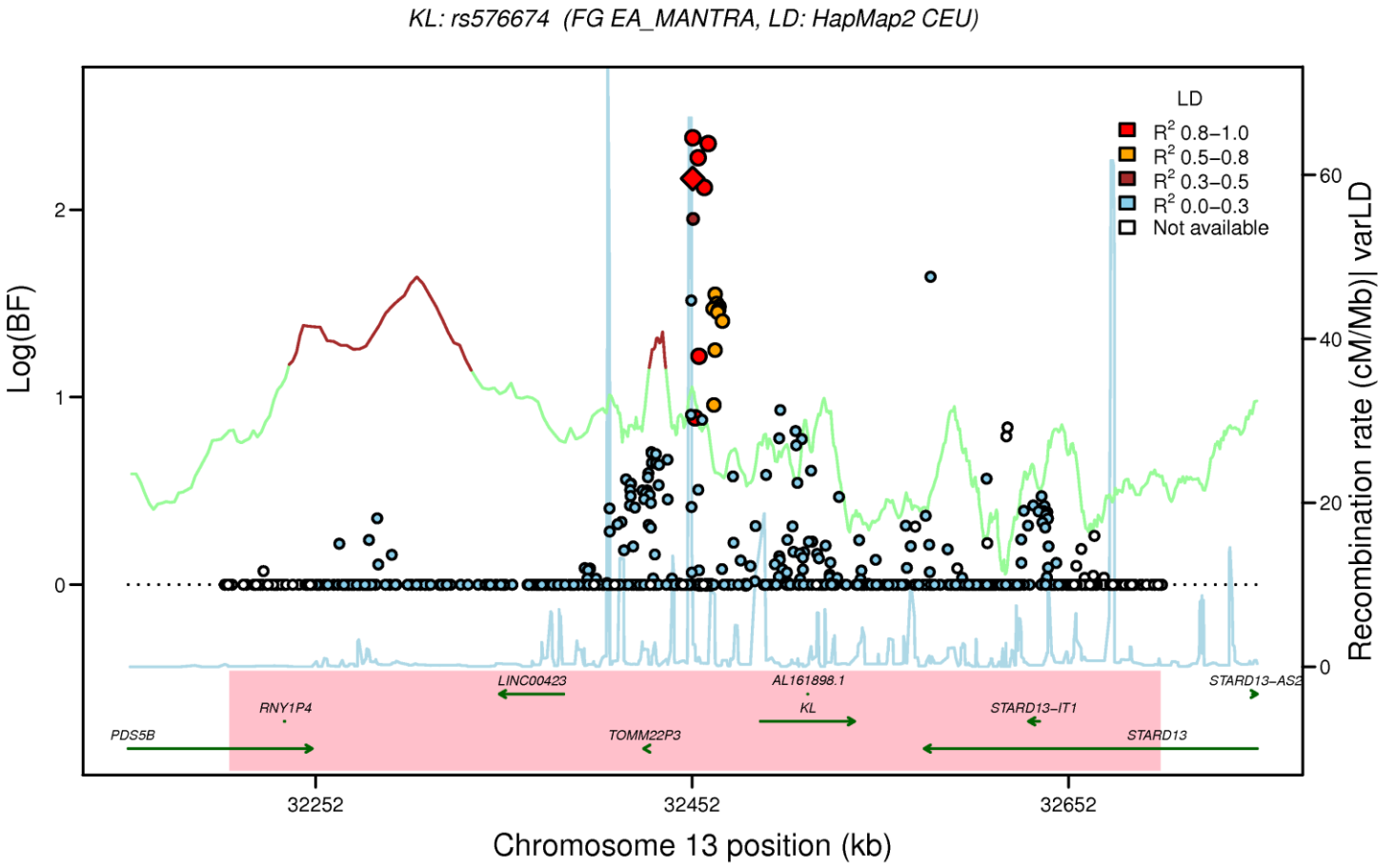
KL: rs576674 (FG EA_MANTRA, LD: HapMap2 CEU)
LD
R2 0.8–1.0
R2 0.5–0.8
R2 0.3–0.5
R2 0.0–0.3
Not available
Log(BF)
Recombination rate (cM/Mb)| varLD
LINC00423
AL161898.1
STARD13–AS2
RNY1P4
KL
STARD13–IT1
PDS5B
TOMM22P3
STARD13
32252
32452
32652
Chromosome 13 position (kb)

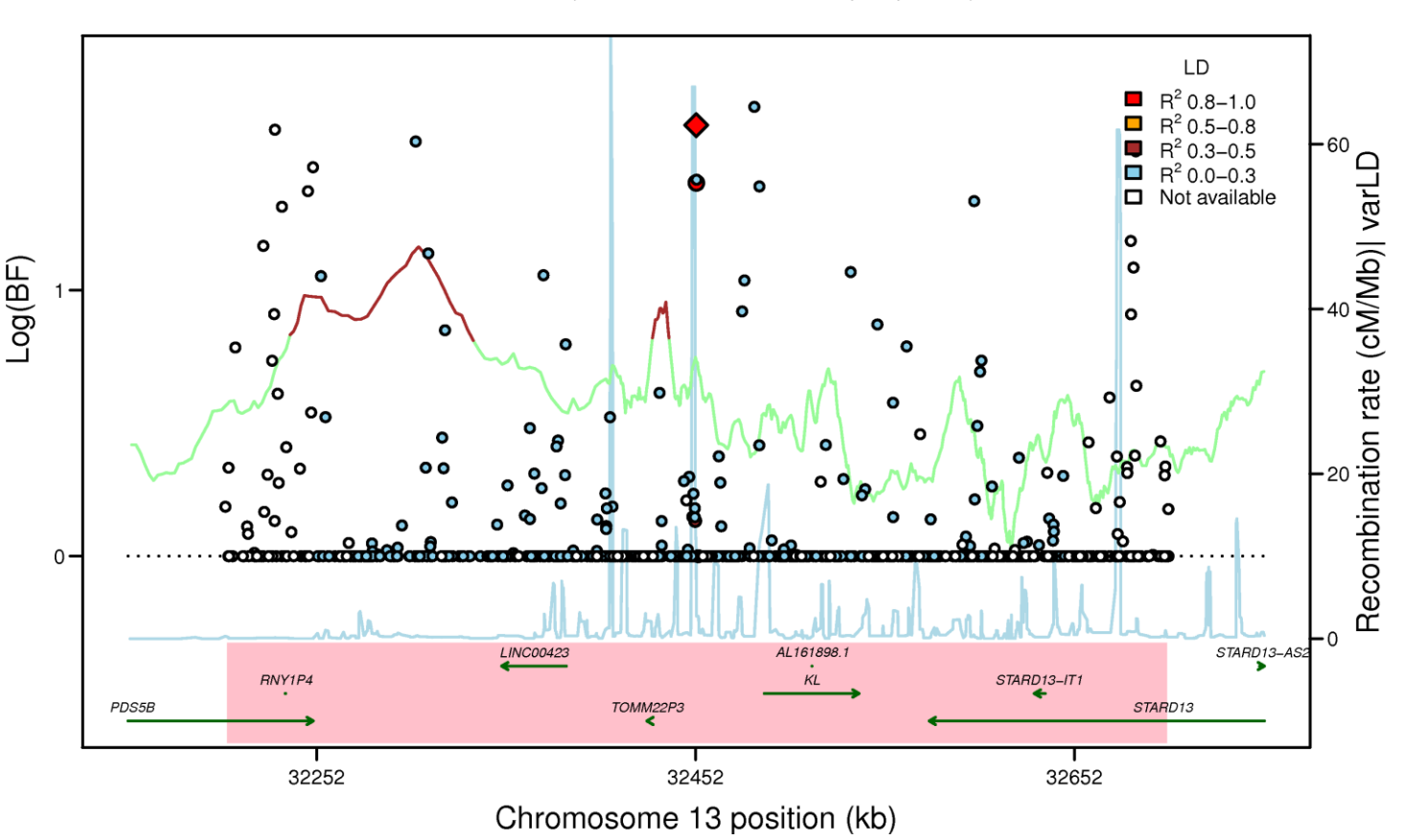
KL: rs576674 (FG AA_MANTRA, LD: HapMap2 YRI)
LD
R2 0.8–1.0
R2 0.5–0.8
R2 0.3–0.5
R2 0.0–0.3
Not available
Log(BF)
Recombination rate (cM/Mb)| varLD
LINC00423
AL161898.1
STARD13–AS2
RNY1P4
KL
STARD13–IT1
PDS5B
TOMM22P3
STARD13
32252
32452
32652
Chromosome 13 position (kb)

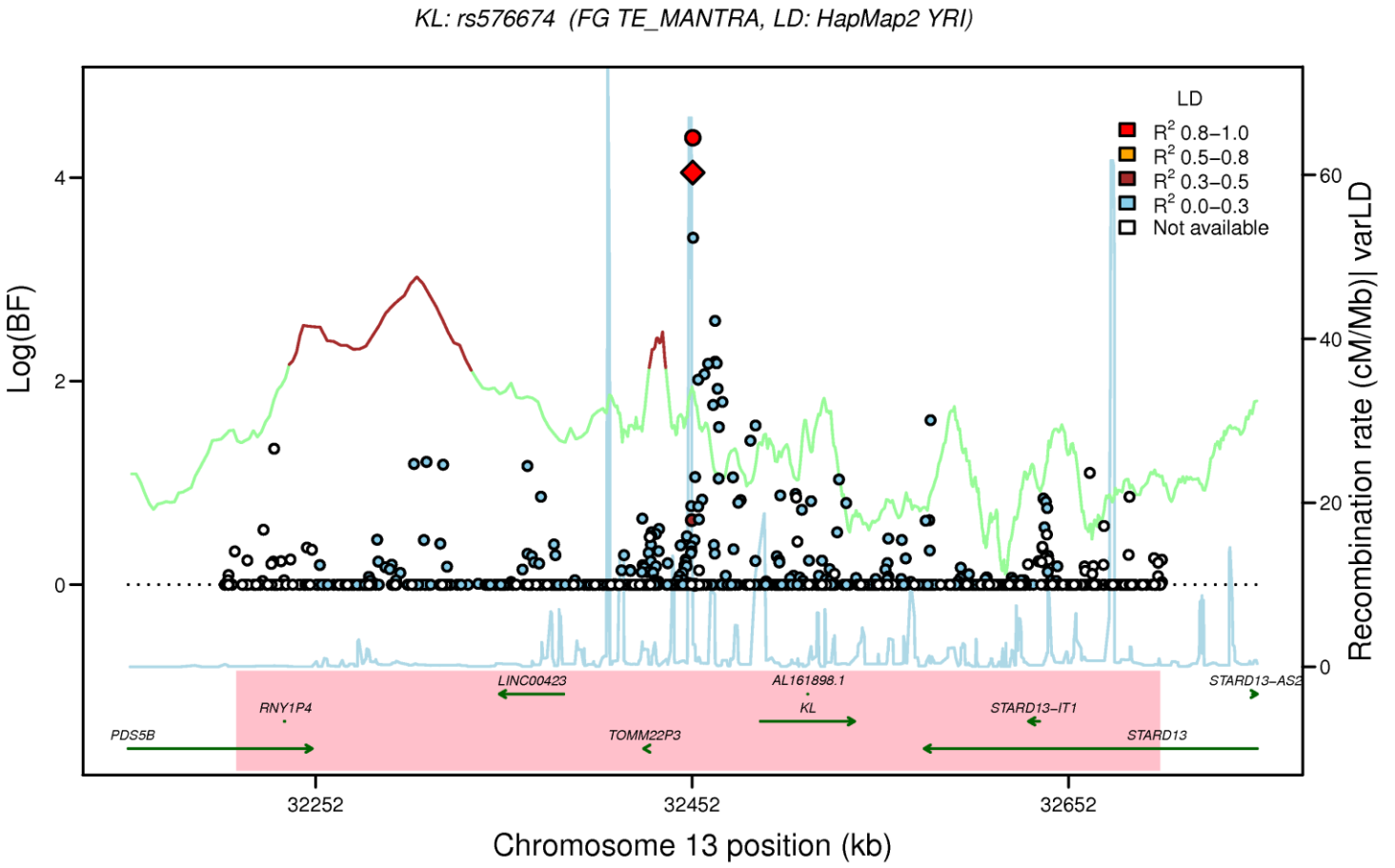
KL: rs576674 (FG TE_MANTRA, LD: HapMap2 YRI)
LD
R2 0.8–1.0
R2 0.5–0.8
R2 0.3–0.5
R2 0.0–0.3
Not available
Log(BF)
Recombination rate (cM/Mb)| varLD
LINC00423
AL161898.1
STARD13–AS2
RNY1P4
KL
STARD13–IT1
PDS5B
TOMM22P3
STARD13
32252
32452
32652
Chromosome 13 position (kb)

Figure S3D

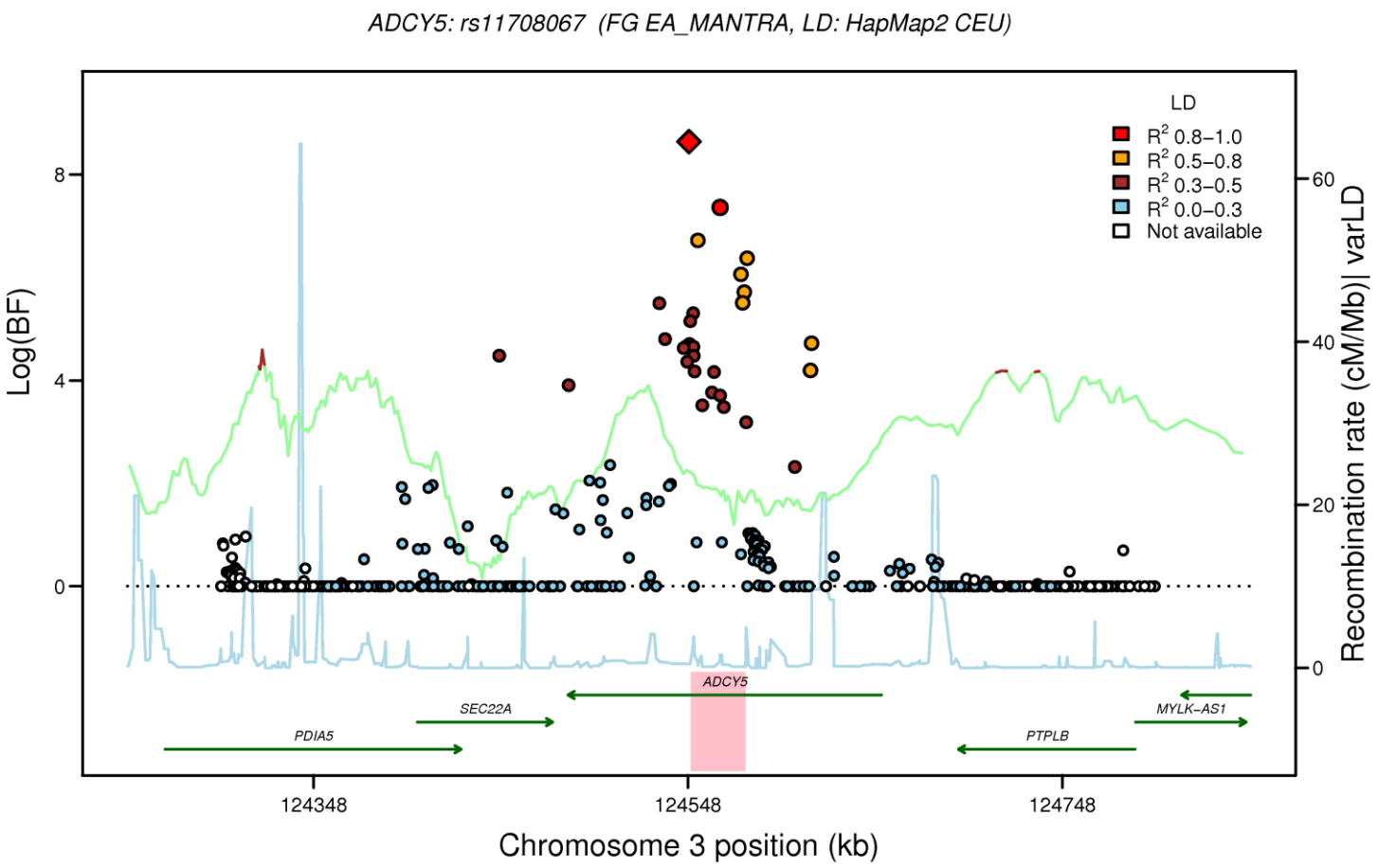
ADCY5: rs11708067 (FG EA_MANTRA, LD: HapMap2 CEU)
LD
R2 0.8–1.0
R2 0.5–0.8
R2 0.3–0.5
R2 0.0–0.3
Not available
Log(BF)
Recombination rate (cM/Mb)| varLD
ADCY5
SEC22A
PDIA5
PTPLB
MYLK–AS1
124348
124548
124748
Chromosome 3 position (kb)

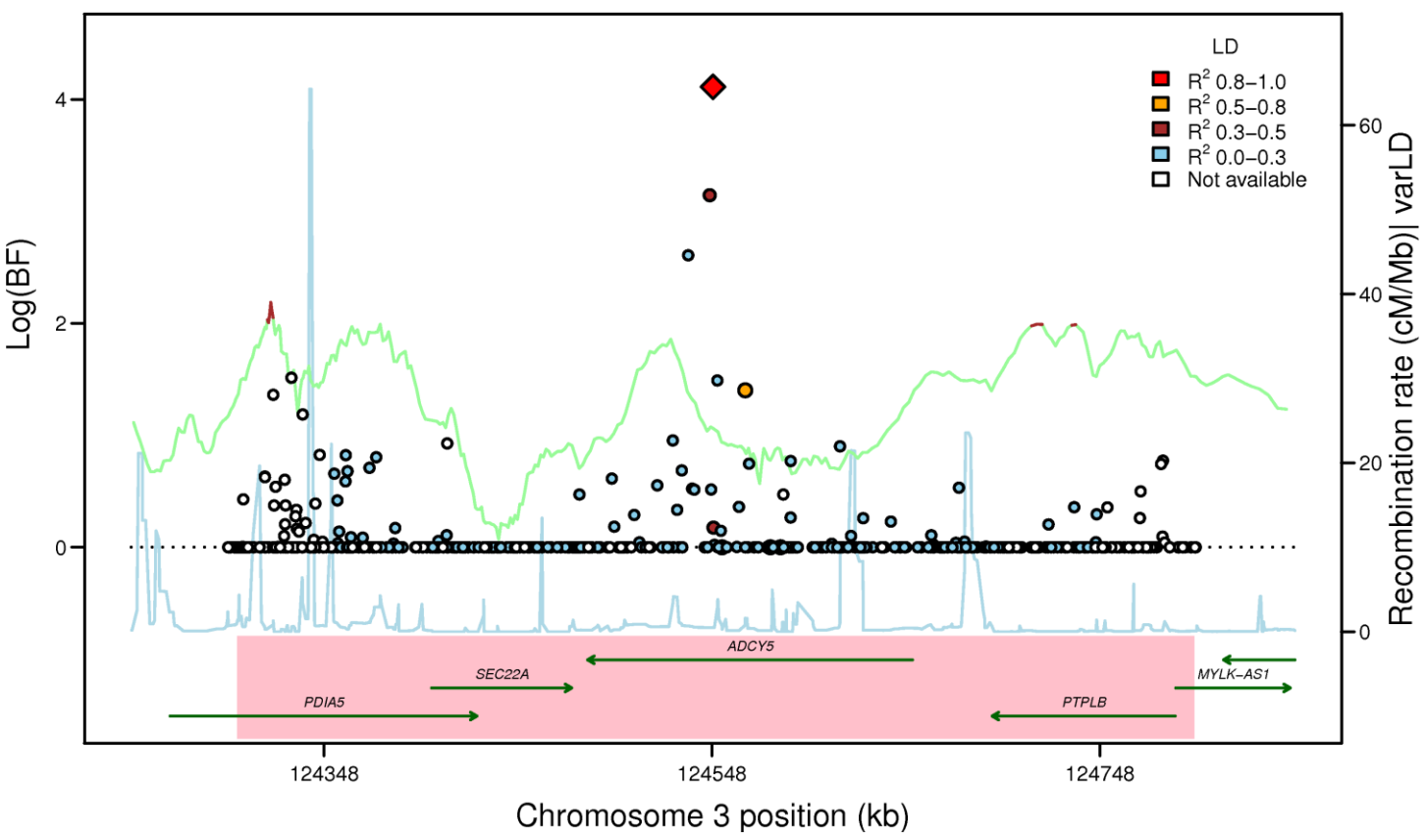
ADCY5: rs11708067 (FG AA_MANTRA, LD: HapMap2 YRI)
LD
R2 0.8–1.0
R2 0.5–0.8
R2 0.3–0.5
R2 0.0–0.3
Not available
Log(BF)
Recombination rate (cM/Mb)| varLD
ADCY5
SEC22A
PDIA5
PTPLB
MYLK–AS1
124348
124548
124748
Chromosome 3 position (kb)

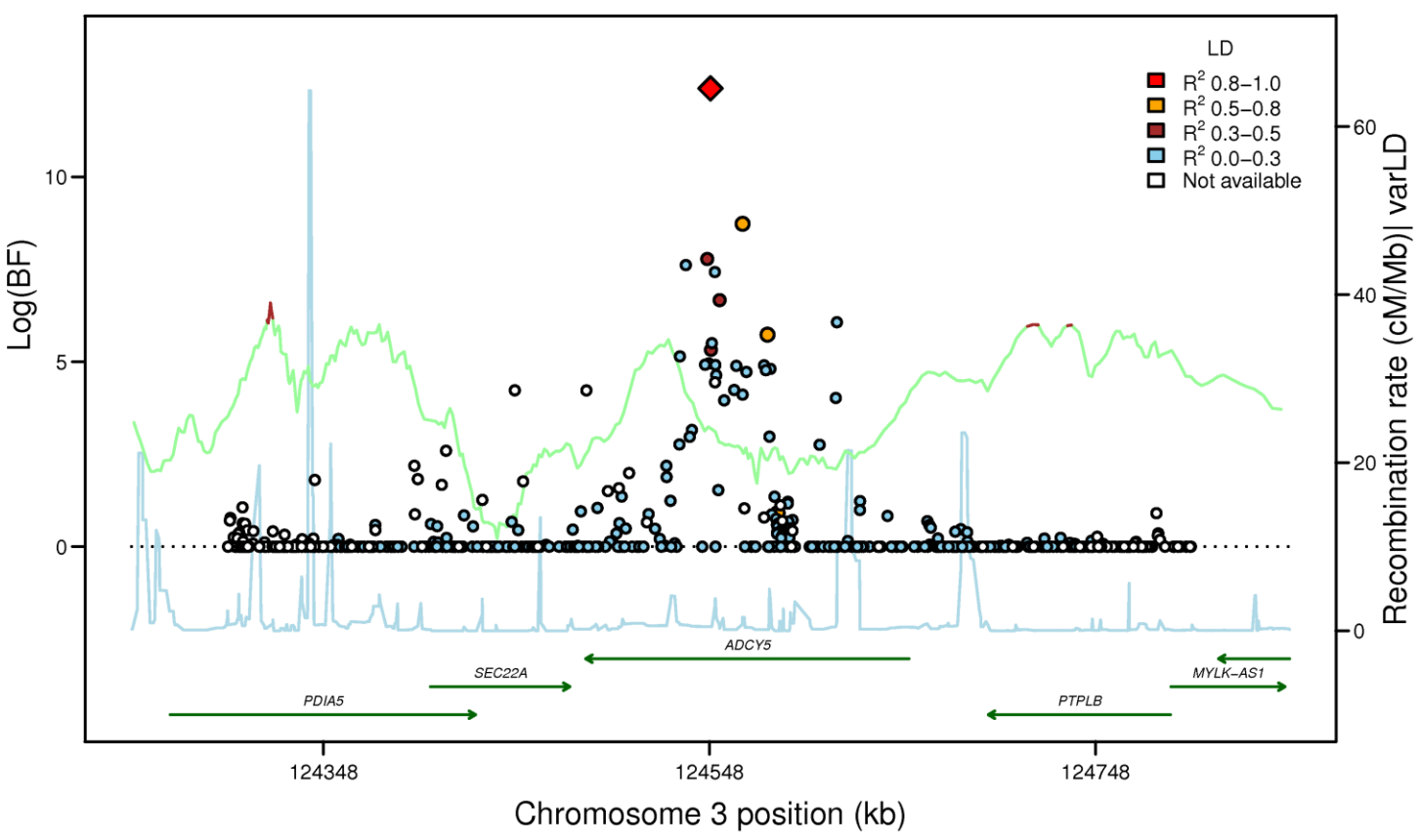
ADCY5: rs11708067 (FG TE_MANTRA, LD: HapMap2 YRI)
LD
R2 0.8–1.0
R2 0.5–0.8
R2 0.3–0.5
R2 0.0–0.3
Not available
Log(BF)
Recombination rate (cM/Mb)| varLD
ADCY5
SEC22A
PDIA5
PTPLB
MYLK–AS1
124348
124548
124748
Chromosome 3 position (kb)

Figure S3E

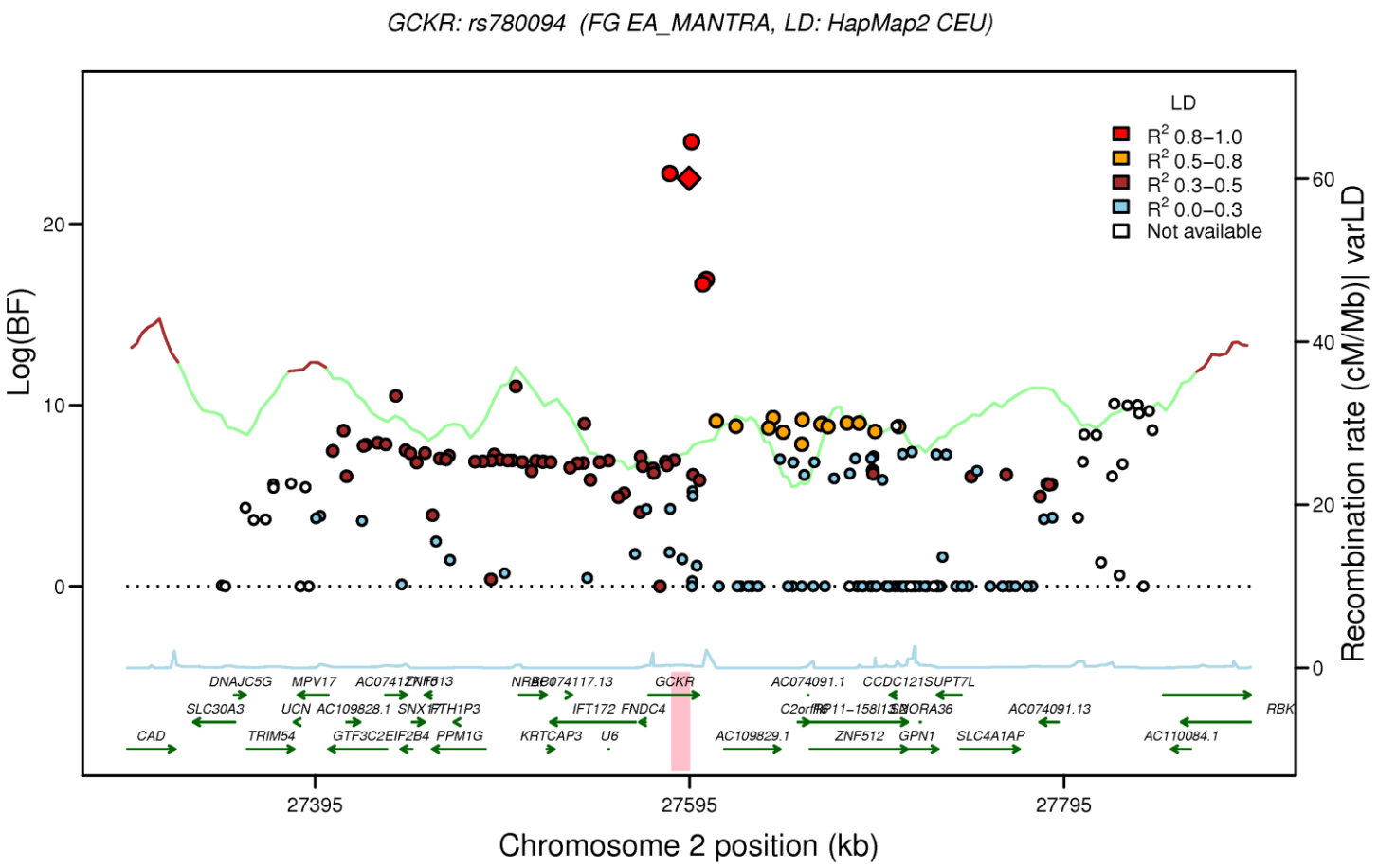
GCKR: rs780094 (FG EA_MANTRA, LD: HapMap2 CEU)
LD
R2 0.8–1.0
R2 0.5–0.8
R2 0.3–0.5
R2 0.0–0.3
Not available
Log(BF)
Recombination rate (cM/Mb)| varLD
Chromosome 2 position (kb)
27395
27595
27795
DNAJC5G MPV17 AC074117.13 GCKR AC074091.1 CCDC121SUPT7L
SLC30A3 UCN AC109828.1 IFT172 FNDC4 AC074091.13
CAD TRIM54 GTF3C2EIF2B4 PPM1G KRTCAP3 U6 AC109829.1 ZNF512 GPN1 SLC4A1AP AC110084.1

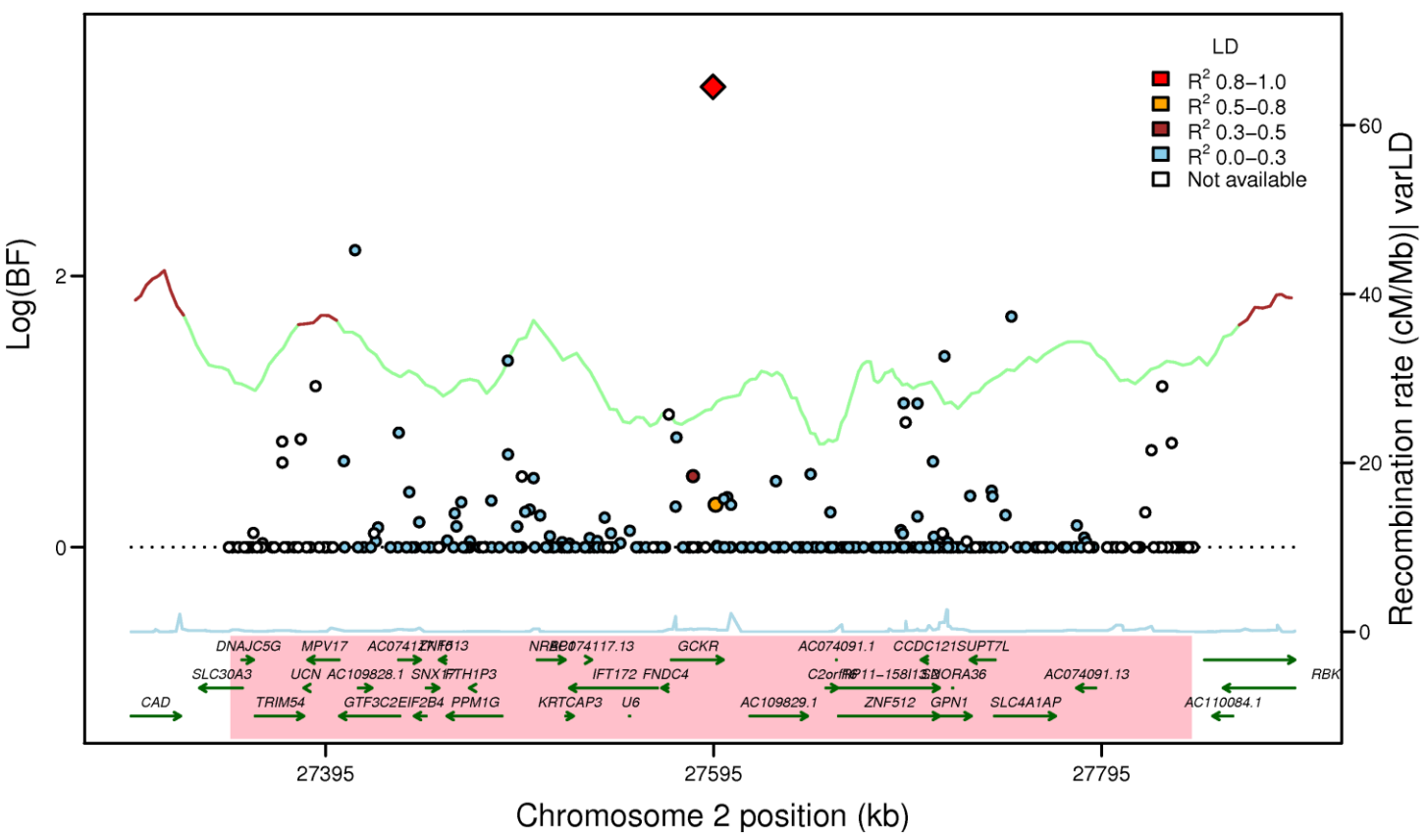
GCKR: rs780094 (FG AA_MANTRA, LD: HapMap2 YRI)
LD
R2 0.8–1.0
R2 0.5–0.8
R2 0.3–0.5
R2 0.0–0.3
Not available
Log(BF)
Recombination rate (cM/Mb)| varLD
Chromosome 2 position (kb)
27395
27595
27795
DNAJC5G MPV17 AC074117.13 GCKR AC074091.1 CCDC121SUPT7L
SLC30A3 UCN AC109828.1 IFT172 FNDC4 AC074091.13
CAD TRIM54 GTF3C2EIF2B4 PPM1G KRTCAP3 U6 AC109829.1 ZNF512 GPN1 SLC4A1AP AC110084.1

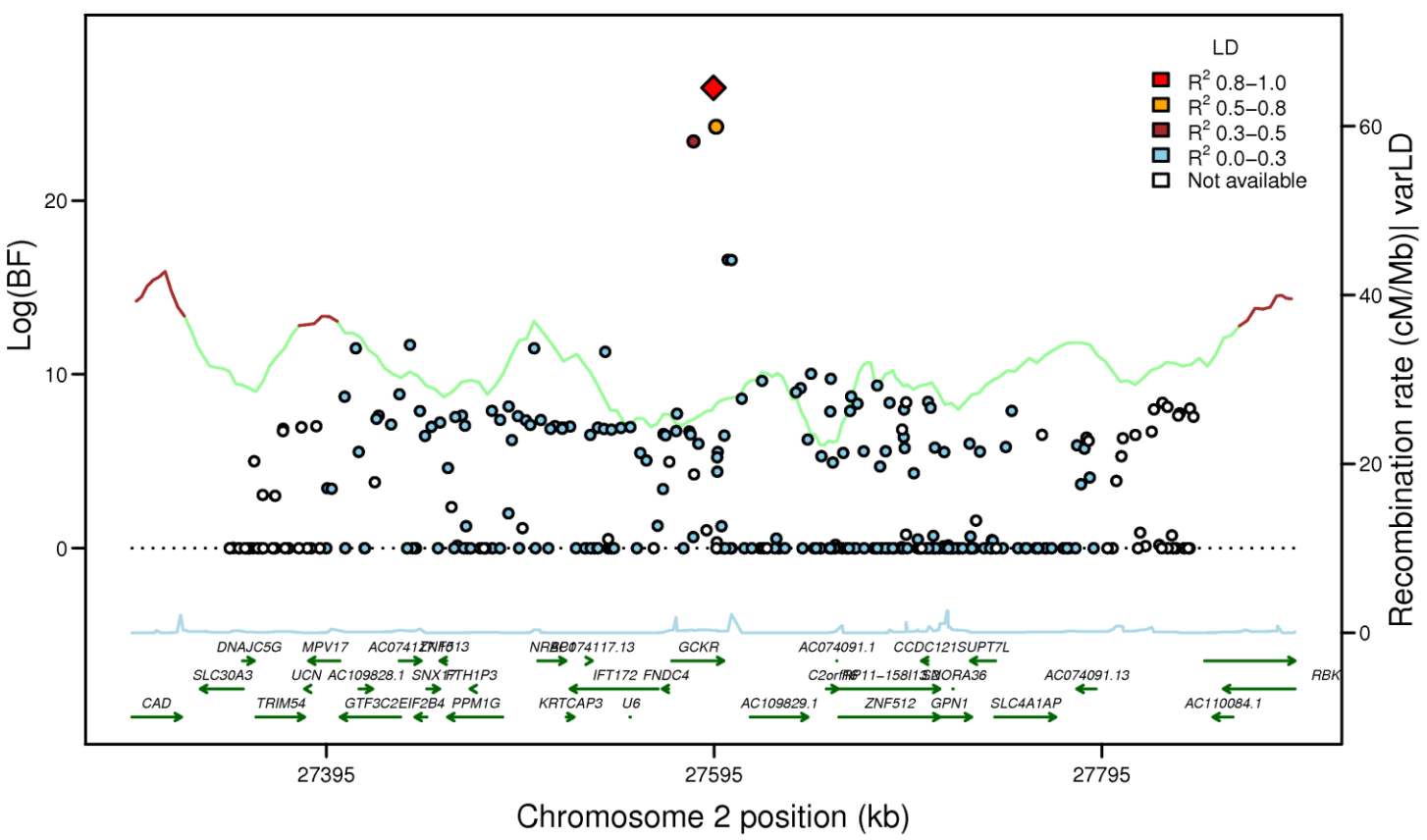
GCKR: rs780094 (FG TE_MANTRA, LD: HapMap2 YRI)
LD
R2 0.8–1.0
R2 0.5–0.8
R2 0.3–0.5
R2 0.0–0.3
Not available
Log(BF)
Recombination rate (cM/Mb)| varLD
Chromosome 2 position (kb)
27395
27595
27795
DNAJC5G MPV17 AC074117.13 GCKR AC074091.1 CCDC121SUPT7L
SLC30A3 UCN AC109828.1 IFT172 FNDC4 AC074091.13
CAD TRIM54 GTF3C2EIF2B4 PPM1G KRTCAP3 U6 AC109829.1 ZNF512 GPN1 SLC4A1AP AC110084.1

Figure S3F

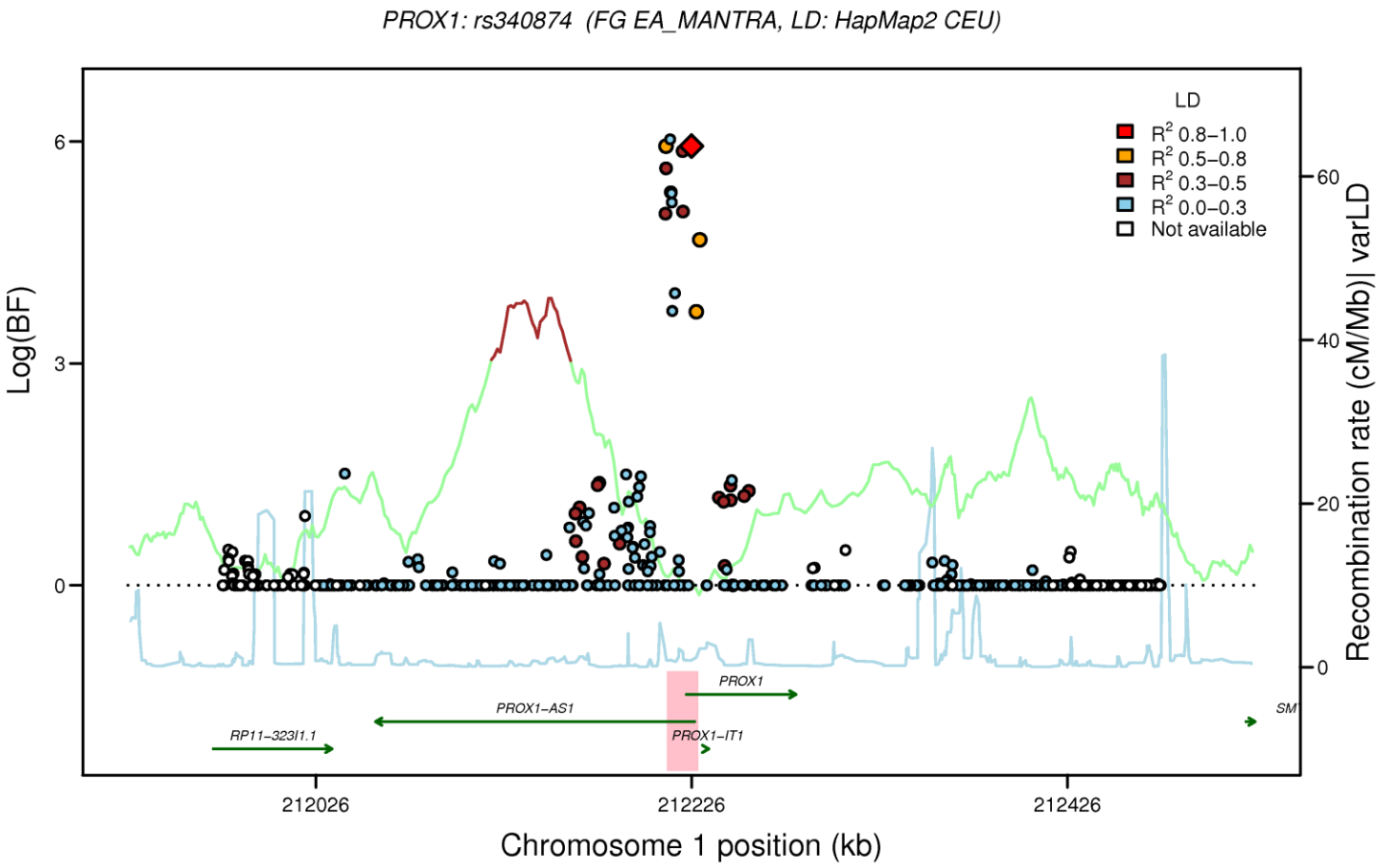
PROX1: rs340874 (FG EA_MANTRA, LD: HapMap2 CEU)
LD
R2 0.8–1.0
R2 0.5–0.8
R2 0.3–0.5
R2 0.0–0.3
Not available
Log(BF)
Recombination rate (cM/Mb)| varLD
PROX1
PROX1–AS1
RP11–323I1.1
PROX1–IT1
212026
212226
212426
Chromosome 1 position (kb)

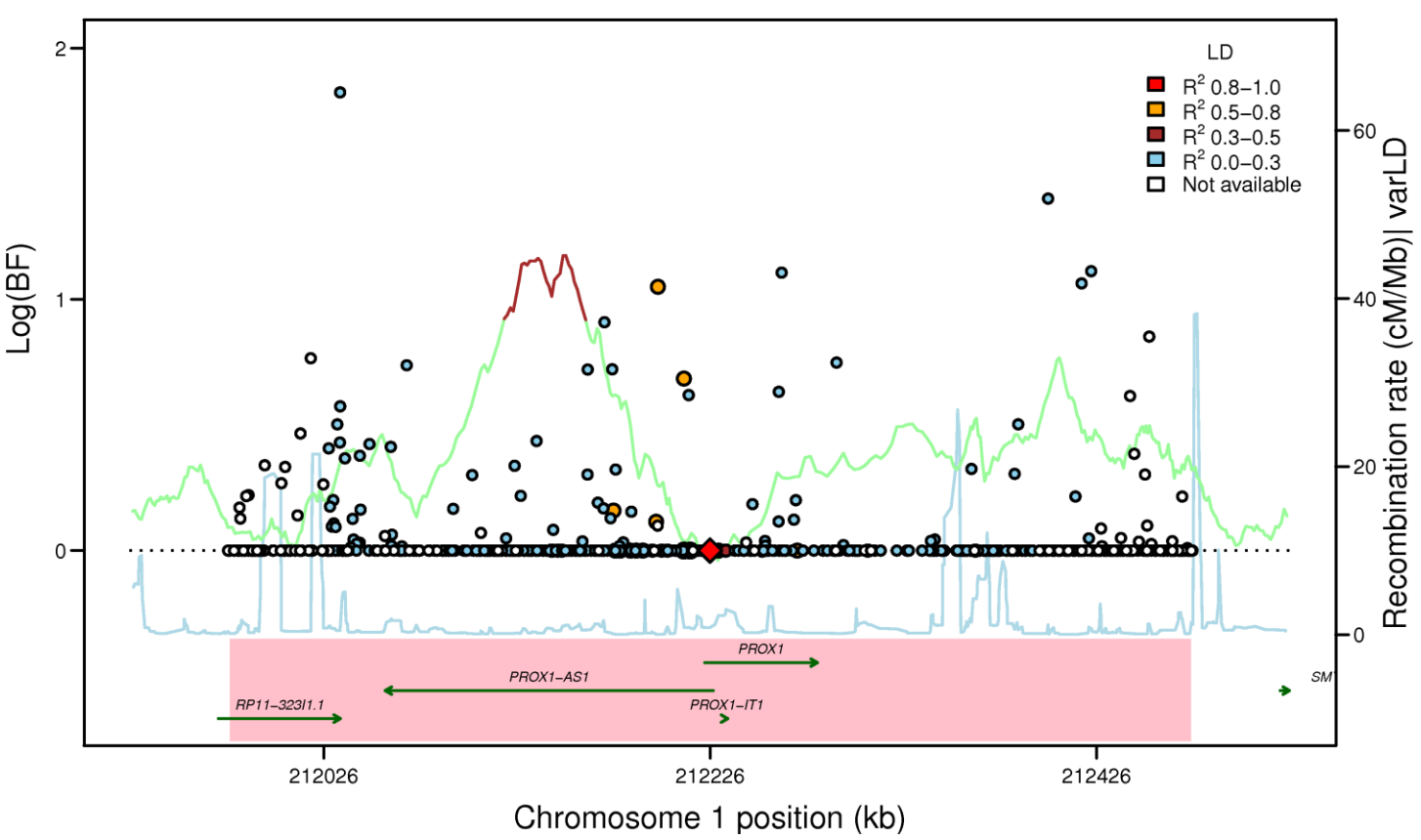
PROX1: rs340874 (FG AA_MANTRA, LD: HapMap2 YRI)
LD
R2 0.8–1.0
R2 0.5–0.8
R2 0.3–0.5
R2 0.0–0.3
Not available
Log(BF)
Recombination rate (cM/Mb)| varLD
PROX1
PROX1–AS1
RP11–323I1.1
PROX1–IT1
212026
212226
212426
Chromosome 1 position (kb)

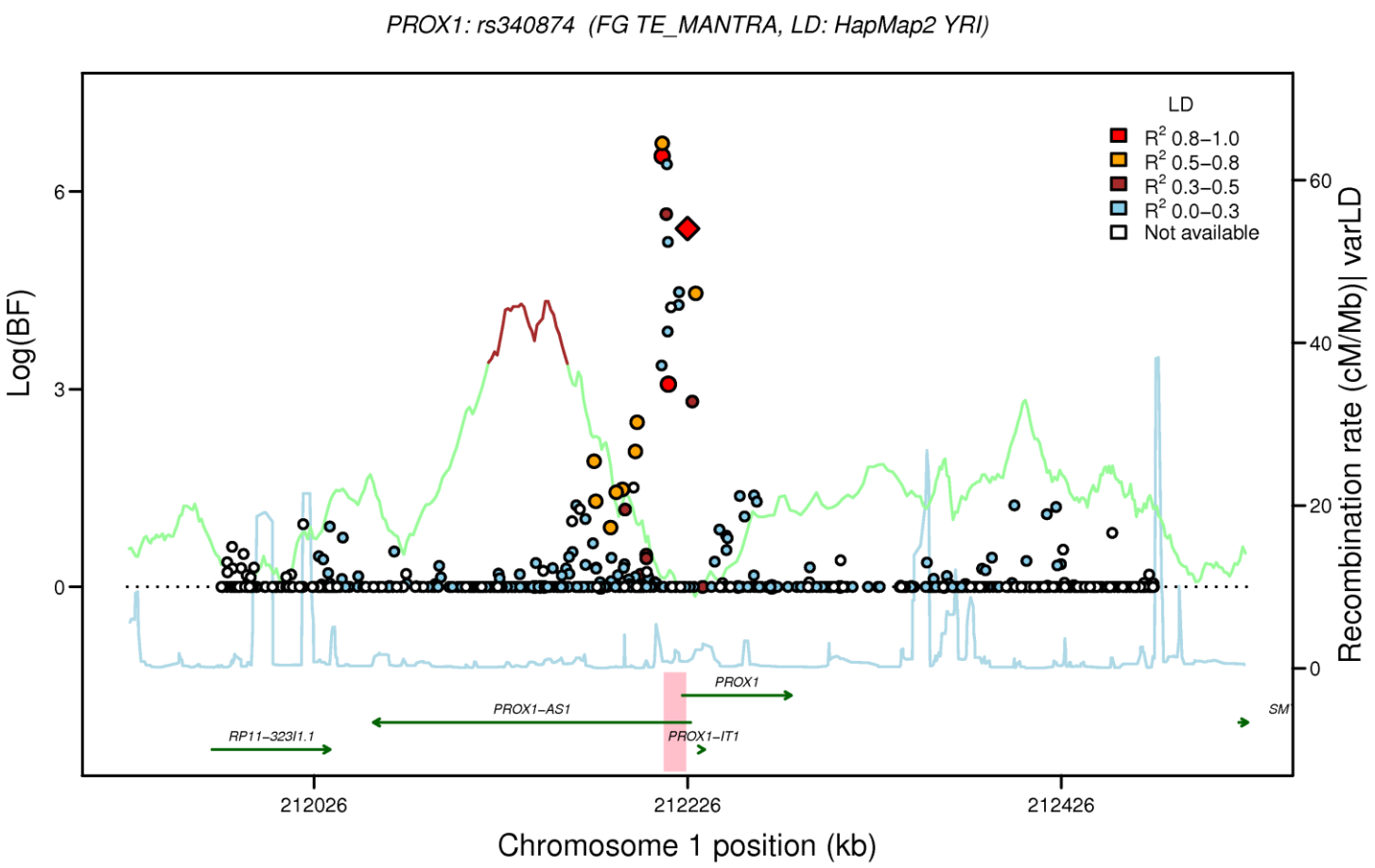
PROX1: rs340874 (FG TE_MANTRA, LD: HapMap2 YRI)
LD
R2 0.8–1.0
R2 0.5–0.8
R2 0.3–0.5
R2 0.0–0.3
Not available
Log(BF)
Recombination rate (cM/Mb)| varLD
PROX1
PROX1–AS1
RP11–323I1.1
PROX1–IT1
212026
212226
212426
Chromosome 1 position (kb)

Figure S3G

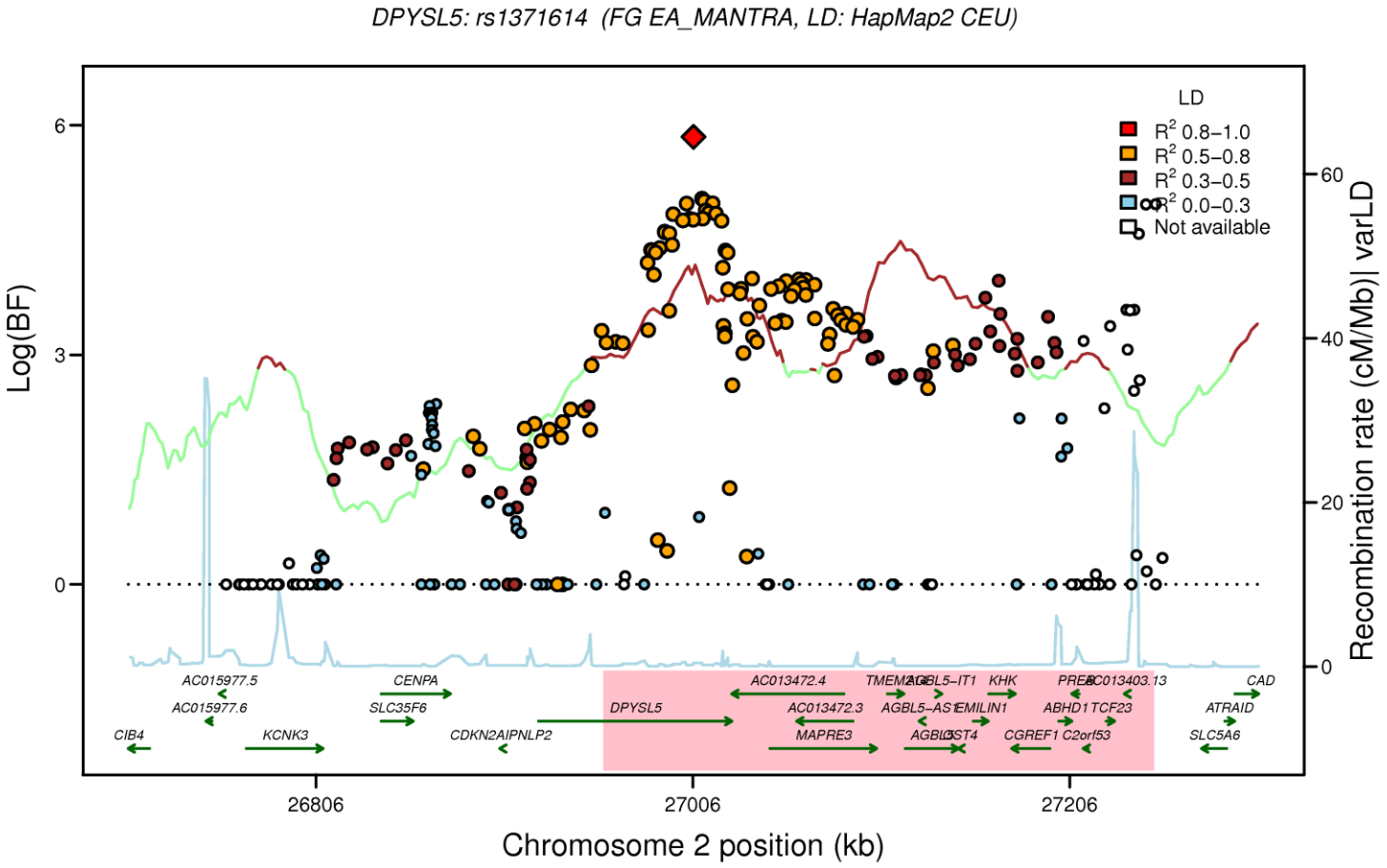
DPYSL5: rs1371614 (FG EA_MANTRA, LD: HapMap2 CEU)
LD
R2 0.8–1.0
R2 0.5–0.8
R2 0.3–0.5
R2 0.0–0.3
Not available
Log(BF)
Recombination rate (cM/Mb)| varLD
Chromosome 2 position (kb)
26806
27006
27206
AC015977.5
AC015977.6
CIB4
CENPA
SLC35F6
KCNK3
CDKN2AIPNLP2
DPYSL5
AC013472.4
AC013472.3
MAPRE3
KHK
EMILIN1
ABHD1
TCF23
C2orf53
ATRAID
SLC5A6
CAD

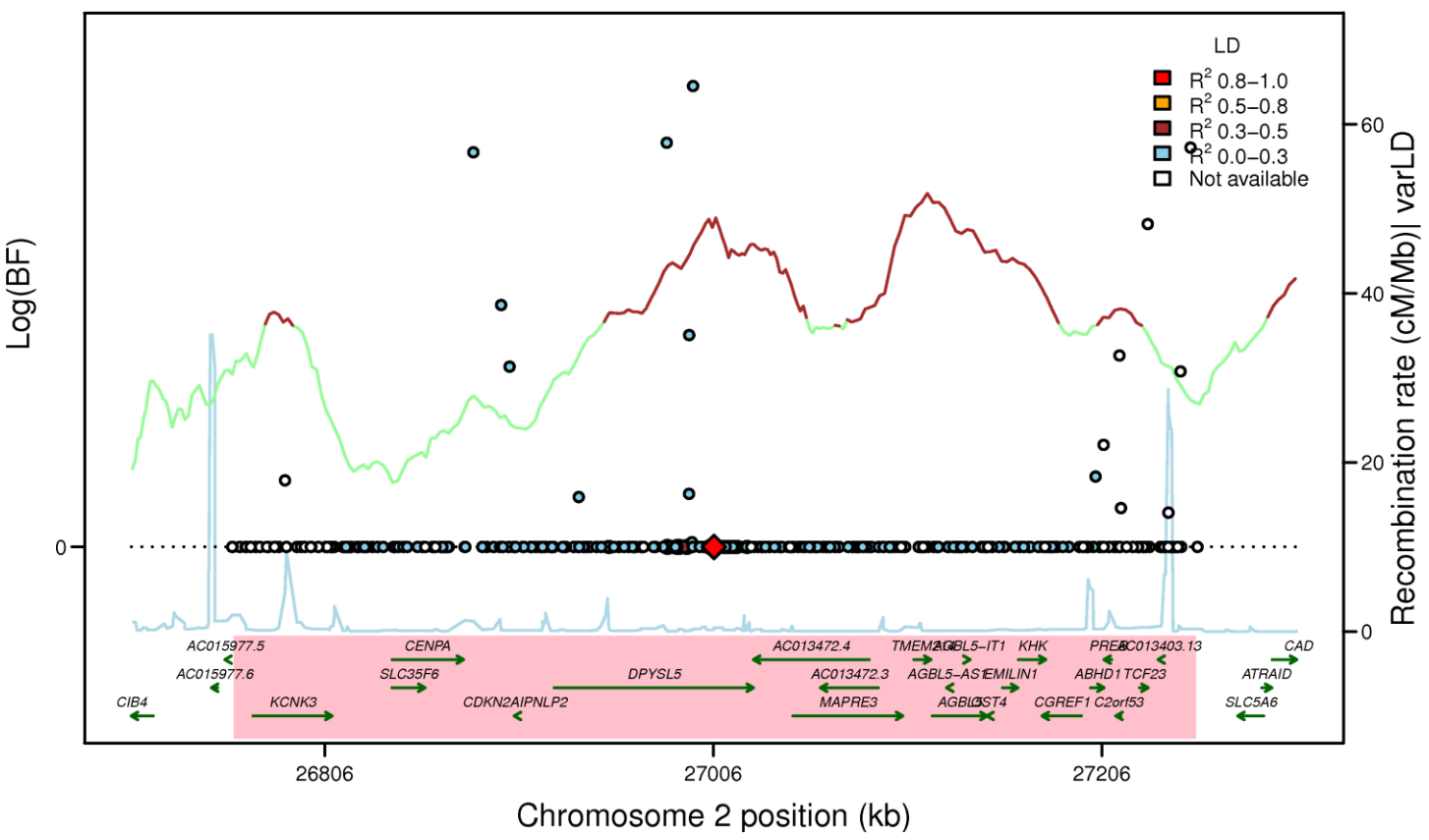
DPYSL5: rs1371614 (FG AA_MANTRA, LD: HapMap2 YRI)
LD
R2 0.8–1.0
R2 0.5–0.8
R2 0.3–0.5
R2 0.0–0.3
Not available
Log(BF)
Recombination rate (cM/Mb)| varLD
Chromosome 2 position (kb)
26806
27006
27206
AC015977.5
AC015977.6
CIB4
CENPA
SLC35F6
KCNK3
CDKN2AIPNLP2
DPYSL5
AC013472.4
AC013472.3
MAPRE3
KHK
EMILIN1
ABHD1
TCF23
C2orf53
ATRAID
SLC5A6
CAD

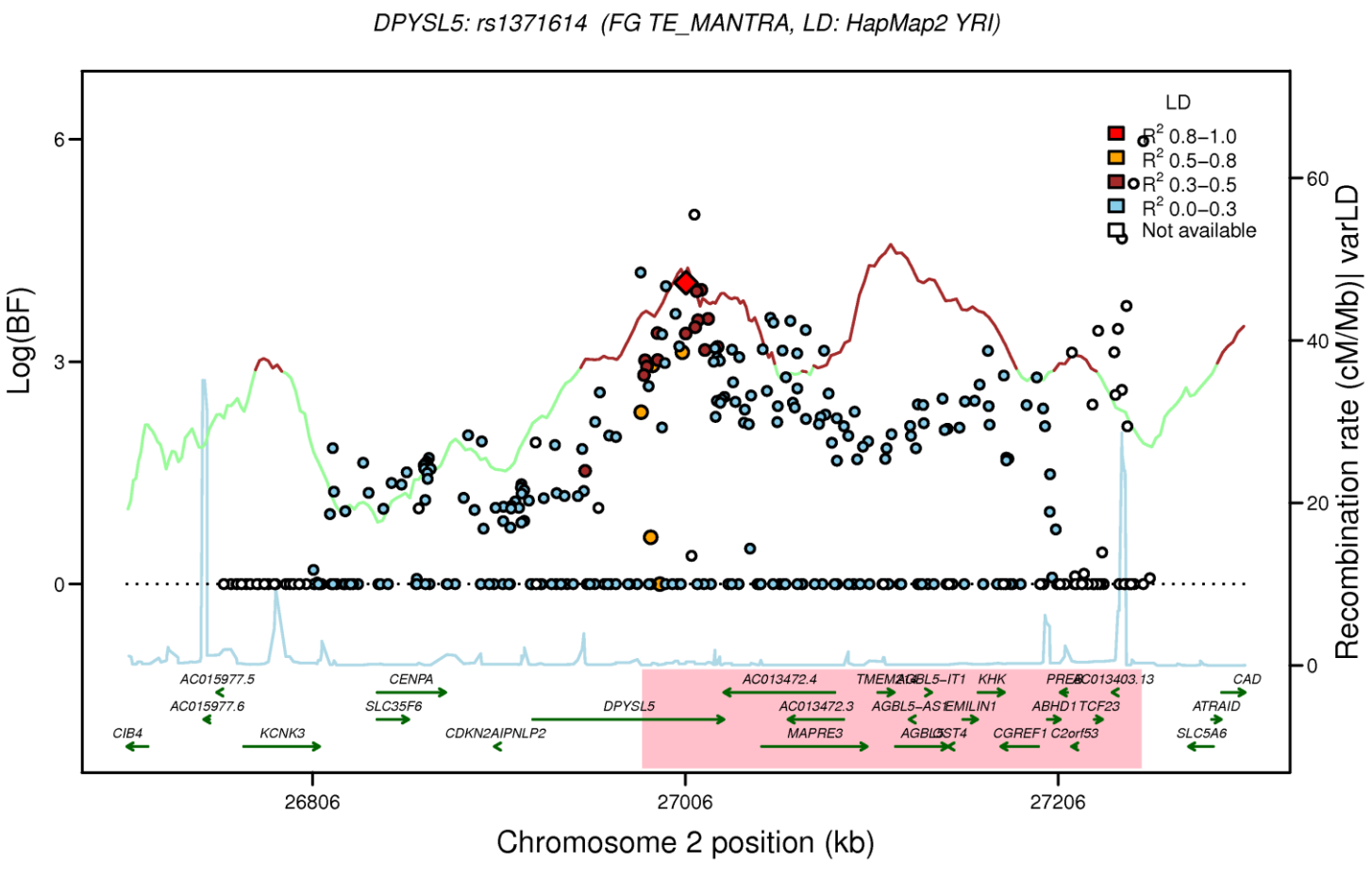
DPYSL5: rs1371614 (FG TE_MANTRA, LD: HapMap2 YRI)
LD
R2 0.8–1.0
R2 0.5–0.8
R2 0.3–0.5
R2 0.0–0.3
Not available
Log(BF)
Recombination rate (cM/Mb)| varLD
Chromosome 2 position (kb)
26806
27006
27206
AC015977.5
AC015977.6
CIB4
CENPA
SLC35F6
KCNK3
CDKN2AIPNLP2
DPYSL5
AC013472.4
AC013472.3
MAPRE3
KHK
EMILIN1
ABHD1
TCF23
C2orf53
ATRAID
SLC5A6
CAD

Figure S3H

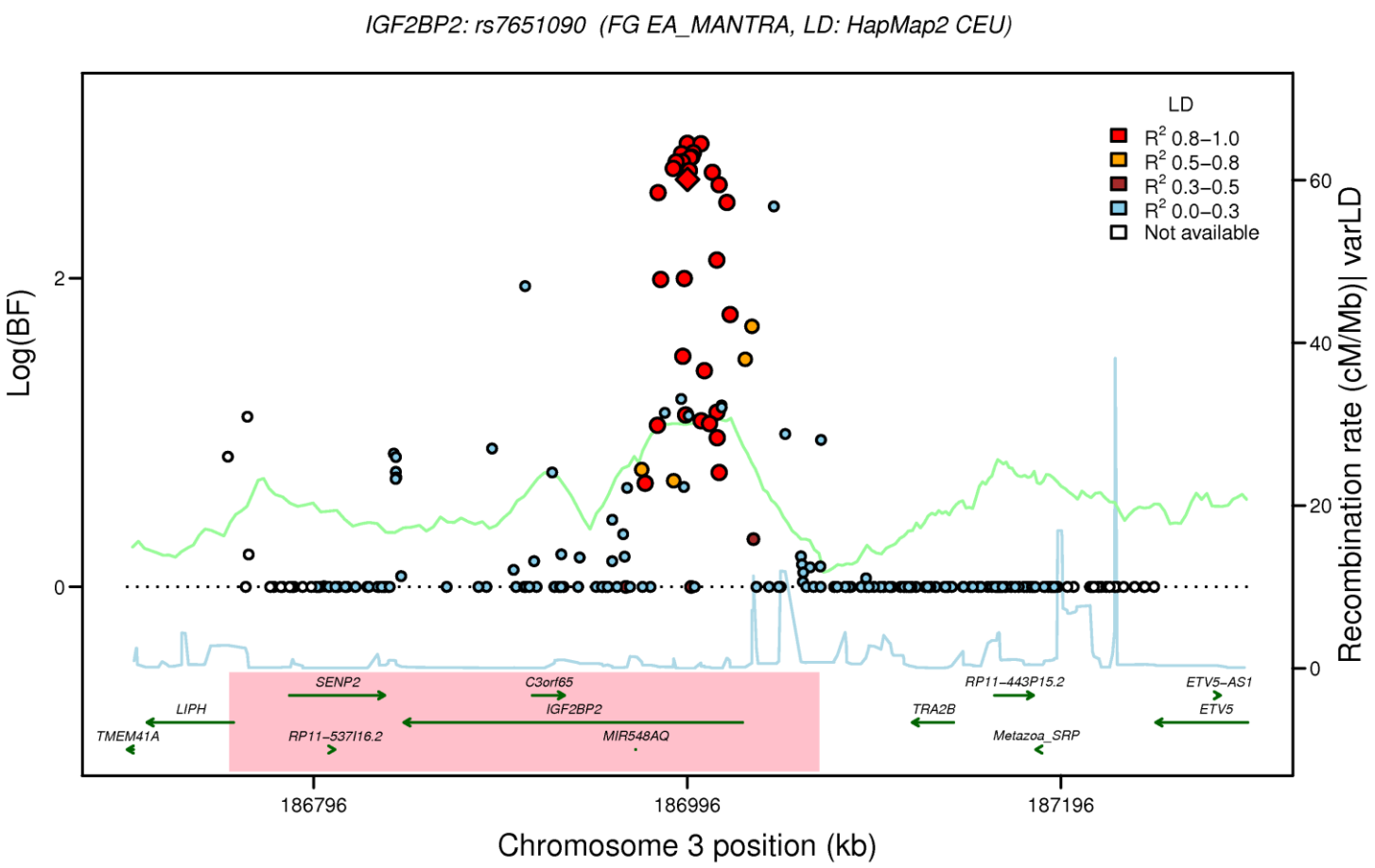
IGF2BP2: rs7651090 (FG EA_MANTRA, LD: HapMap2 CEU)
LD
R2 0.8–1.0
R2 0.5–0.8
R2 0.3–0.5
R2 0.0–0.3
Not available
Log(BF)
Recombination rate (cM/Mb)| varLD
SENP2
C3orf65
RP11–443P15.2
ETV5–AS1
LIPH
IGF2BP2
TRA2B
ETV5
TMEM41A
RP11–537I16.2
MIR548AQ
Metazoa_SRP
186796
186996
187196
Chromosome 3 position (kb)

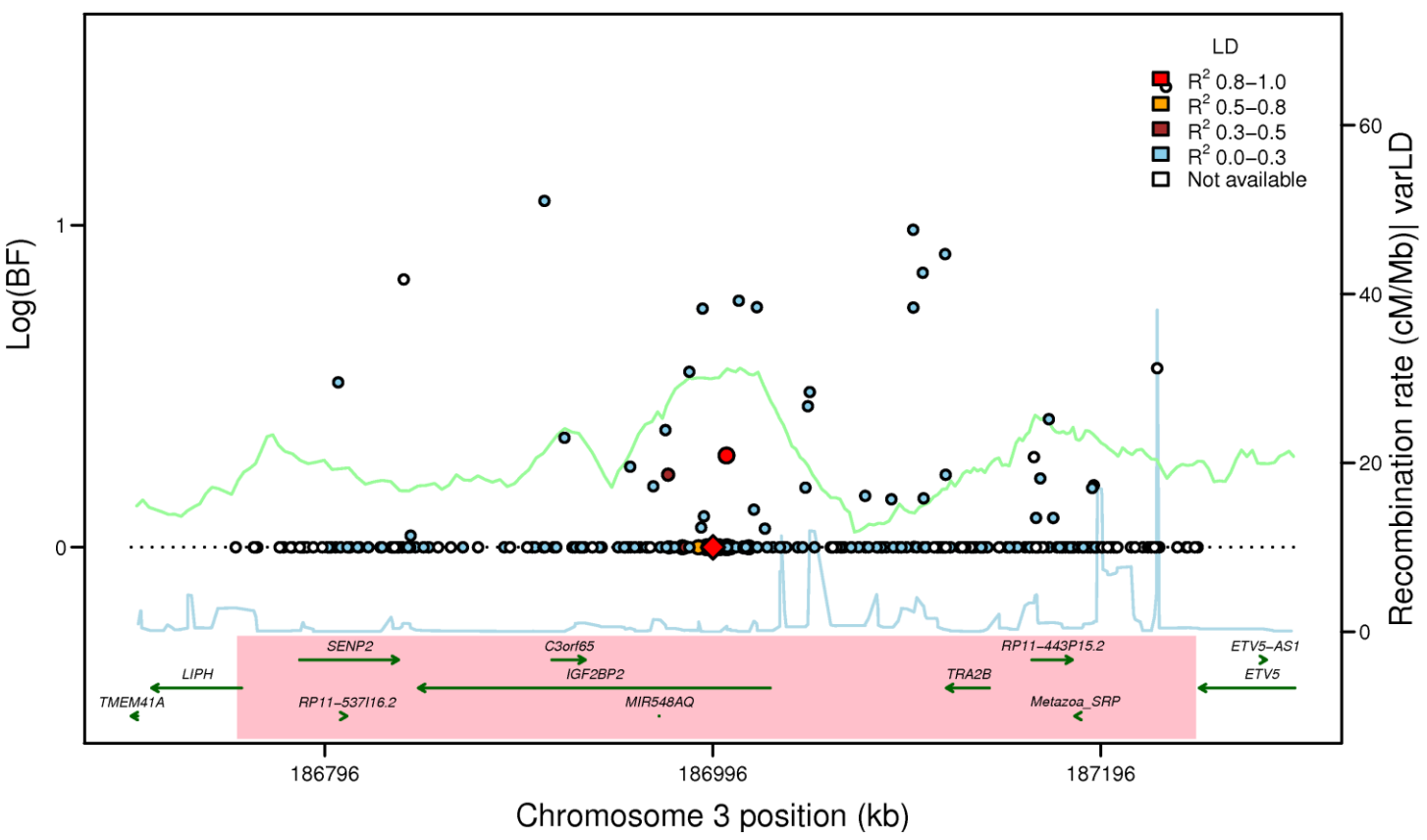
IGF2BP2: rs7651090 (FG AA_MANTRA, LD: HapMap2 YRI)
LD
R2 0.8–1.0
R2 0.5–0.8
R2 0.3–0.5
R2 0.0–0.3
Not available
Log(BF)
Recombination rate (cM/Mb)| varLD
SENP2
C3orf65
RP11–443P15.2
ETV5–AS1
LIPH
IGF2BP2
TRA2B
ETV5
TMEM41A
RP11–537I16.2
MIR548AQ
Metazoa_SRP
186796
186996
187196
Chromosome 3 position (kb)

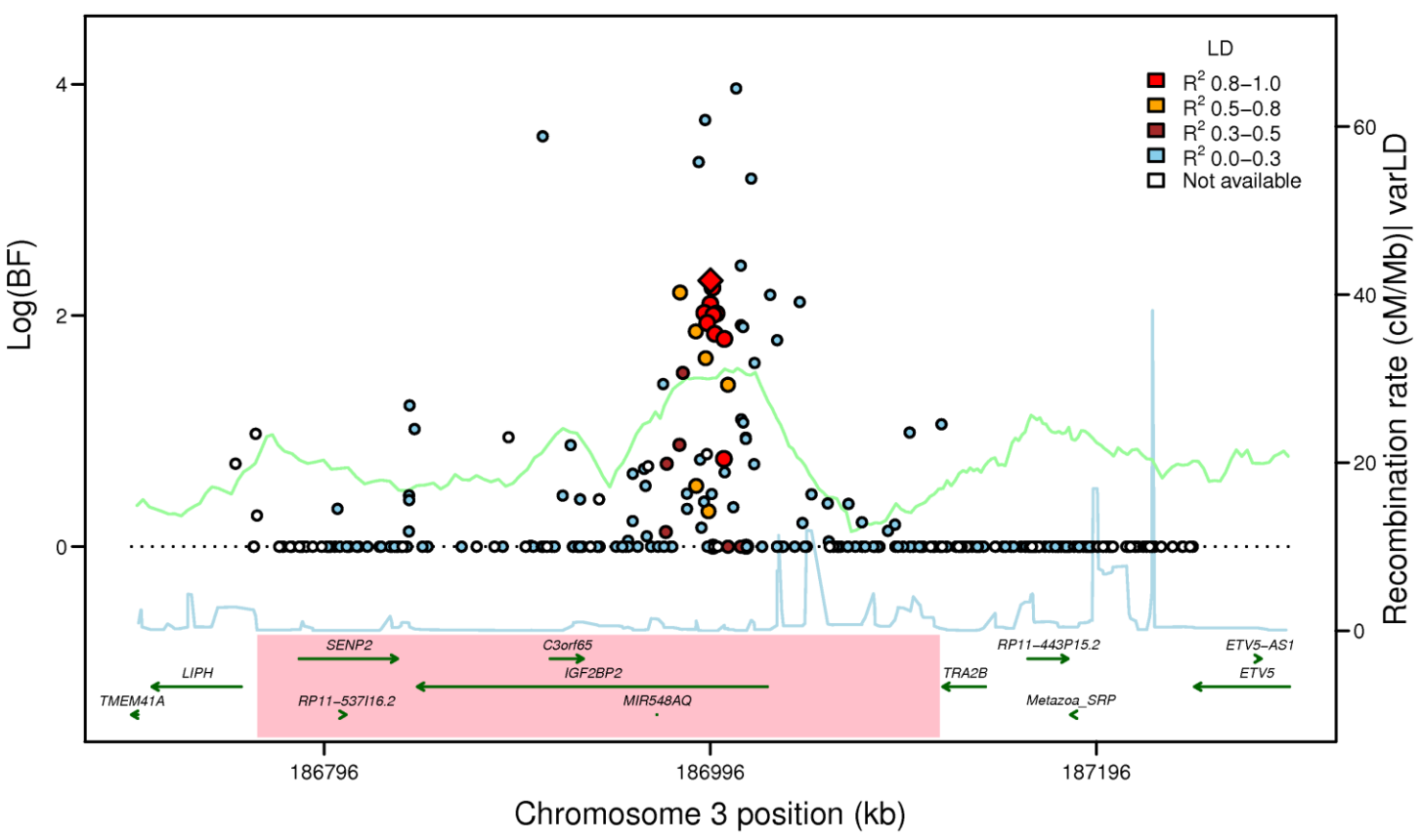
IGF2BP2: rs7651090 (FG TE_MANTRA, LD: HapMap2 YRI)
LD
R2 0.8–1.0
R2 0.5–0.8
R2 0.3–0.5
R2 0.0–0.3
Not available
Log(BF)
Recombination rate (cM/Mb)| varLD
SENP2
C3orf65
RP11–443P15.2
ETV5–AS1
LIPH
IGF2BP2
TRA2B
ETV5
TMEM41A
RP11–537I16.2
MIR548AQ
Metazoa_SRP
186796
186996
187196
Chromosome 3 position (kb)

Figure S3I

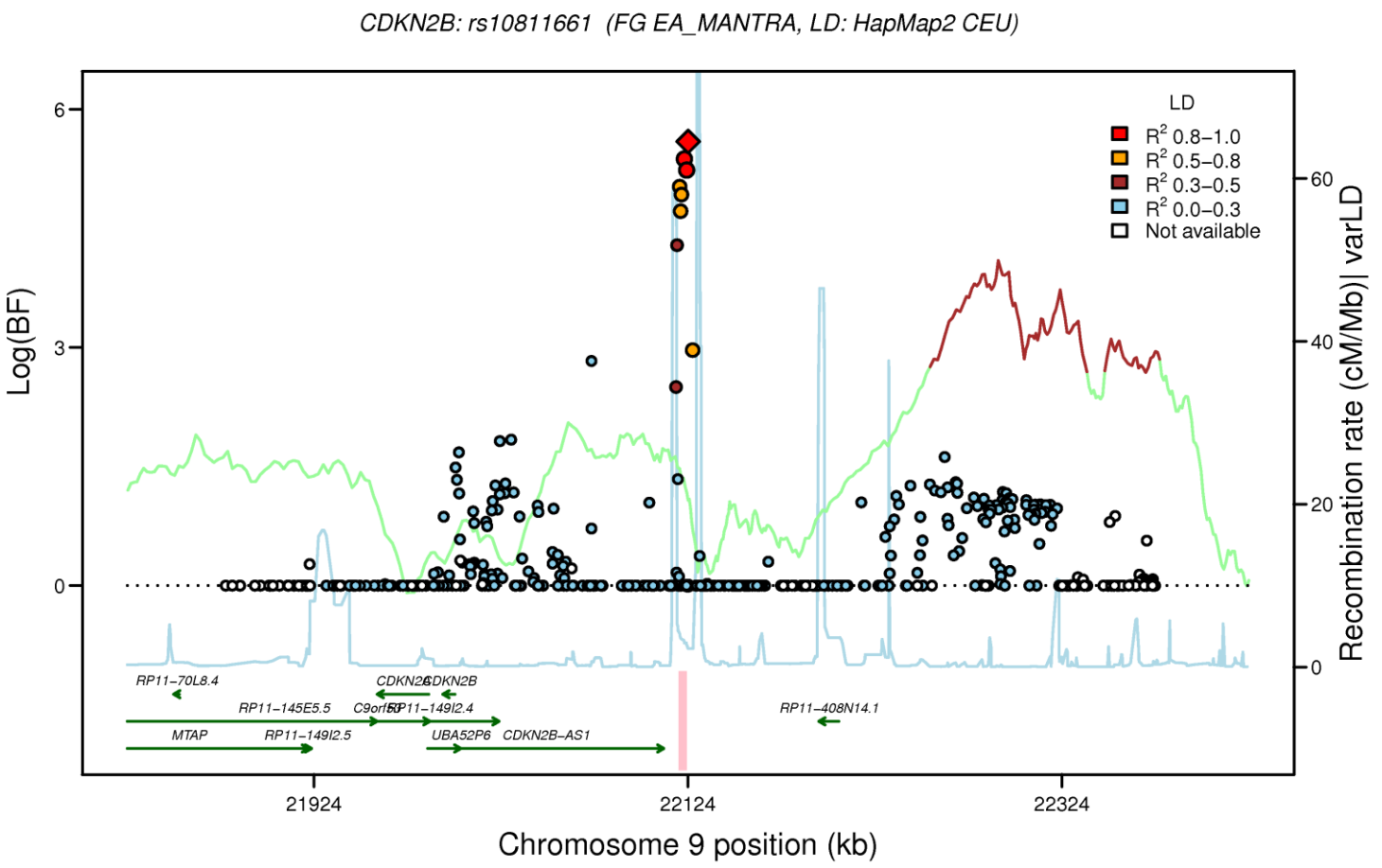
CDKN2B: rs10811661 (FG EA_MANTRA, LD: HapMap2 CEU)
LD
R2 0.8–1.0
R2 0.5–0.8
R2 0.3–0.5
R2 0.0–0.3
Not available
Log(BF)
Recombination rate (cM/Mb)| varLD
RP11–70L8.4
CDKN2A
CDKN2B
RP11–145E5.5
C9orf53
RP11–149I2.4
RP11–408N14.1
MTAP
RP11–149I2.5
UBA52P6
CDKN2B–AS1
21924
22124
22324
Chromosome 9 position (kb)

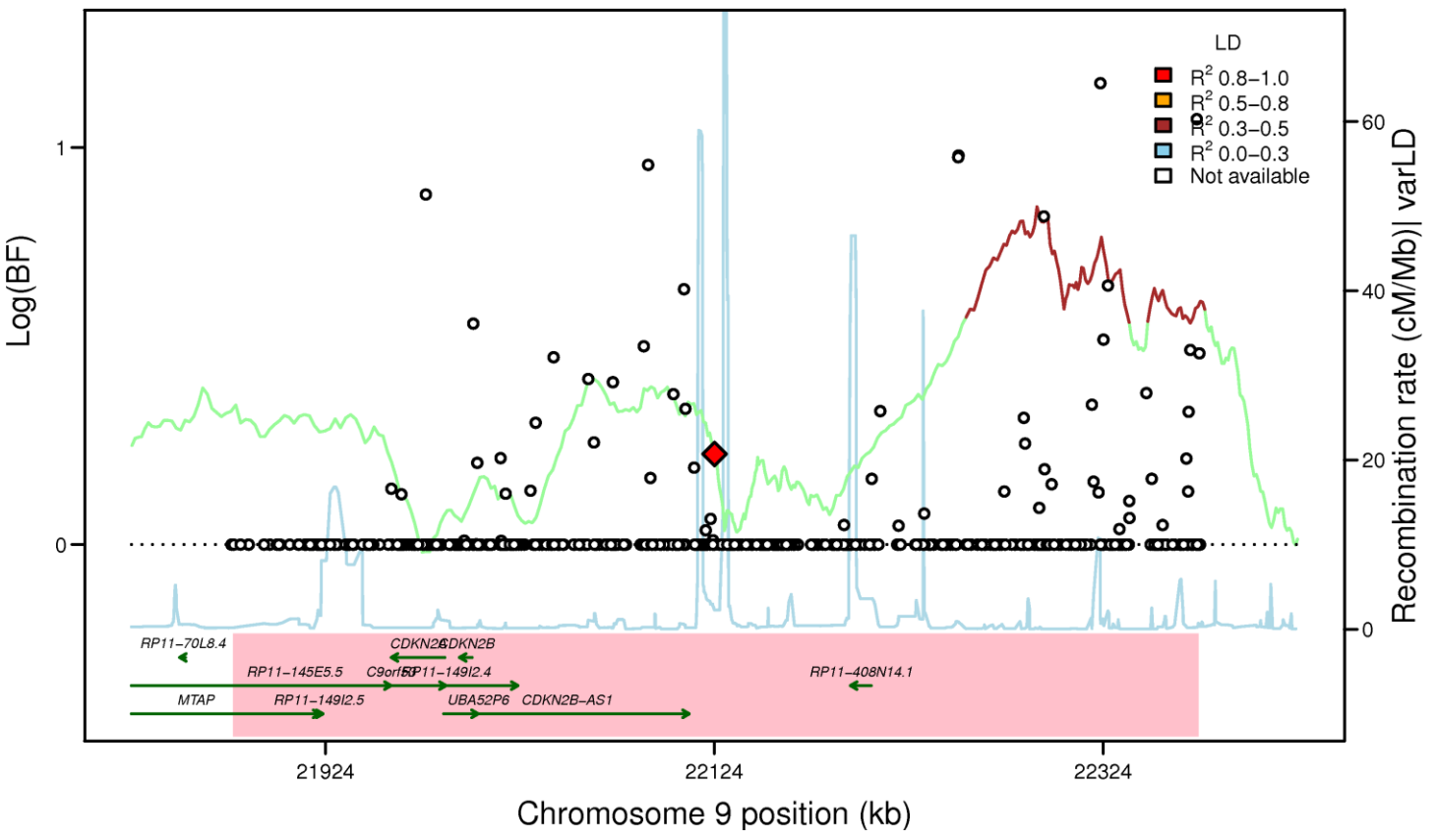
CDKN2B: rs10811661 (FG AA_MANTRA, LD: HapMap2 YRI)
LD
R2 0.8–1.0
R2 0.5–0.8
R2 0.3–0.5
R2 0.0–0.3
Not available
Log(BF)
Recombination rate (cM/Mb)| varLD
RP11–70L8.4
CDKN2A
CDKN2B
RP11–145E5.5
C9orf53
RP11–149I2.4
RP11–408N14.1
MTAP
RP11–149I2.5
UBA52P6
CDKN2B–AS1
21924
22124
22324
Chromosome 9 position (kb)

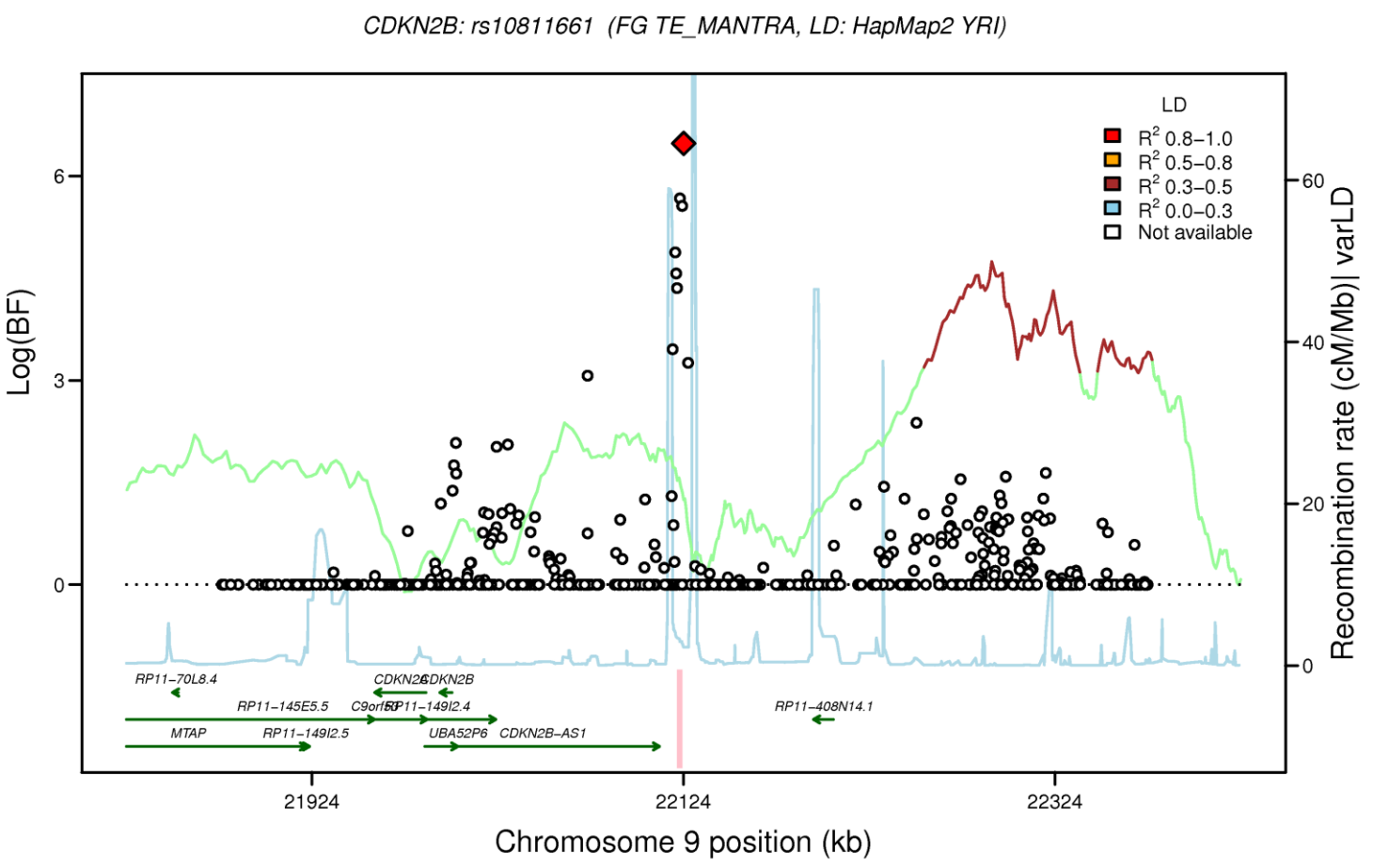
CDKN2B: rs10811661 (FG TE_MANTRA, LD: HapMap2 YRI)
LD
R2 0.8–1.0
R2 0.5–0.8
R2 0.3–0.5
R2 0.0–0.3
Not available
Log(BF)
Recombination rate (cM/Mb)| varLD
RP11–70L8.4
CDKN2A
CDKN2B
RP11–145E5.5
C9orf53
RP11–149I2.4
RP11–408N14.1
MTAP
RP11–149I2.5
UBA52P6
CDKN2B–AS1
21924
22124
22324
Chromosome 9 position (kb)

Figure S3J

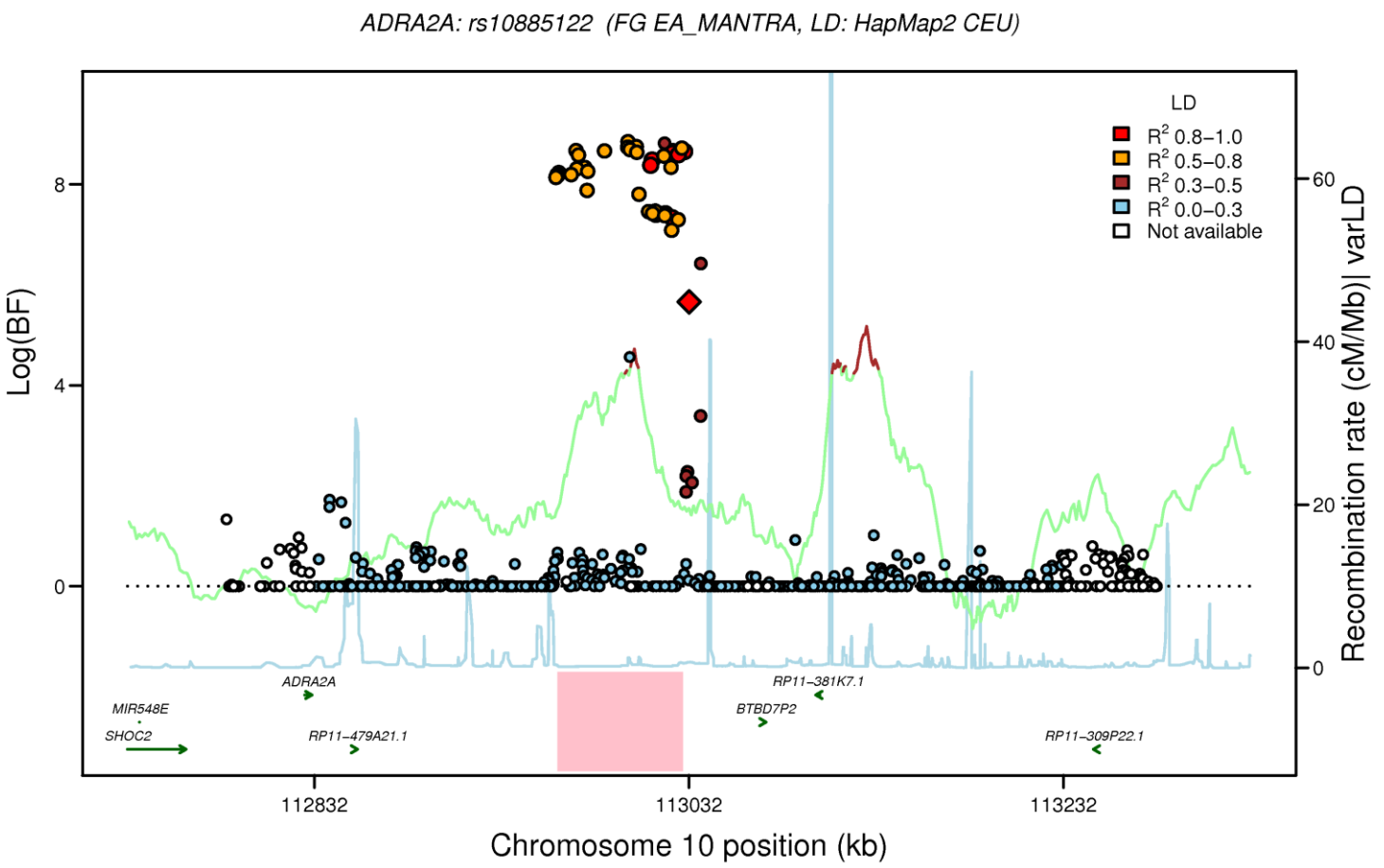
ADRA2A: rs10885122 (FG EA_MANTRA, LD: HapMap2 CEU)
LD
R2 0.8–1.0
R2 0.5–0.8
R2 0.3–0.5
R2 0.0–0.3
Not available
Log(BF)
Recombination rate (cM/Mb)| varLD
ADRA2A
RP11–381K7.1
MIR548E
BTBD7P2
SHOC2
RP11–479A21.1
RP11–309P22.1
112832
113032
113232
Chromosome 10 position (kb)

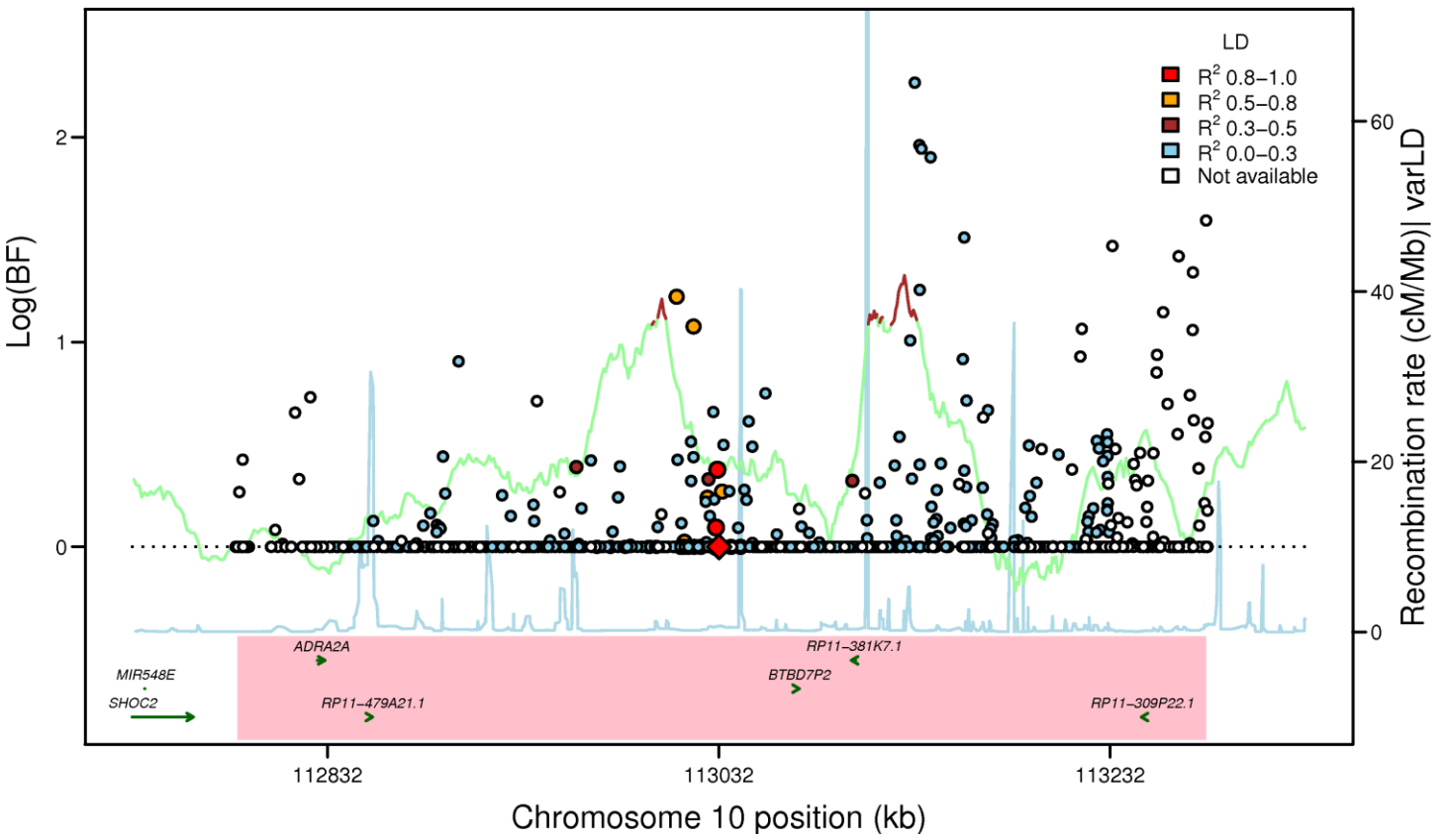
ADRA2A: rs10885122 (FG AA_MANTRA, LD: HapMap2 YRI)
LD
R2 0.8–1.0
R2 0.5–0.8
R2 0.3–0.5
R2 0.0–0.3
Not available
Log(BF)
Recombination rate
ADRA2A
RP11–381K7.1
MIR548E
BTBD7P2
SHOC2
RP11–479A21.1
RP11–309P22.1
112832
113032
113232
Chromosome 10 position (kb)

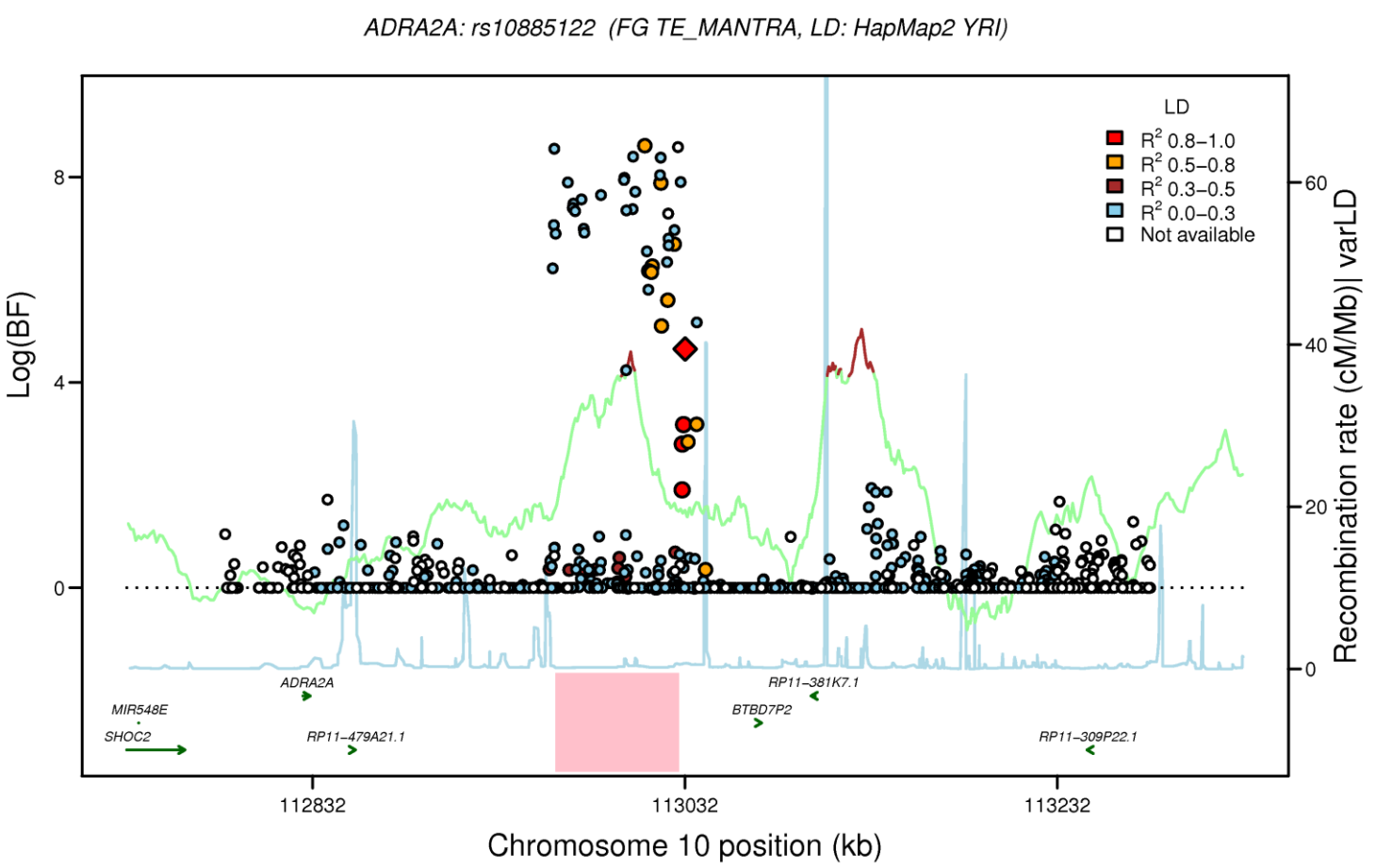
ADRA2A: rs10885122 (FG TE_MANTRA, LD: HapMap2 YRI)
LD
R2 0.8–1.0
R2 0.5–0.8
R2 0.3–0.5
R2 0.0–0.3
Not available
Log(BF)
Recombination rate (cM/Mb)| varLD
ADRA2A
RP11–381K7.1
MIR548E
BTBD7P2
SHOC2
RP11–479A21.1
RP11–309P22.1
112832
113032
113232
Chromosome 10 position (kb)

Figure S3K

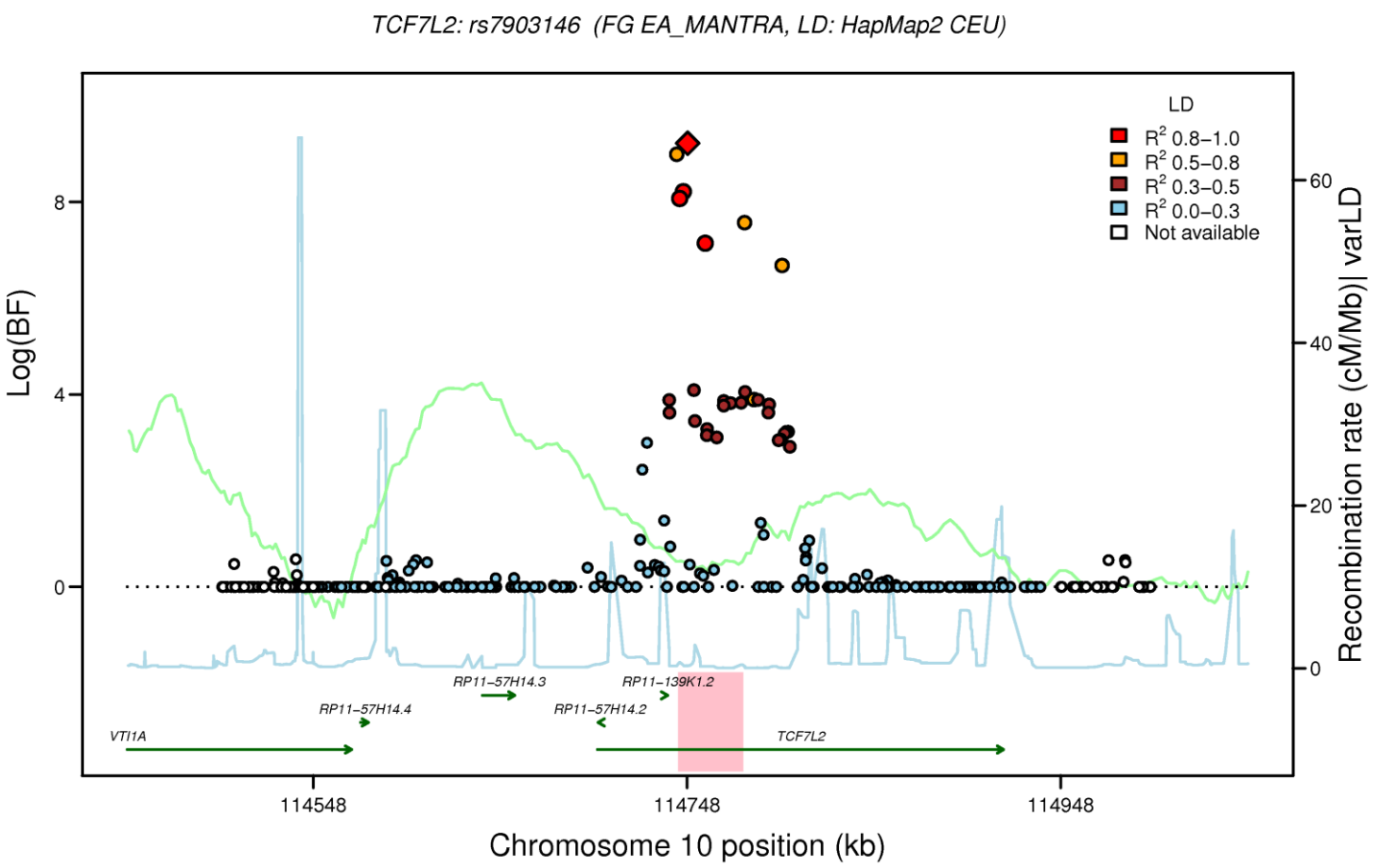
TCF7L2: rs7903146 (FG EA_MANTRA, LD: HapMap2 CEU)
LD
R2 0.8–1.0
R2 0.5–0.8
R2 0.3–0.5
R2 0.0–0.3
Not available
Log(BF)
Recombination rate (cM/Mb)| varLD
RP11–57H14.3
RP11–139K1.2
RP11–57H14.4
RP11–57H14.2
VTI1A
TCF7L2
114548
114748
114948
Chromosome 10 position (kb)

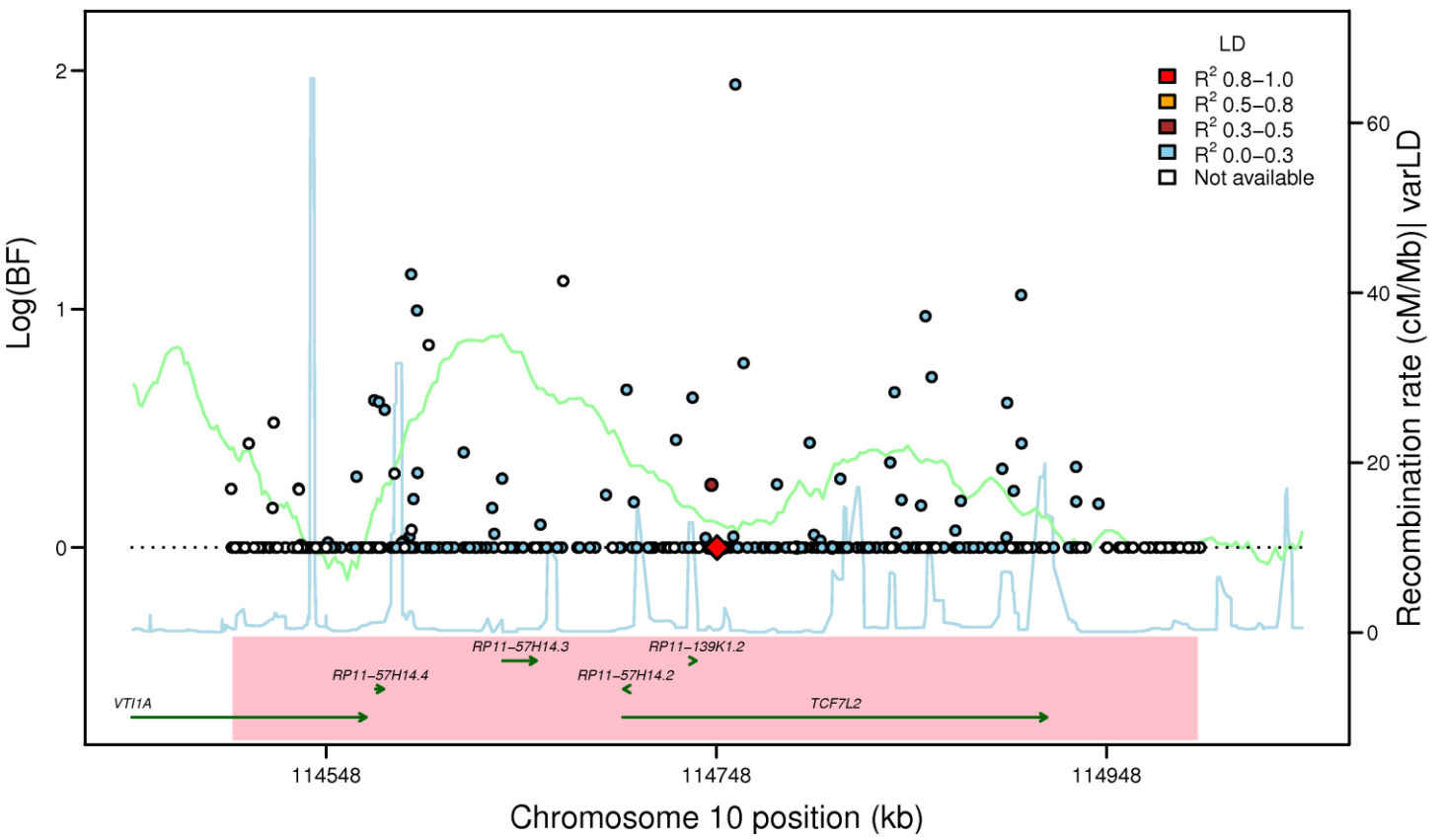
TCF7L2: rs7903146 (FG AA_MANTRA, LD: HapMap2 YRI)
LD
R2 0.8–1.0
R2 0.5–0.8
R2 0.3–0.5
R2 0.0–0.3
Not available
Log(BF)
Recombination rate (cM/Mb)| varLD
RP11–57H14.3
RP11–139K1.2
RP11–57H14.4
RP11–57H14.2
VTI1A
TCF7L2
114548
114748
114948
Chromosome 10 position (kb)

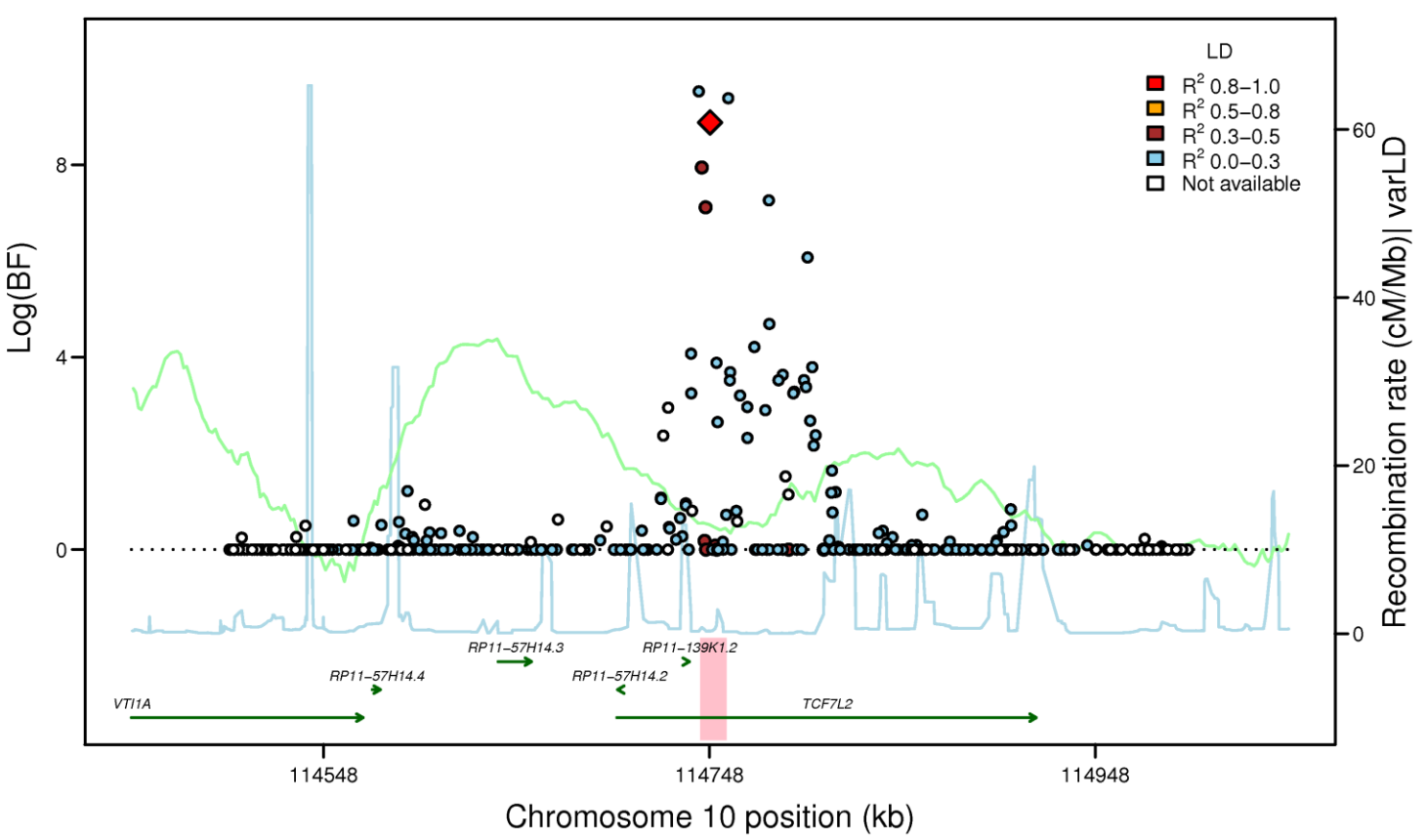
TCF7L2: rs7903146 (FG TE_MANTRA, LD: HapMap2 YRI)
LD
R2 0.8–1.0
R2 0.5–0.8
R2 0.3–0.5
R2 0.0–0.3
Not available
Log(BF)
Recombination rate (cM/Mb)| varLD
RP11–57H14.3
RP11–139K1.2
RP11–57H14.4
RP11–57H14.2
VTI1A
TCF7L2
114548
114748
114948
Chromosome 10 position (kb)

Figure S3L

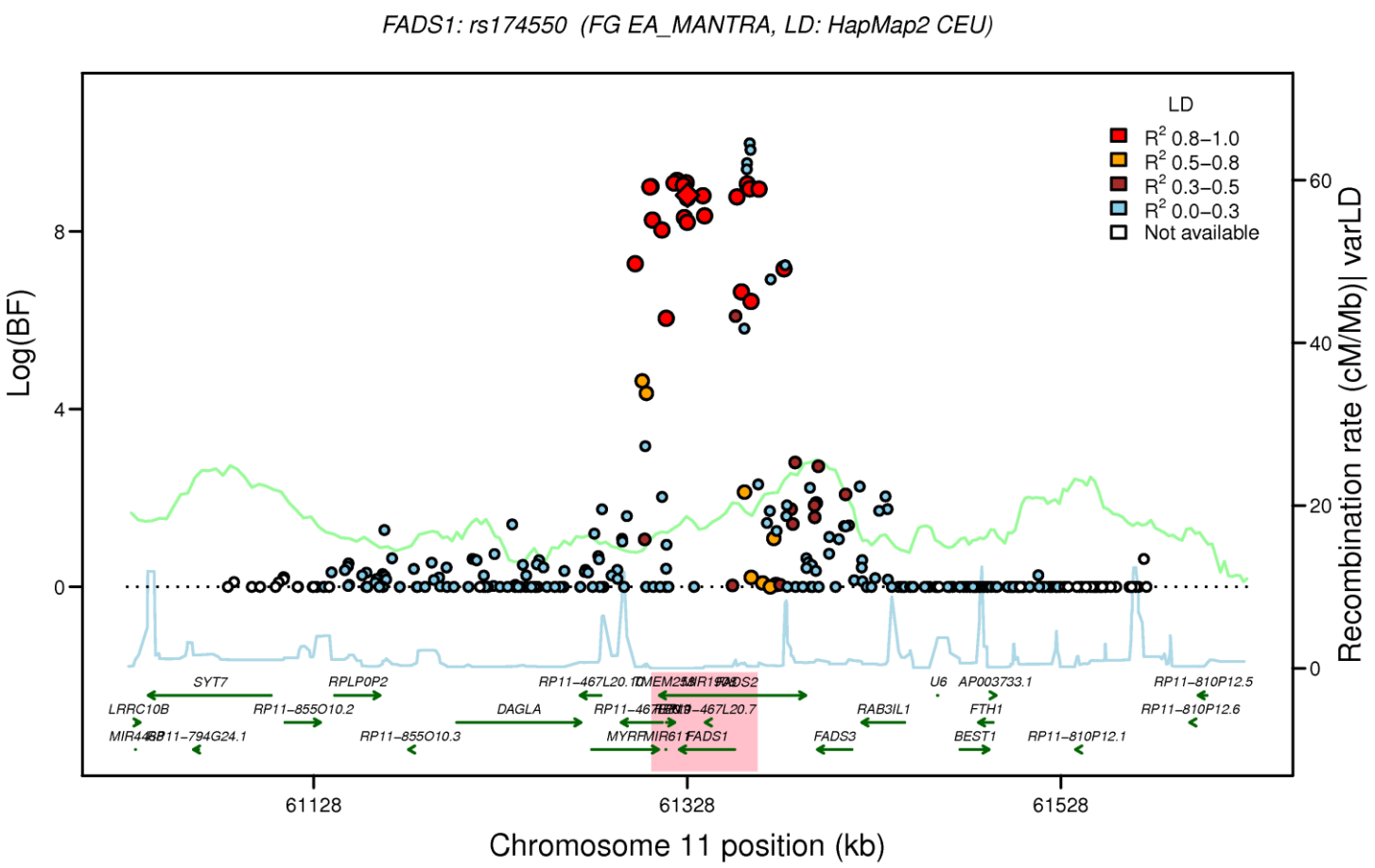
FADS1: rs174550 (FG EA_MANTRA, LD: HapMap2 CEU)
LD
R2 0.8–1.0
R2 0.5–0.8
R2 0.3–0.5
R2 0.0–0.3
Not available
Log(BF)
Recombination rate (cM/Mb)| varLD
SYT7
RPLP0P2
RP11–467L20.10
DMEM256
MIR1908
FADS2
U6
AP003733.1
RP11–810P12.5
LRRC10B
RP11–855O10.2
DAGLA
RP11–467L20.7
RAB3IL1
FTH1
RP11–810P12.6
MIR4482
RP11–794G24.1
RP11–855O10.3
MYRFL
MIR611
FADS1
FADS3
BEST1
RP11–810P12.1
61128
61328
61528
Chromosome 11 position (kb)

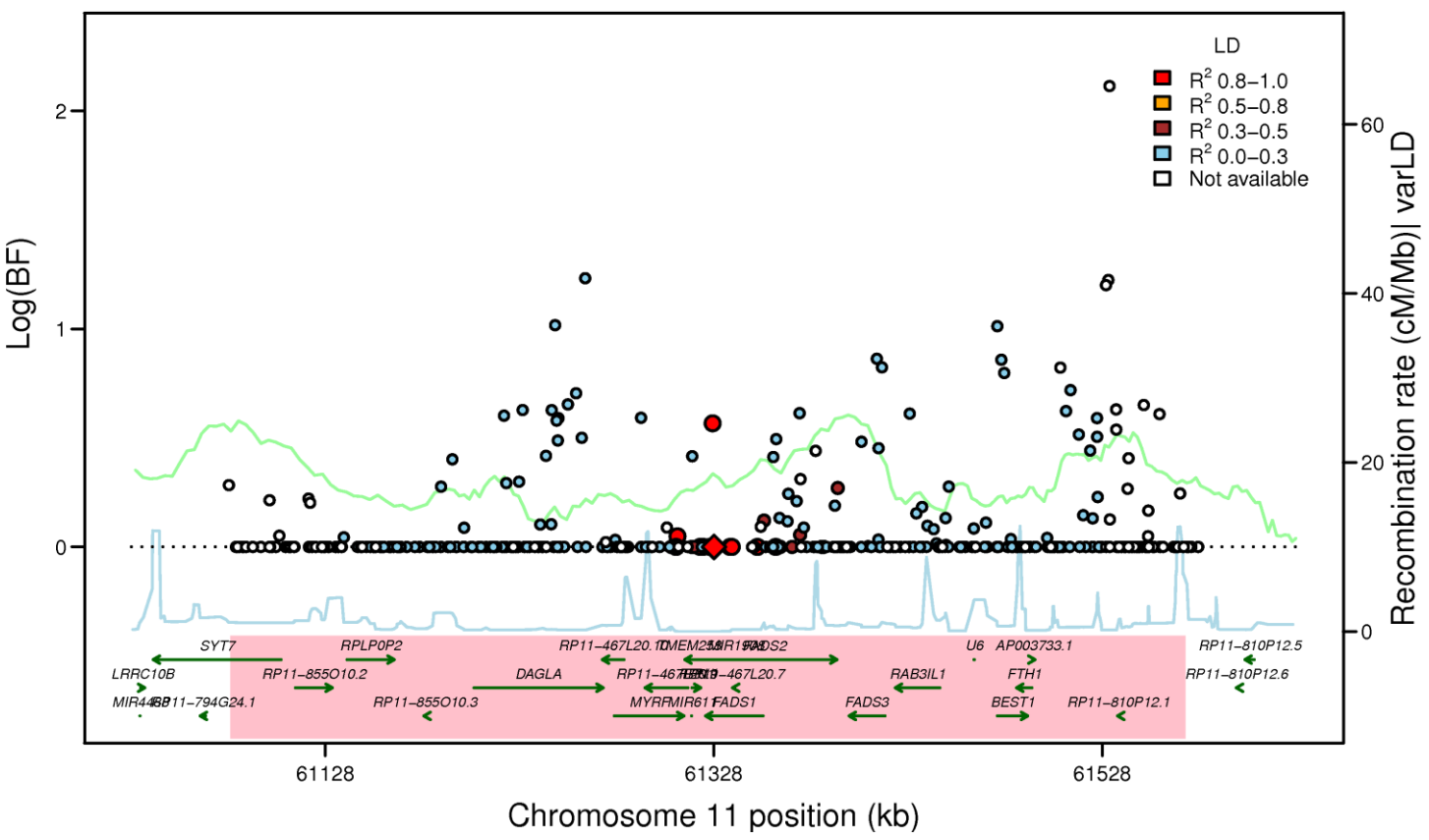
FADS1: rs174550 (FG AA_MANTRA, LD: HapMap2 YRI)
LD
R2 0.8–1.0
R2 0.5–0.8
R2 0.3–0.5
R2 0.0–0.3
Not available
Log(BF)
Recombination rate (cM/Mb)| varLD
SYT7
RPLP0P2
RP11–467L20.10
DMEM256
MIR1908
FADS2
U6
AP003733.1
RP11–810P12.5
LRRC10B
RP11–855O10.2
DAGLA
RP11–467L20.7
RAB3IL1
FTH1
RP11–810P12.6
MIR4482
RP11–794G24.1
RP11–855O10.3
MYRFL
MIR611
FADS1
FADS3
BEST1
RP11–810P12.1
61128
61328
61528
Chromosome 11 position (kb)

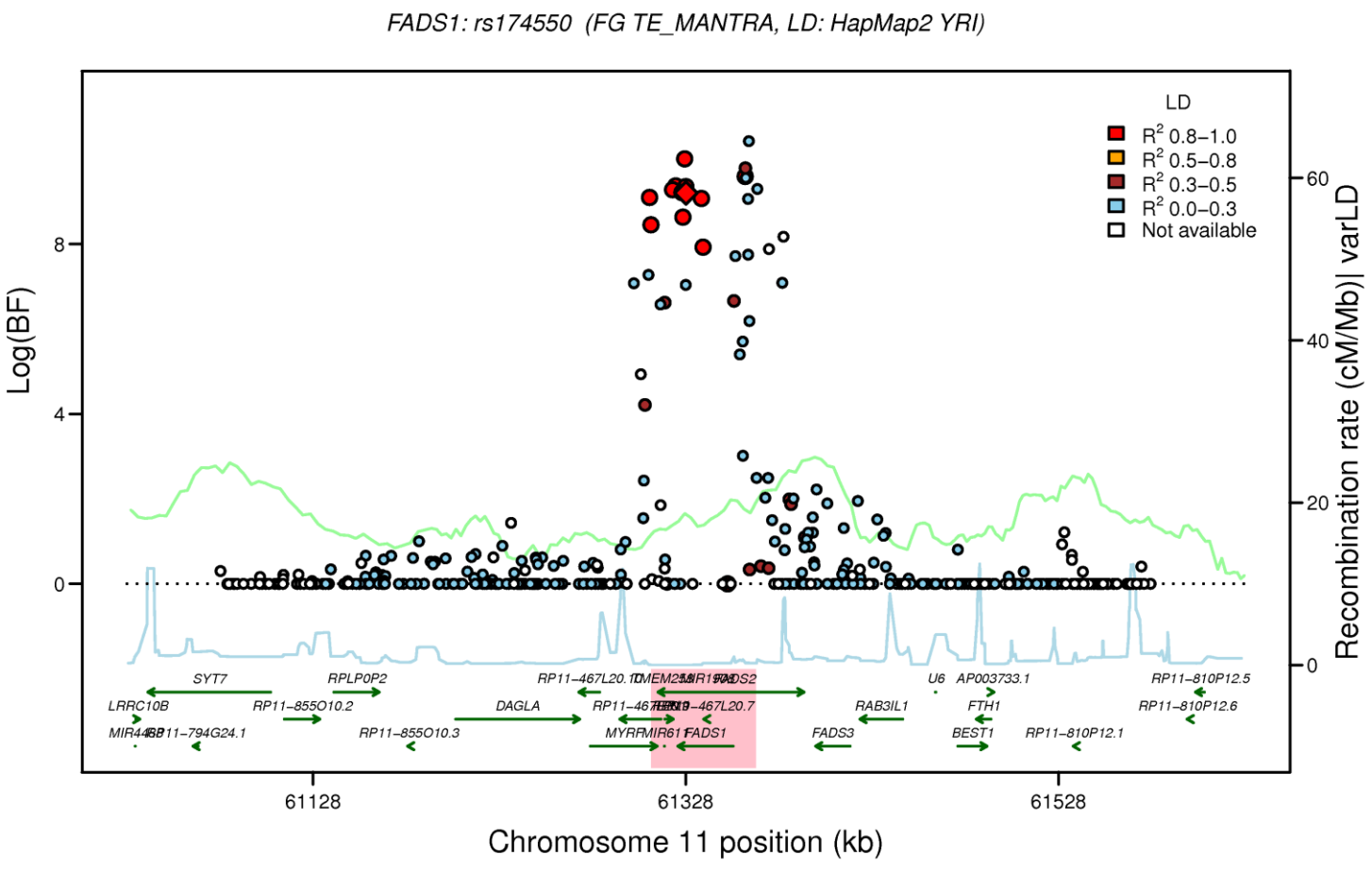
FADS1: rs174550 (FG TE_MANTRA, LD: HapMap2 YRI)
LD
R2 0.8–1.0
R2 0.5–0.8
R2 0.3–0.5
R2 0.0–0.3
Not available
Log(BF)
Recombination rate (cM/Mb)| varLD
SYT7
RPLP0P2
RP11–467L20.10
DMEM256
MIR1908
FADS2
U6
AP003733.1
RP11–810P12.5
LRRC10B
RP11–855O10.2
DAGLA
RP11–467L20.7
RAB3IL1
FTH1
RP11–810P12.6
MIR4482
RP11–794G24.1
RP11–855O10.3
MYRFL
MIR611
FADS1
FADS3
BEST1
RP11–810P12.1
61128
61328
61528
Chromosome 11 position (kb)

Figure S3M

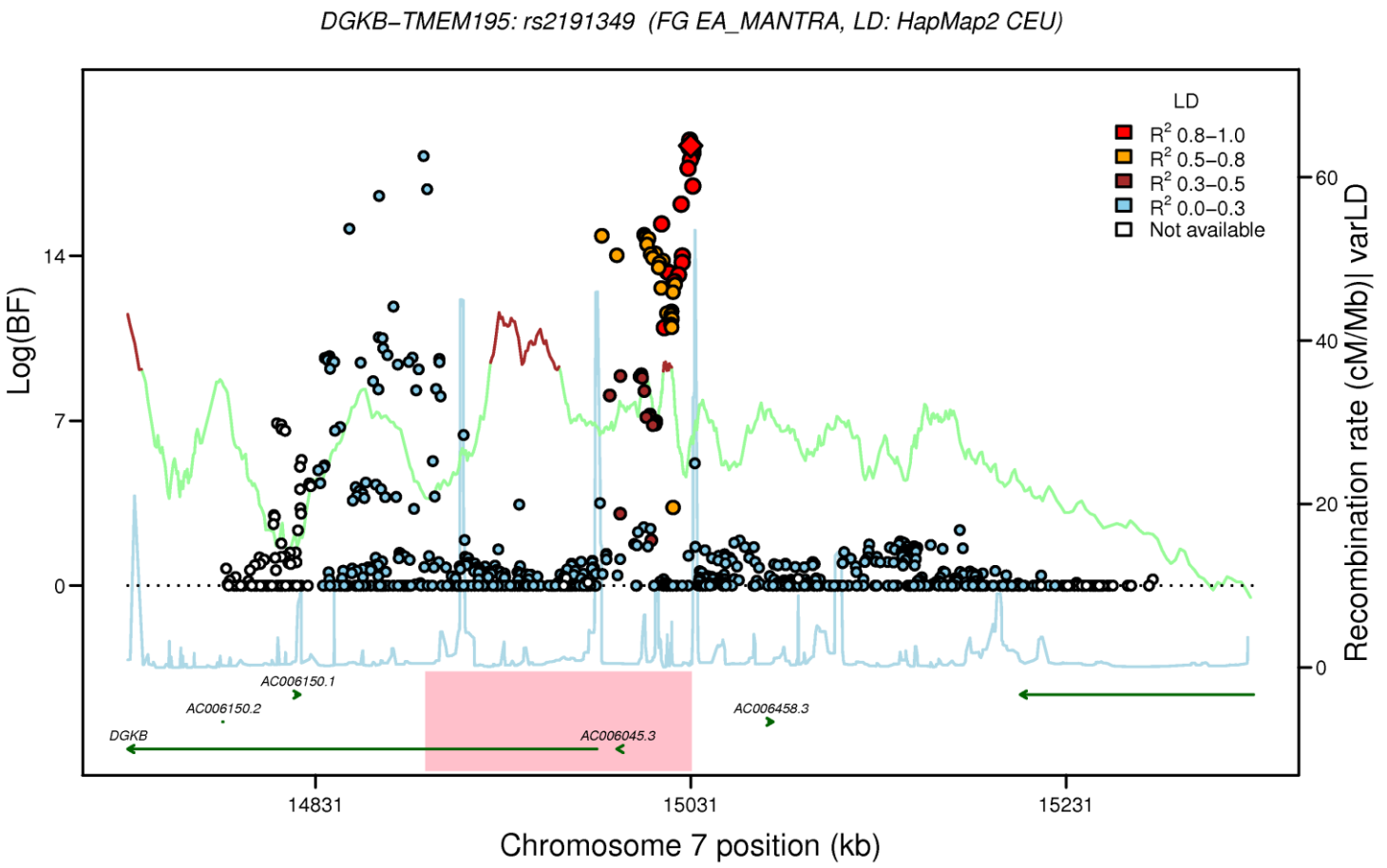
DGKB–TMEM195: rs2191349 (FG EA_MANTRA, LD: HapMap2 CEU)
LD
R2 0.8–1.0
R2 0.5–0.8
R2 0.3–0.5
R2 0.0–0.3
Not available
Log(BF)
14
7
0
Recombination rate (cM/Mb)| varLD
60
40
20
0
AC006150.1
AC006150.2
AC006458.3
DGKB
AC006045.3
14831
15031
15231
Chromosome 7 position (kb)

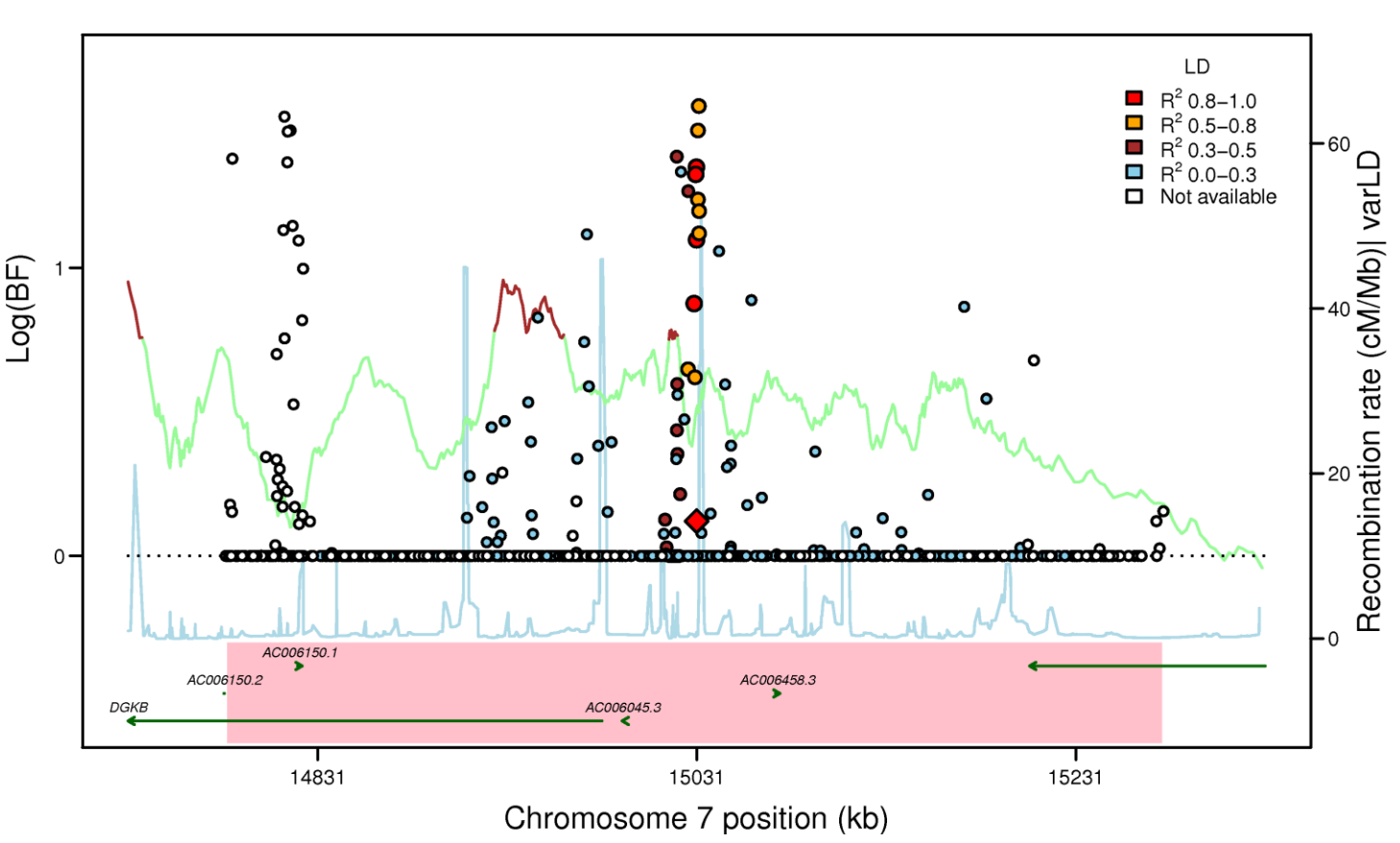
DGKB–TMEM195: rs2191349 (FG AA_MANTRA, LD: HapMap2 YRI)
LD
R2 0.8–1.0
R2 0.5–0.8
R2 0.3–0.5
R2 0.0–0.3
Not available
Log(BF)
1
0
Recombination rate (cM/Mb)| varLD
60
40
20
0
AC006150.1
AC006150.2
AC006458.3
DGKB
AC006045.3
14831
15031
15231
Chromosome 7 position (kb)

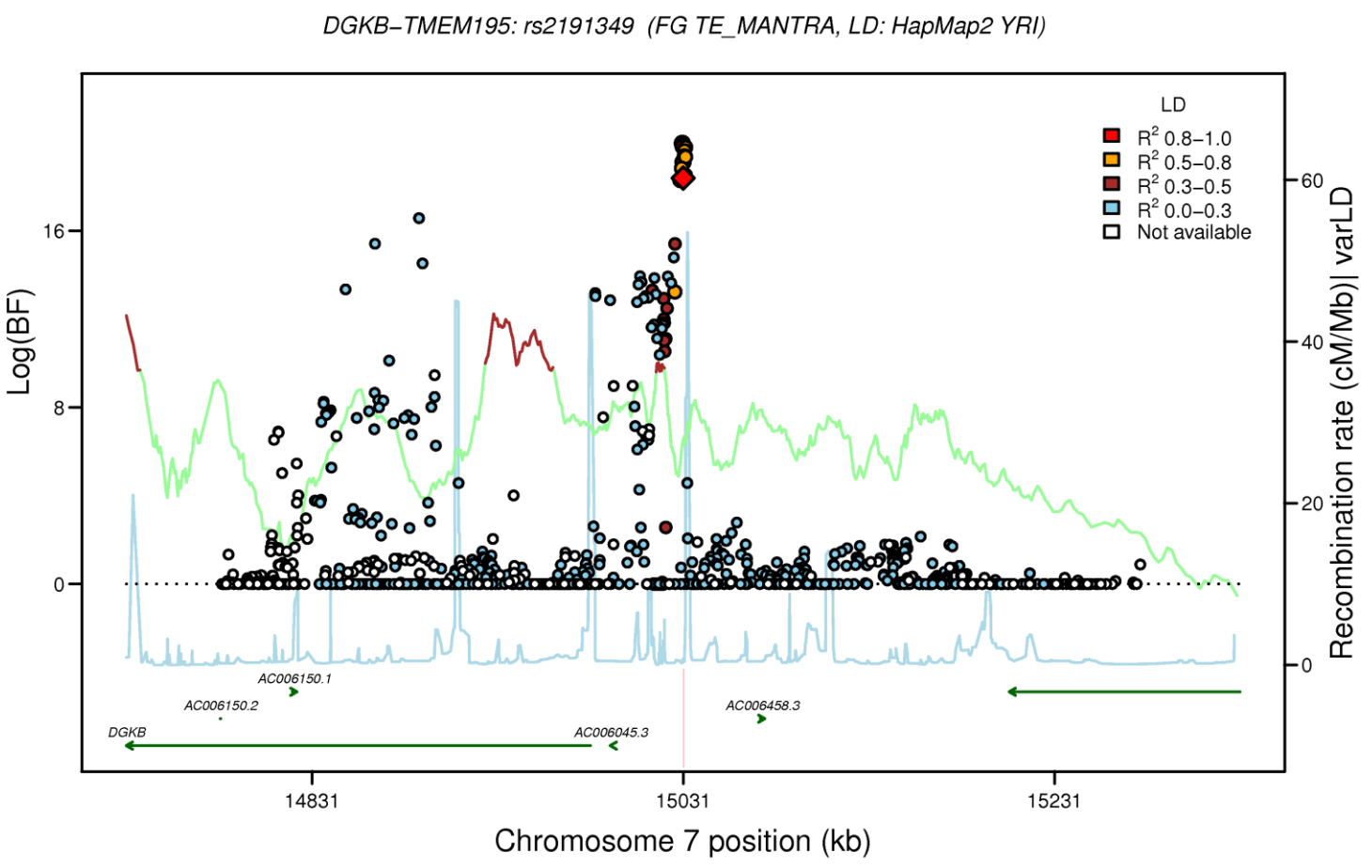
DGKB–TMEM195: rs2191349 (FG TE_MANTRA, LD: HapMap2 YRI)
LD
R2 0.8–1.0
R2 0.5–0.8
R2 0.3–0.5
R2 0.0–0.3
Not available
Log(BF)
16
8
0
Recombination rate (cM/Mb)| varLD
60
40
20
0
AC006150.1
AC006150.2
AC006458.3
DGKB
AC006045.3
14831
15031
15231
Chromosome 7 position (kb)

Figure S3N

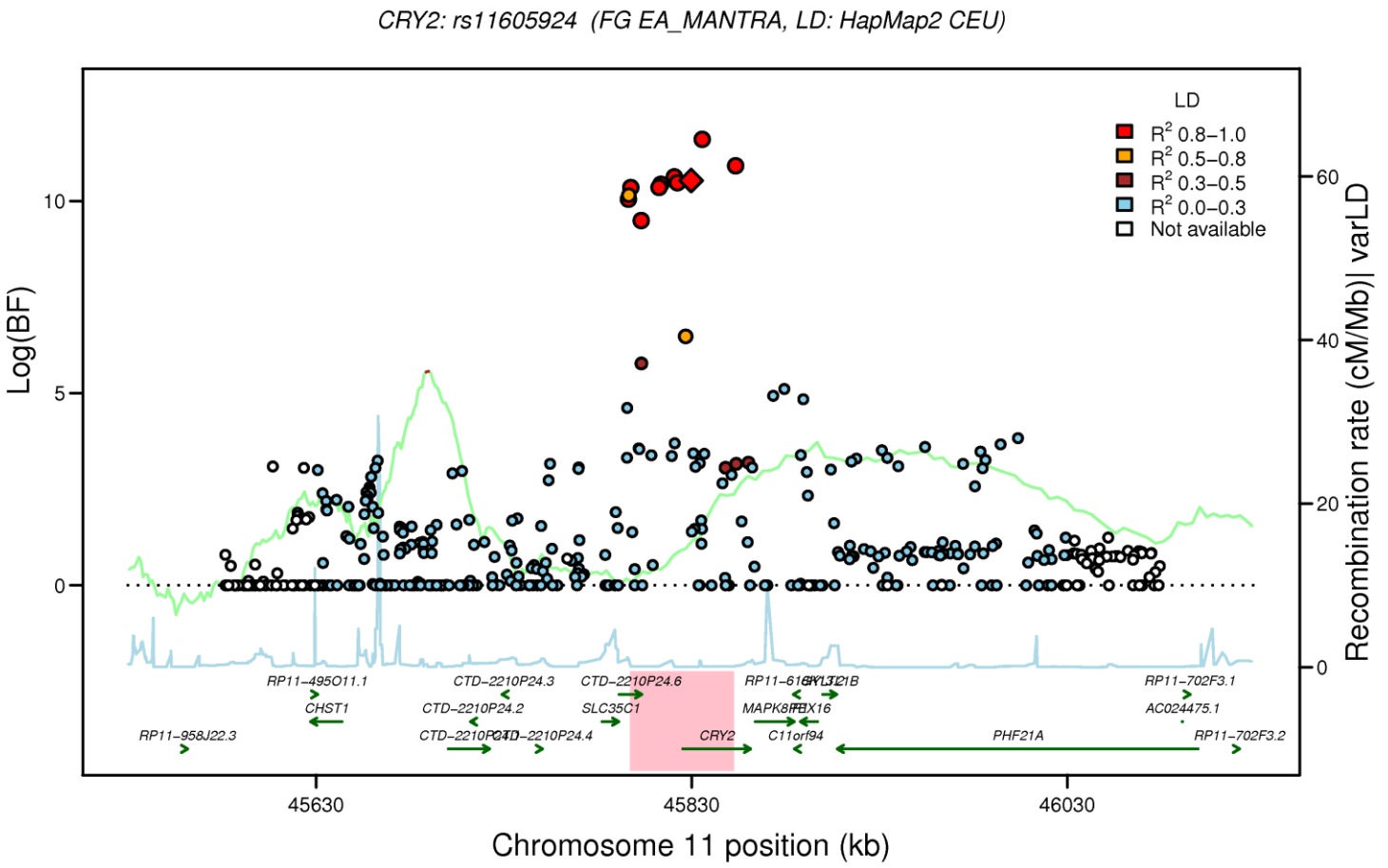
CRY2: rs11605924 (FG EA_MANTRA, LD: HapMap2 CEU)
LD
R2 0.8–1.0
R2 0.5–0.8
R2 0.3–0.5
R2 0.0–0.3
Not available
Log(BF)
Recombination rate (cM/Mb)| varLD
RP11–495O11.1
CHST1
RP11–958J22.3
CTD–2210P24.3
CTD–2210P24.2
CTD–2210P24.4
CTD–2210P24.6
SLC35C1
CRY2
C11orf94
PHF21A
RP11–702F3.1
AC024475.1
RP11–702F3.2
45630
45830
46030
Chromosome 11 position (kb)

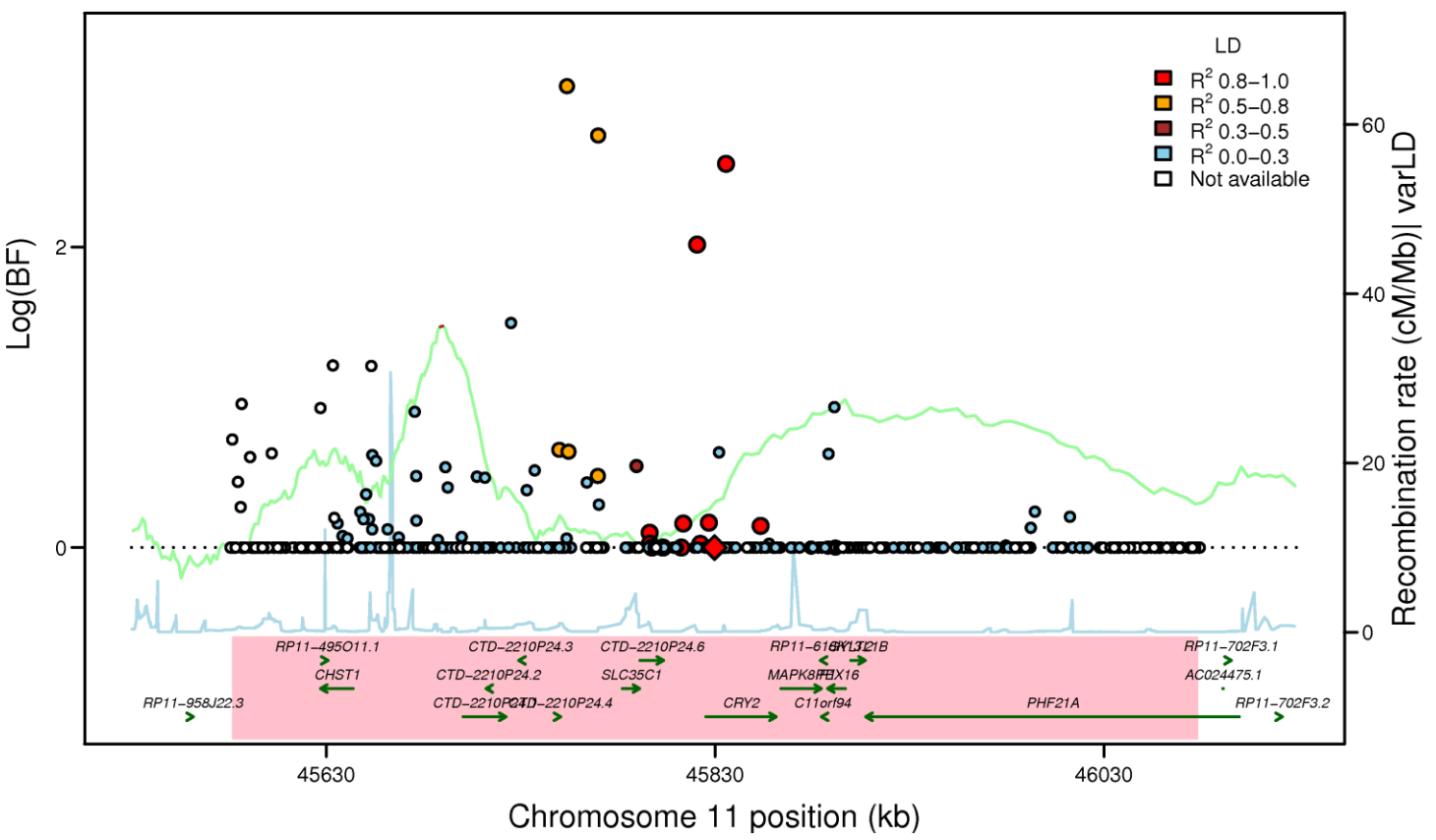
CRY2: rs11605924 (FG AA_MANTRA, LD: HapMap2 YRI)
LD
R2 0.8–1.0
R2 0.5–0.8
R2 0.3–0.5
R2 0.0–0.3
Not available
Log(BF)
Recombination rate (cM/Mb)| varLD
RP11–495O11.1
CHST1
RP11–958J22.3
CTD–2210P24.3
CTD–2210P24.2
CTD–2210P24.4
CTD–2210P24.6
SLC35C1
CRY2
C11orf94
PHF21A
RP11–702F3.1
AC024475.1
RP11–702F3.2
45630
45830
46030
Chromosome 11 position (kb)

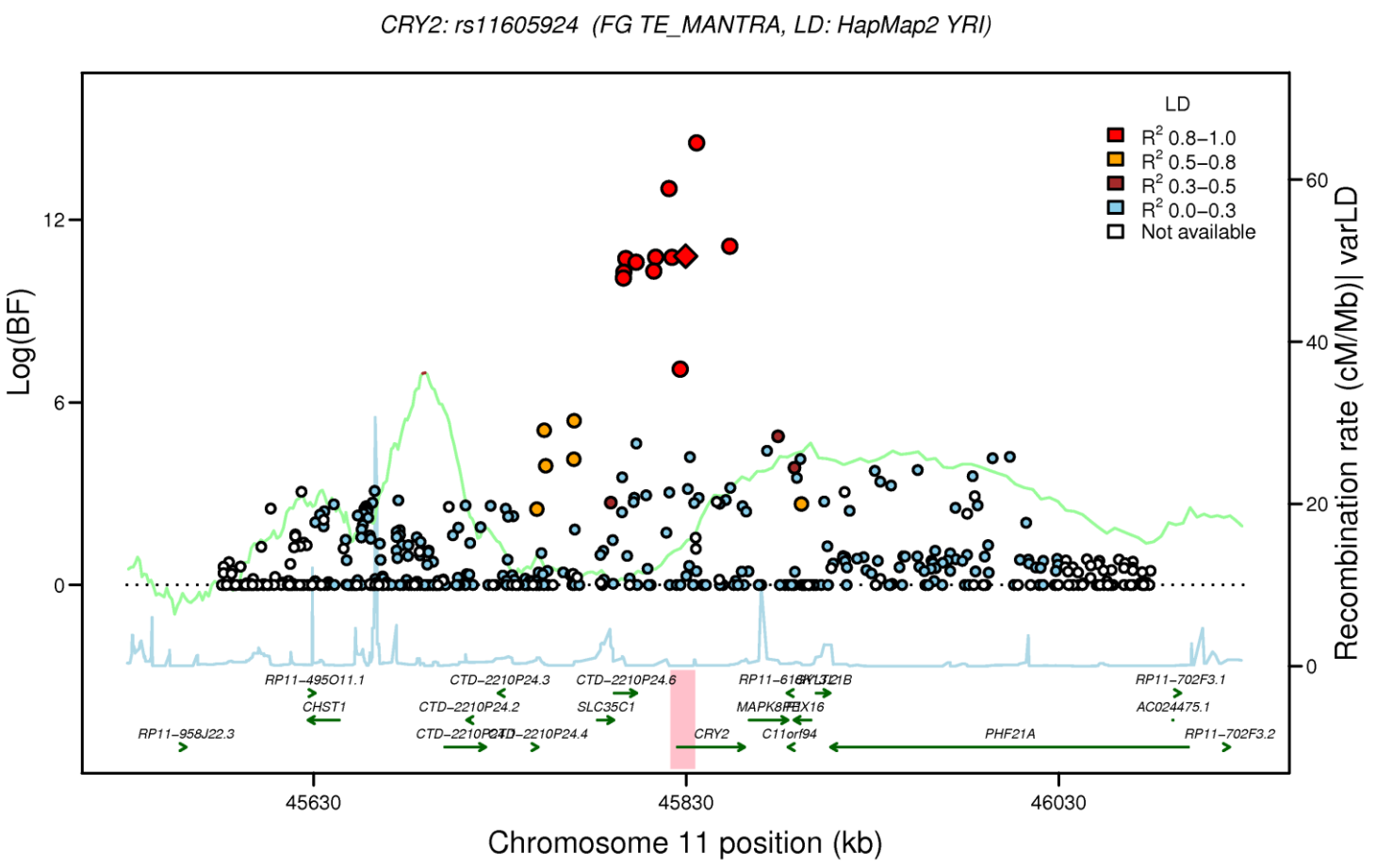
CRY2: rs11605924 (FG TE_MANTRA, LD: HapMap2 YRI)
LD
R2 0.8–1.0
R2 0.5–0.8
R2 0.3–0.5
R2 0.0–0.3
Not available
Log(BF)
Recombination rate (cM/Mb)| varLD
RP11–495O11.1
CHST1
RP11–958J22.3
CTD–2210P24.3
CTD–2210P24.2
CTD–2210P24.4
CTD–2210P24.6
SLC35C1
CRY2
C11orf94
PHF21A
RP11–702F3.1
AC024475.1
RP11–702F3.2
45630
45830
46030
Chromosome 11 position (kb)

Figure S3O

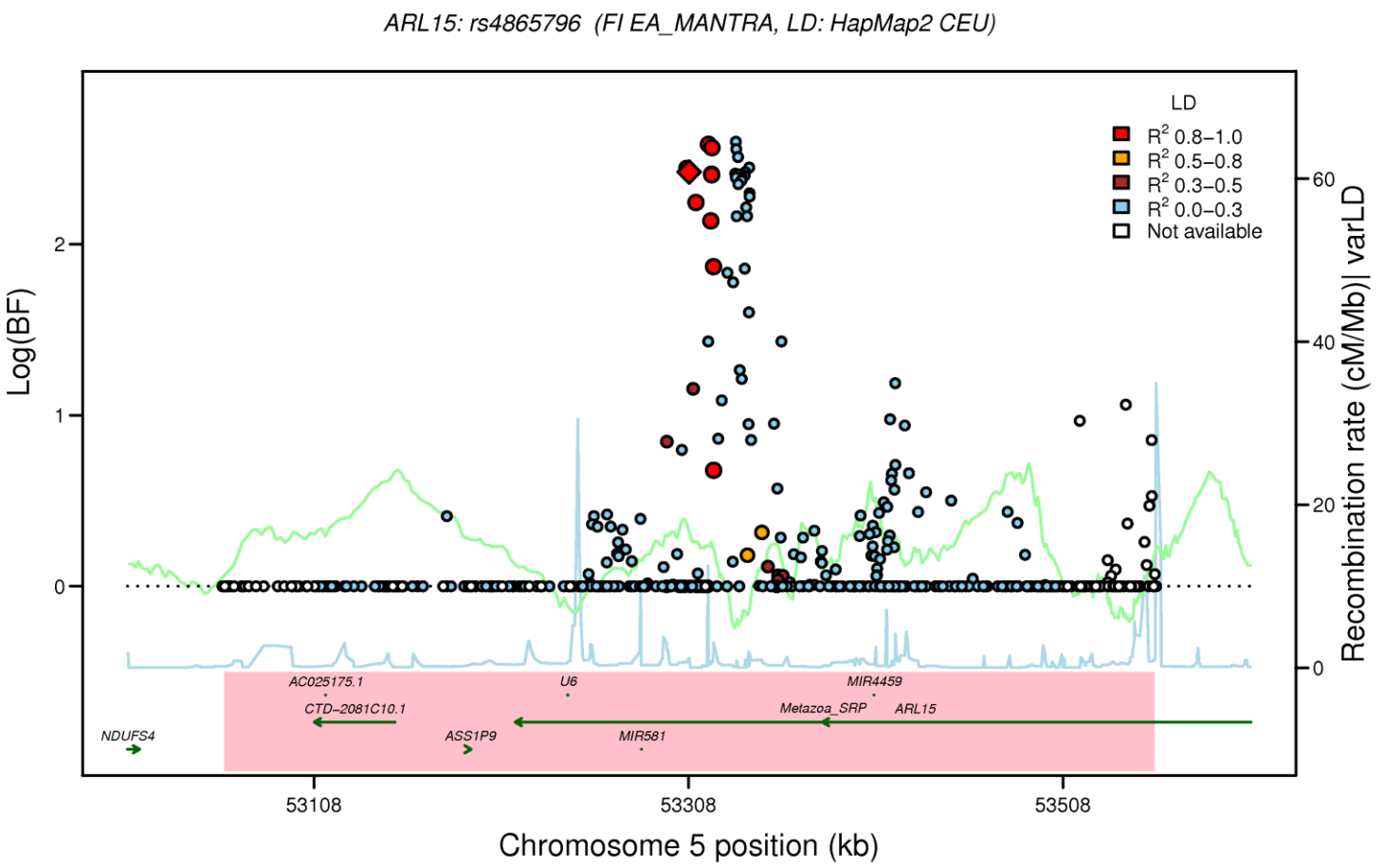
ARL15: rs4865796 (FI EA_MANTRA, LD: HapMap2 CEU)
LD
R2 0.8–1.0
R2 0.5–0.8
R2 0.3–0.5
R2 0.0–0.3
Not available
Log(BF)
Recombination rate (cM/Mb)| varLD
AC025175.1
CTD–2081C10.1
U6
MIR4459
Metazoa_SRP
ARL15
NDUFS4
ASS1P9
MIR581
53108
53308
53508
Chromosome 5 position (kb)

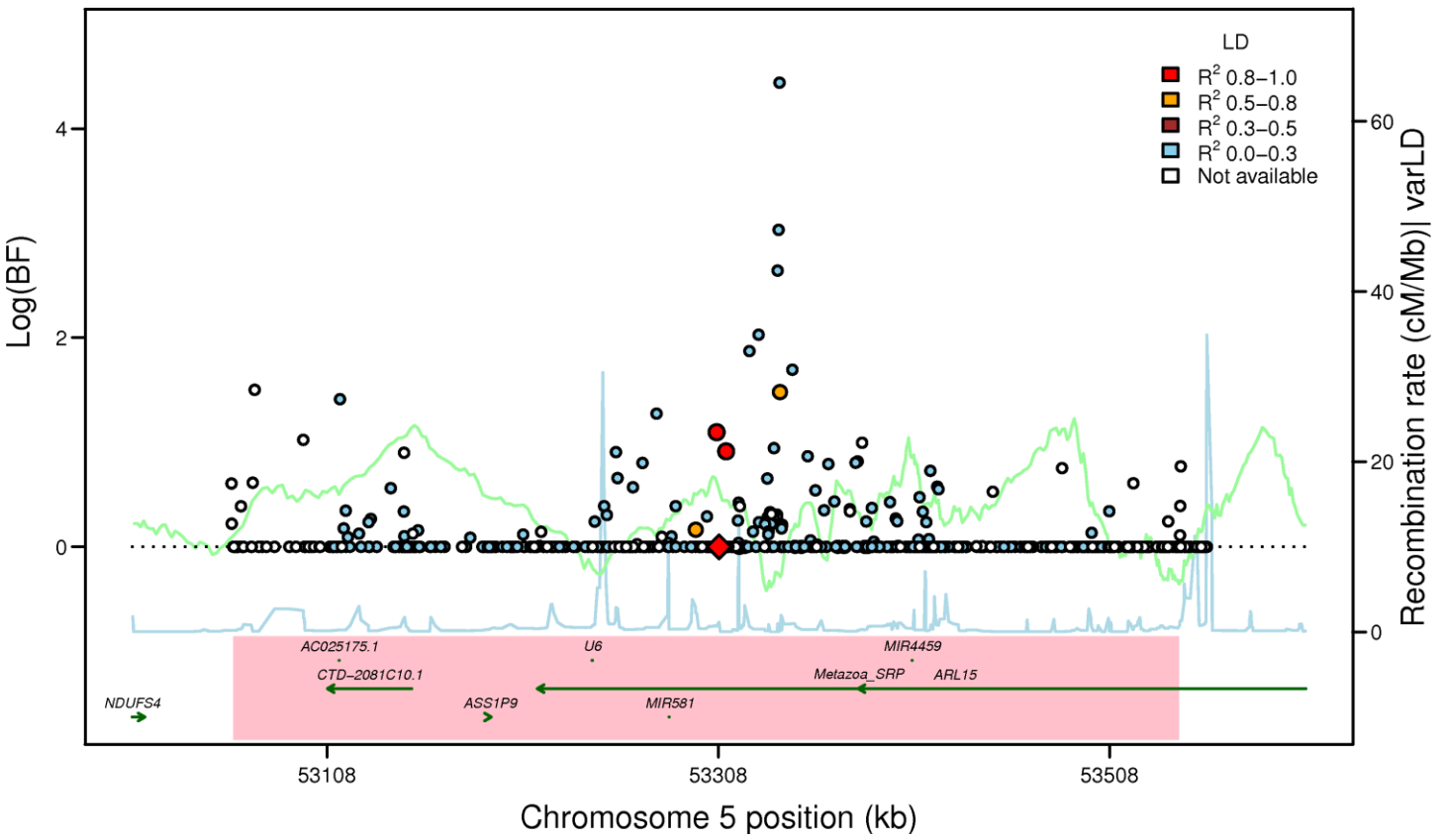
ARL15: rs4865796 (FI AA_MANTRA, LD: HapMap2 YRI)
LD
R2 0.8–1.0
R2 0.5–0.8
R2 0.3–0.5
R2 0.0–0.3
Not available
Log(BF)
Recombination rate
AC025175.1
CTD–2081C10.1
U6
MIR4459
Metazoa_SRP
ARL15
NDUFS4
ASS1P9
MIR581
53108
53308
53508
Chromosome 5 position (kb)

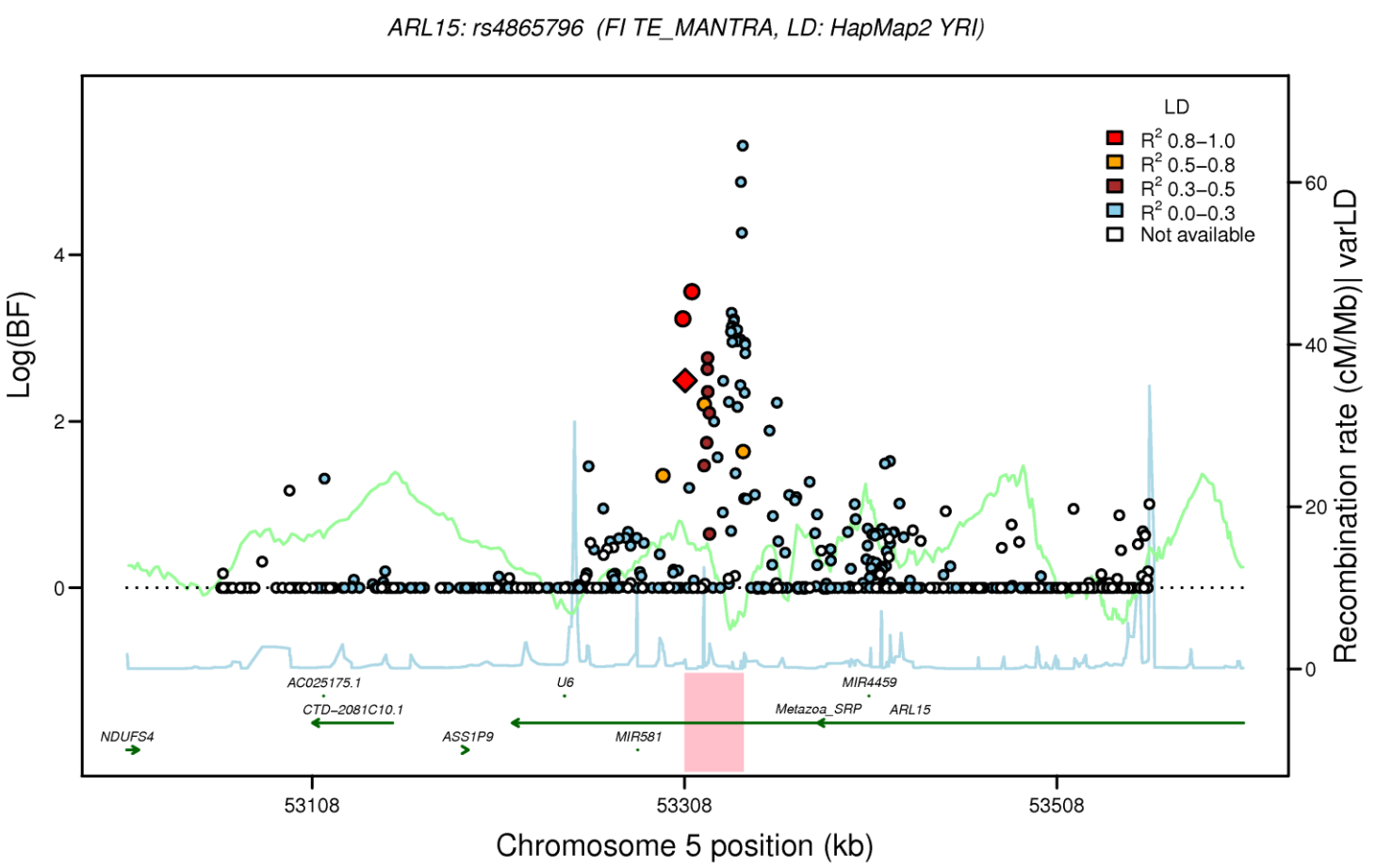
ARL15: rs4865796 (FI TE_MANTRA, LD: HapMap2 YRI)
LD
R2 0.8–1.0
R2 0.5–0.8
R2 0.3–0.5
R2 0.0–0.3
Not available
Log(BF)
Recombination rate (cM/Mb)| varLD
AC025175.1
CTD–2081C10.1
U6
MIR4459
Metazoa_SRP
ARL15
NDUFS4
ASS1P9
MIR581
53108
53308
53508
Chromosome 5 position (kb)

Figure S3P

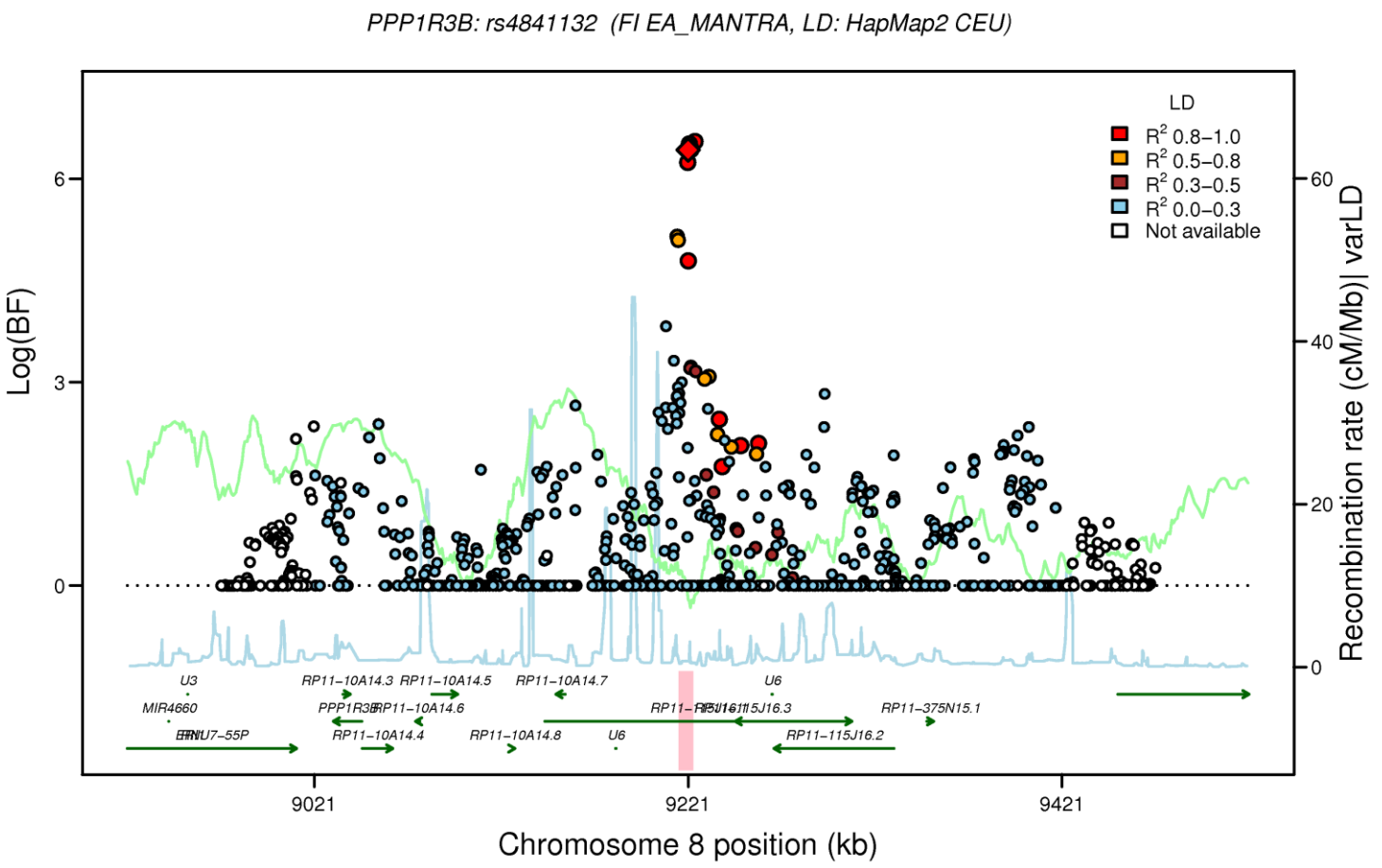
PPP1R3B: rs4841132 (FI EA_MANTRA, LD: HapMap2 CEU)
LD
R2 0.8–1.0
R2 0.5–0.8
R2 0.3–0.5
R2 0.0–0.3
Not available
Log(BF)
Recombination rate (cM/Mb)| varLD
Chromosome 8 position (kb)
9021
9221
9421
U3
MIR4660
RP11–10A14.3
RP11–10A14.5
RP11–10A14.7
U6
RP11–375N15.1
RP11–10A14.4
RP11–10A14.8
RP11–115J16.2

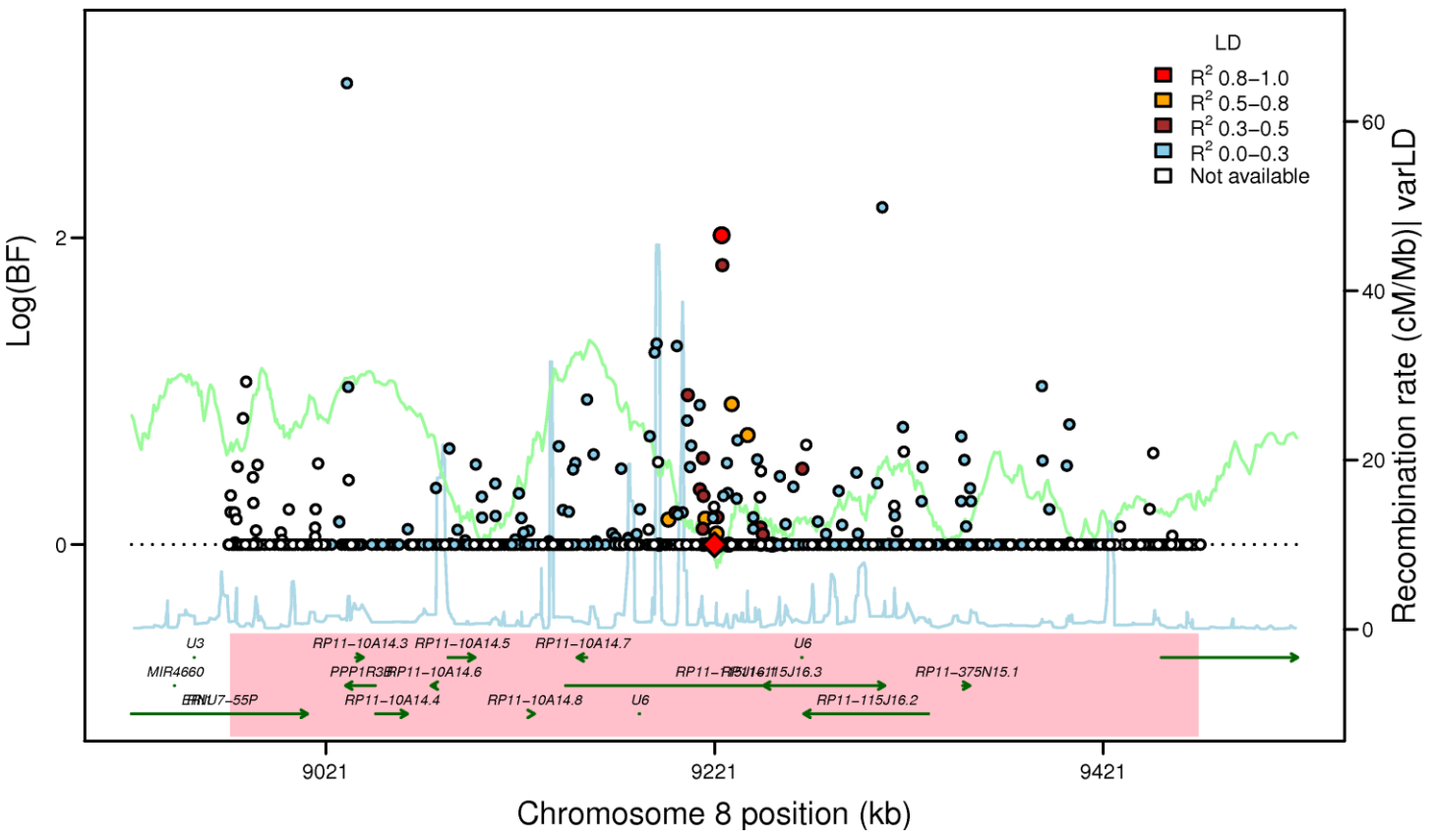
PPP1R3B: rs4841132 (FI AA_MANTRA, LD: HapMap2 YRI)
LD
R2 0.8–1.0
R2 0.5–0.8
R2 0.3–0.5
R2 0.0–0.3
Not available
Log(BF)
Recombination rate (cM/Mb)| varLD
Chromosome 8 position (kb)
9021
9221
9421
U3
MIR4660
RP11–10A14.3
RP11–10A14.5
RP11–10A14.7
U6
RP11–375N15.1
RP11–10A14.4
RP11–10A14.8
RP11–115J16.2

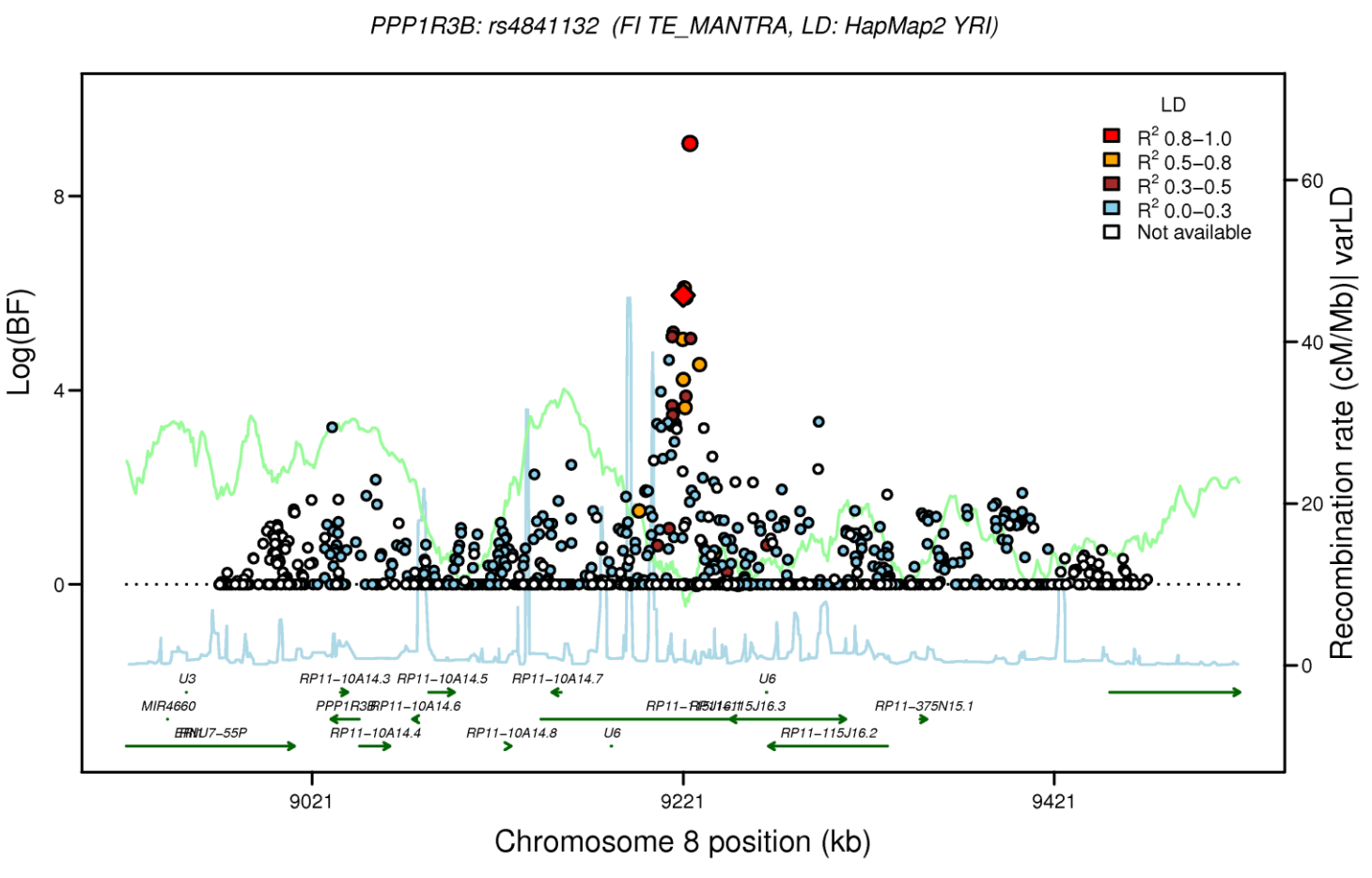
PPP1R3B: rs4841132 (FI TE_MANTRA, LD: HapMap2 YRI)
LD
R2 0.8–1.0
R2 0.5–0.8
R2 0.3–0.5
R2 0.0–0.3
Not available
Log(BF)
Recombination rate (cM/Mb)| varLD
Chromosome 8 position (kb)
9021
9221
9421
U3
MIR4660
RP11–10A14.3
RP11–10A14.5
RP11–10A14.7
U6
RP11–375N15.1
RP11–10A14.4
RP11–10A14.8
RP11–115J16.2

Figure S3Q

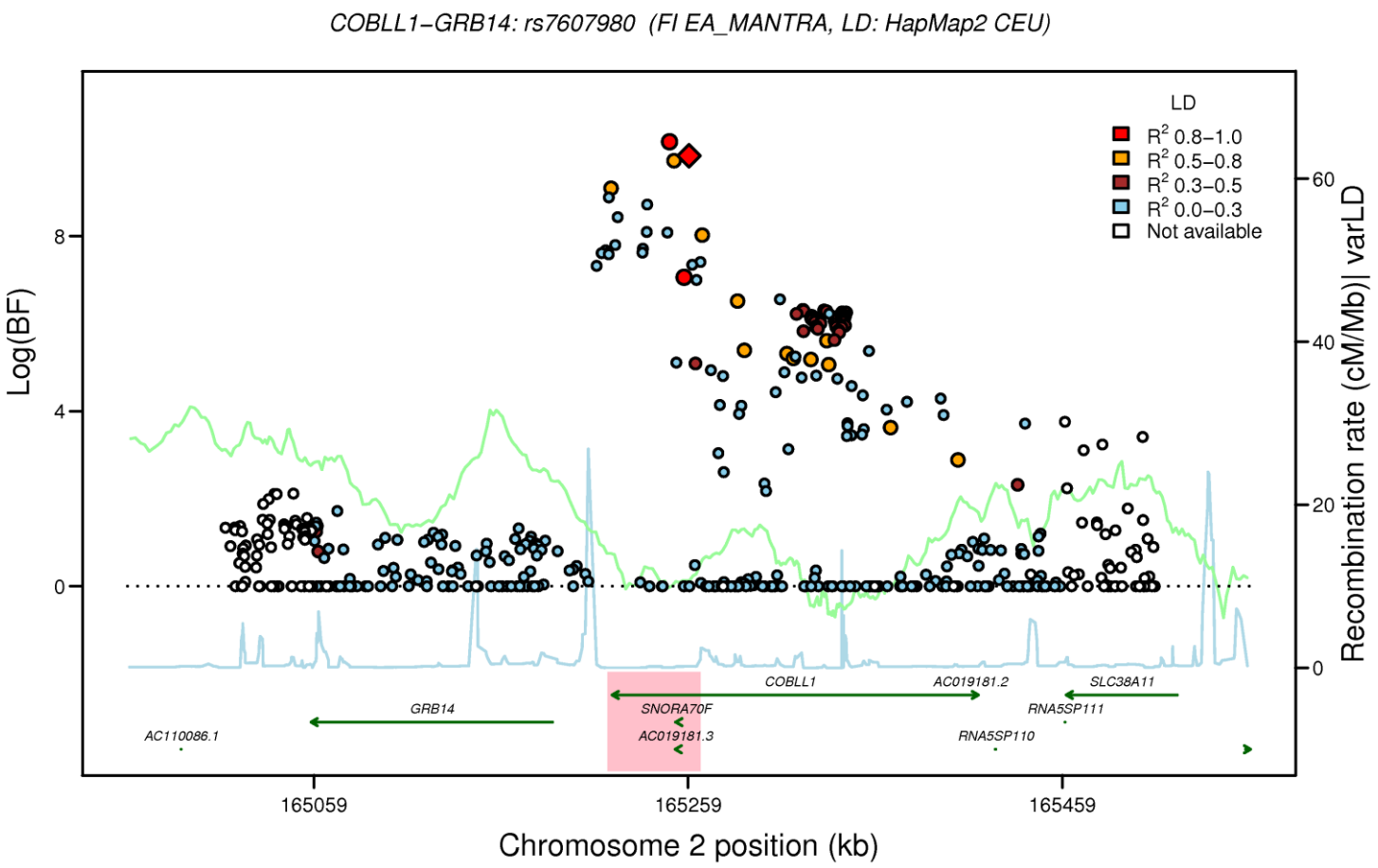
COBLL1–GRB14: rs7607980 (FI EA_MANTRA, LD: HapMap2 CEU)
LD
R2 0.8–1.0
R2 0.5–0.8
R2 0.3–0.5
R2 0.0–0.3
Not available
Log(BF)
Recombination rate (cM/Mb)| varLD
COBLL1
AC019181.2
SLC38A11
GRB14
SNORA70F
RNA5SP111
AC110086.1
AC019181.3
RNA5SP110
165059
165259
165459
Chromosome 2 position (kb)

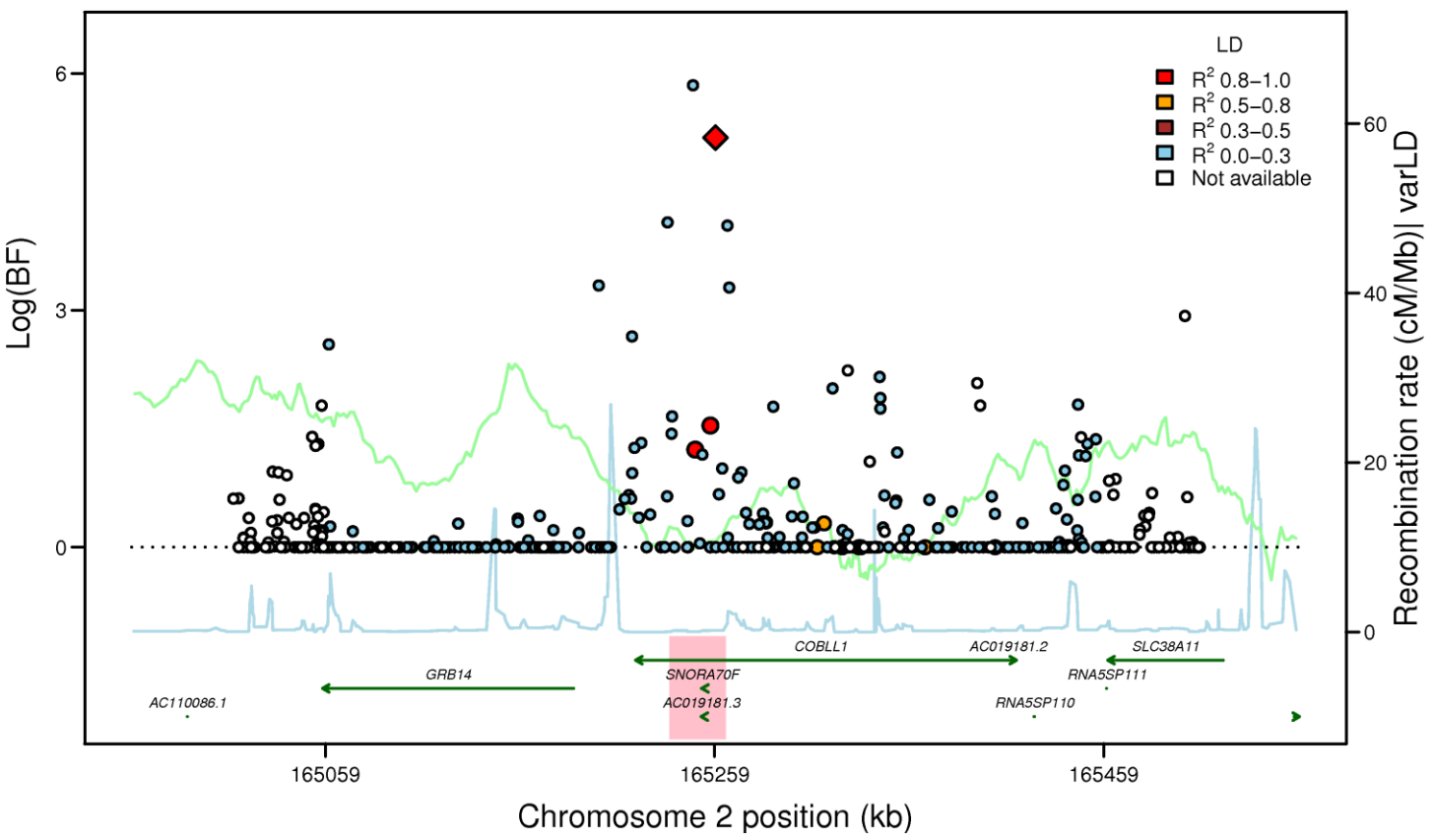
COBLL1–GRB14: rs7607980 (FI AA_MANTRA, LD: HapMap2 YRI)
LD
R2 0.8–1.0
R2 0.5–0.8
R2 0.3–0.5
R2 0.0–0.3
Not available
Log(BF)
Recombination rate (cM/Mb)| varLD
COBLL1
AC019181.2
SLC38A11
GRB14
SNORA70F
RNA5SP111
AC110086.1
AC019181.3
RNA5SP110
165059
165259
165459
Chromosome 2 position (kb)

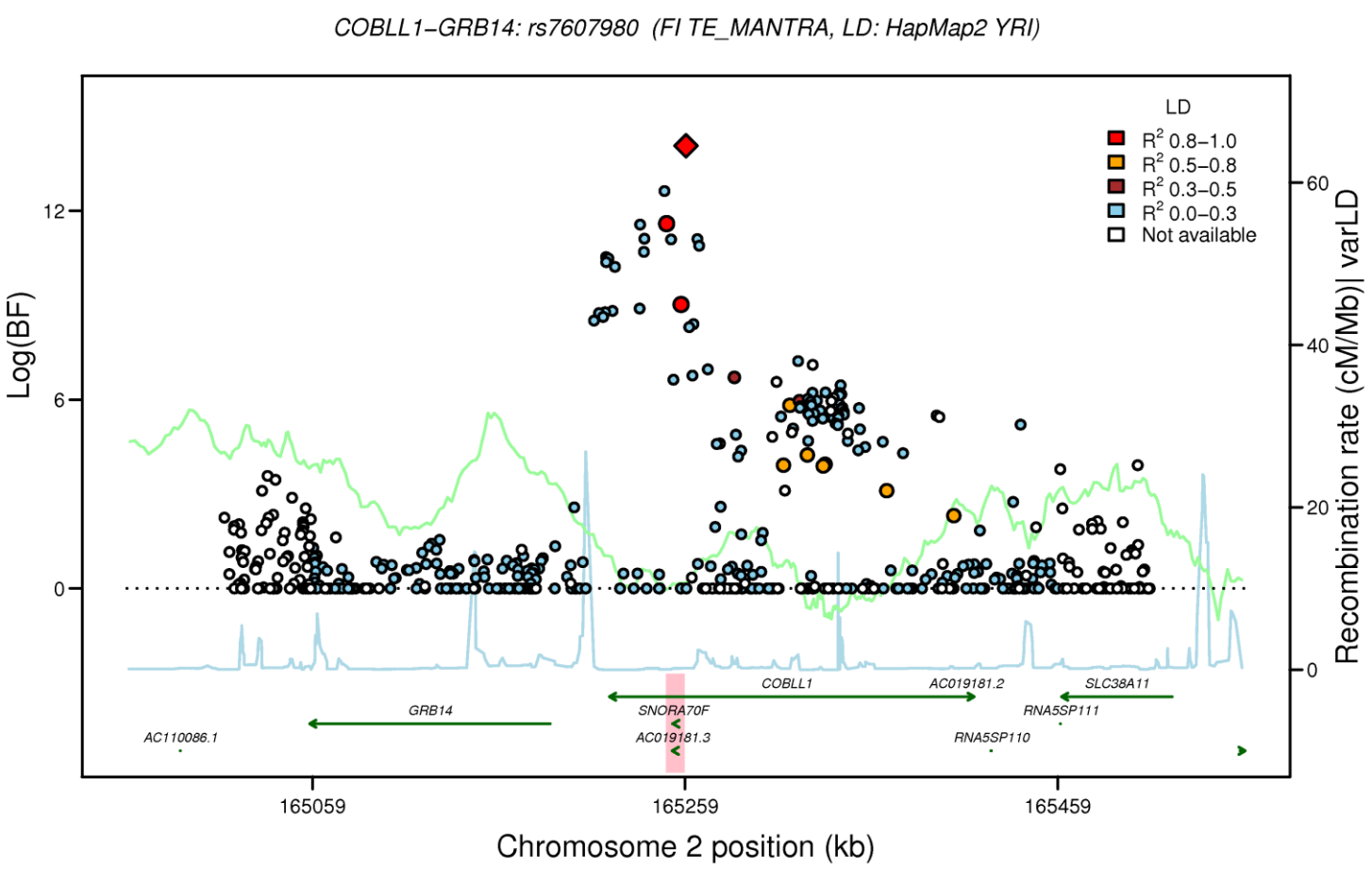
COBLL1–GRB14: rs7607980 (FI TE_MANTRA, LD: HapMap2 YRI)
LD
R2 0.8–1.0
R2 0.5–0.8
R2 0.3–0.5
R2 0.0–0.3
Not available
Log(BF)
Recombination rate (cM/Mb)| varLD
COBLL1
AC019181.2
SLC38A11
GRB14
SNORA70F
RNA5SP111
AC110086.1
AC019181.3
RNA5SP110
165059
165259
165459
Chromosome 2 position (kb)

Figure S3R

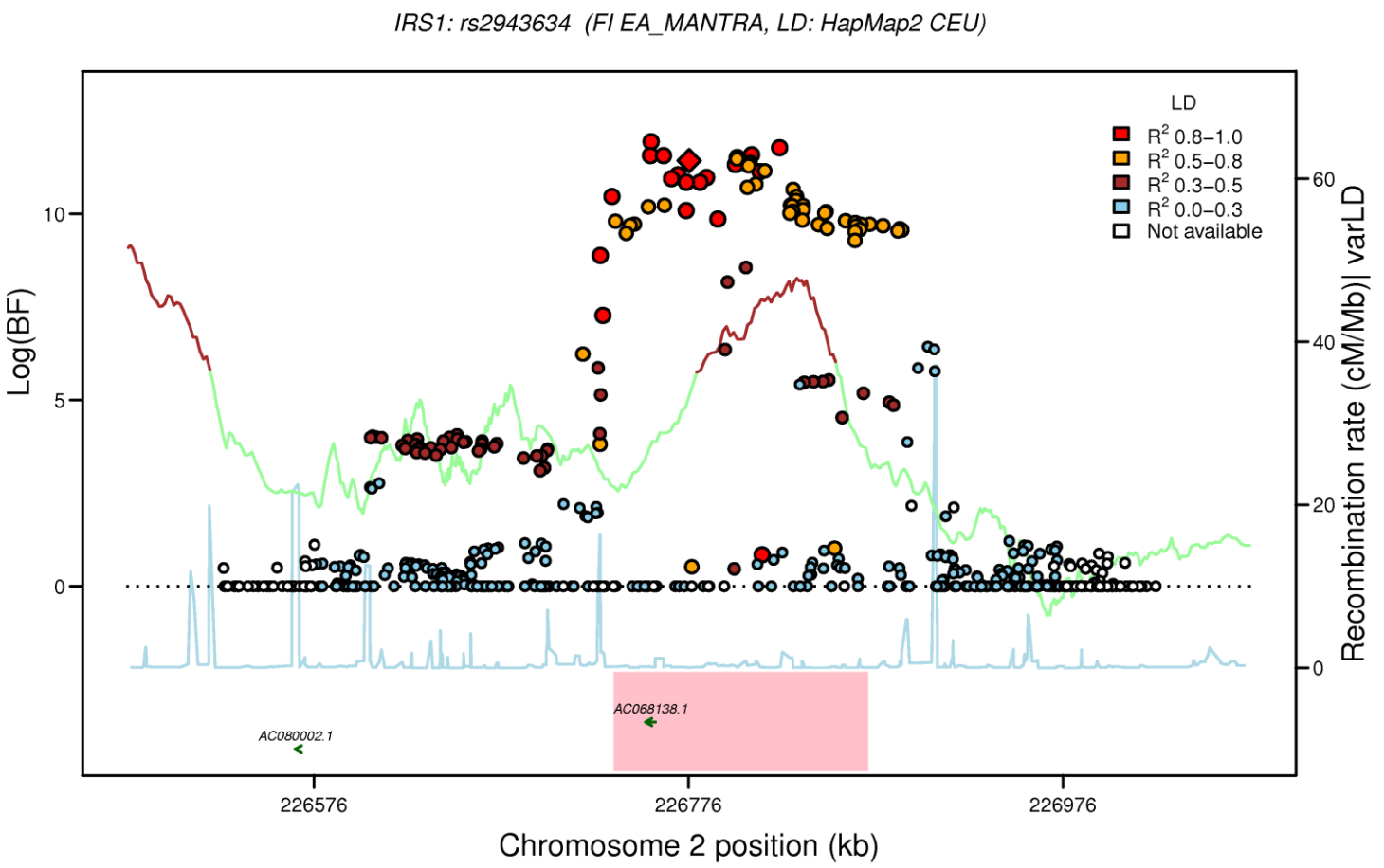
IRS1: rs2943634 (FI EA_MANTRA, LD: HapMap2 CEU)
LD
R² 0.8–1.0
R² 0.5–0.8
R² 0.3–0.5
R² 0.0–0.3
Not available
Log(BF)
Recombination rate (cM/Mb)| varLD
AC080002.1
AC068138.1
226576
226776
226976
Chromosome 2 position (kb)

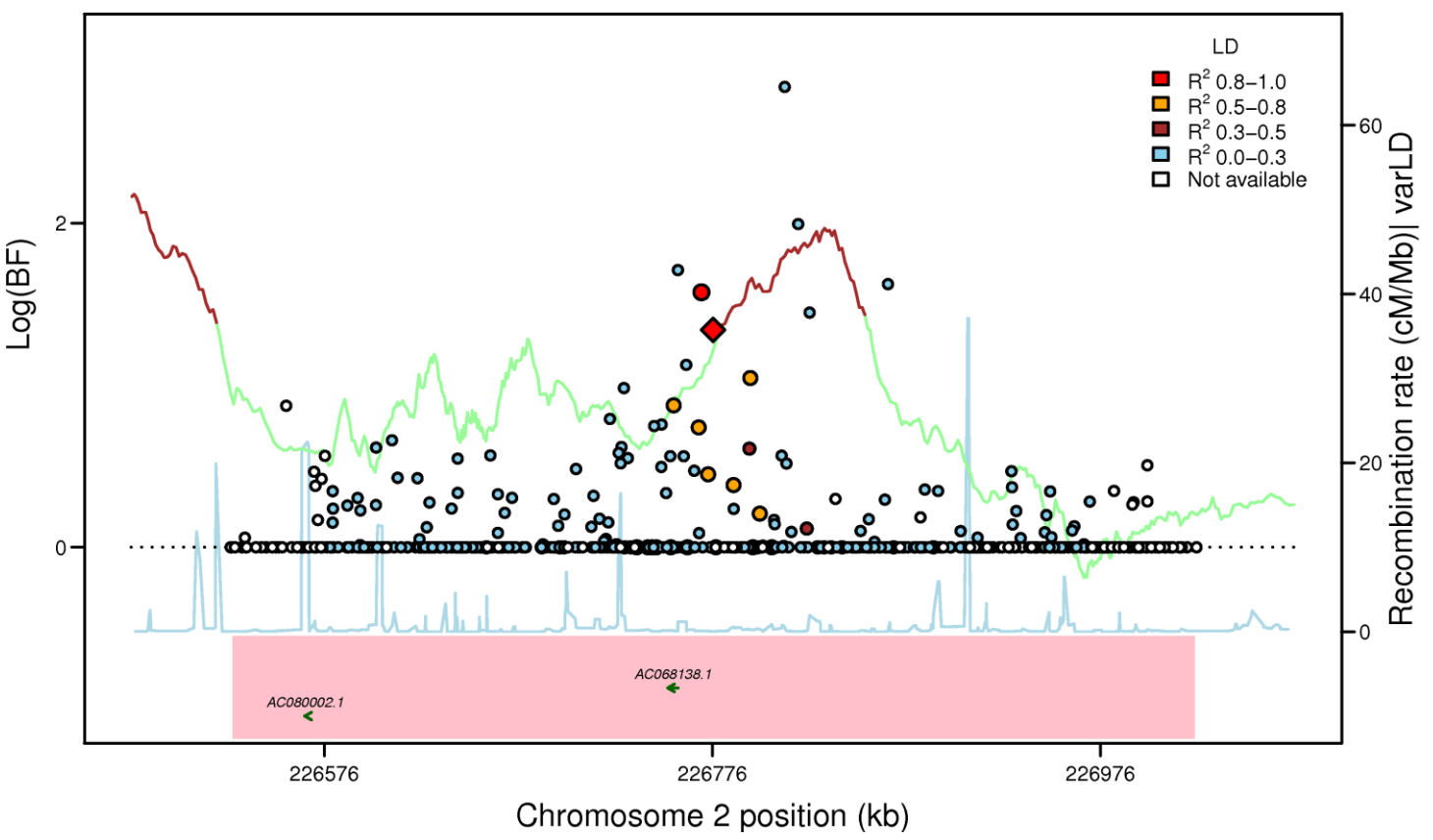
IRS1: rs2943634 (FI AA_MANTRA, LD: HapMap2 YRI)
LD
R² 0.8–1.0
R² 0.5–0.8
R² 0.3–0.5
R² 0.0–0.3
Not available
Log(BF)
Recombination rate (cM/Mb)| varLD
AC080002.1
AC068138.1
226576
226776
226976
Chromosome 2 position (kb)

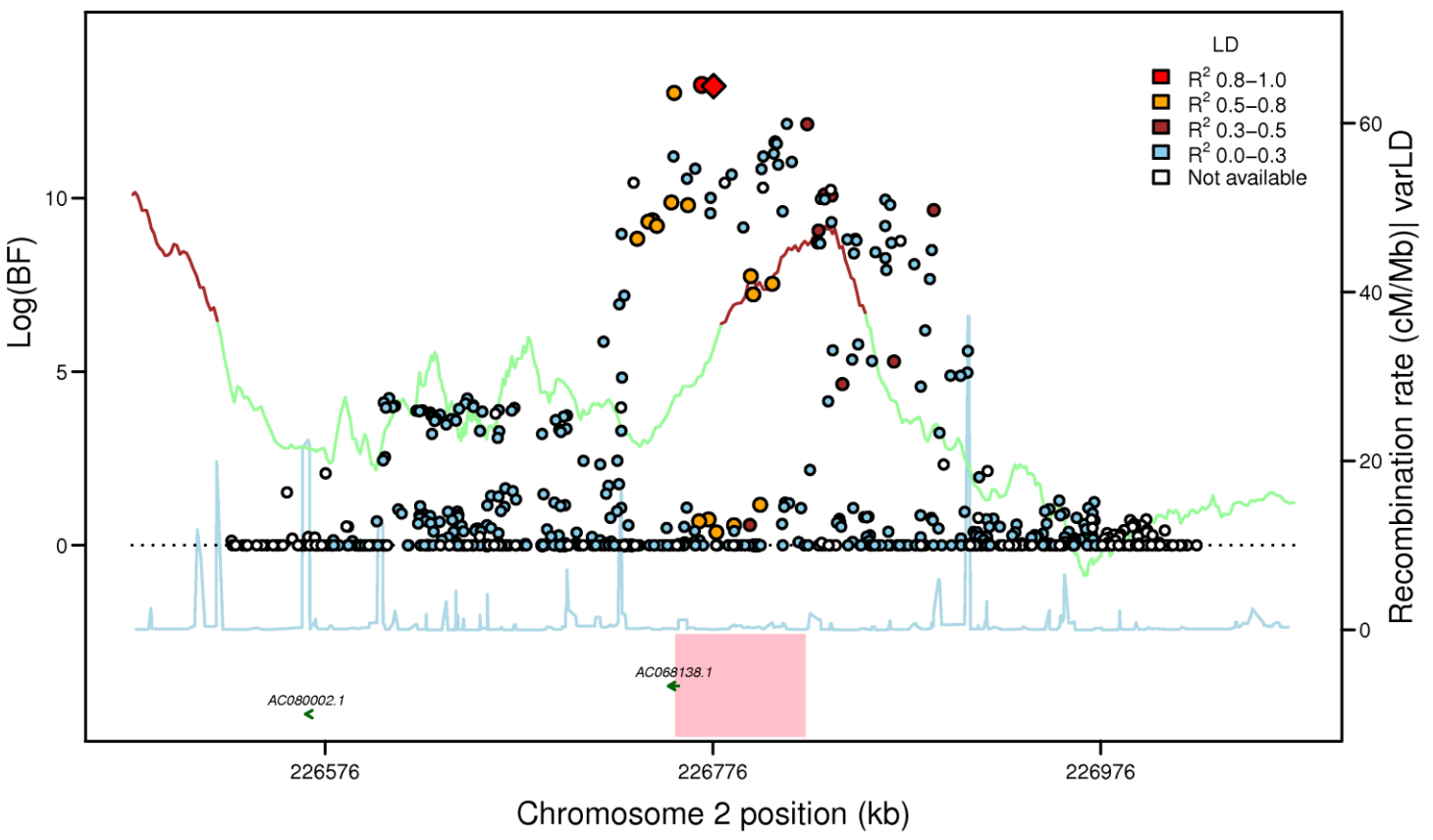
IRS1: rs2943634 (FI TE_MANTRA, LD: HapMap2 YRI)
LD
R² 0.8–1.0
R² 0.5–0.8
R² 0.3–0.5
R² 0.0–0.3
Not available
Log(BF)
Recombination rate (cM/Mb)| varLD
AC080002.1
AC068138.1
226576
226776
226976
Chromosome 2 position (kb)

Figure S3S

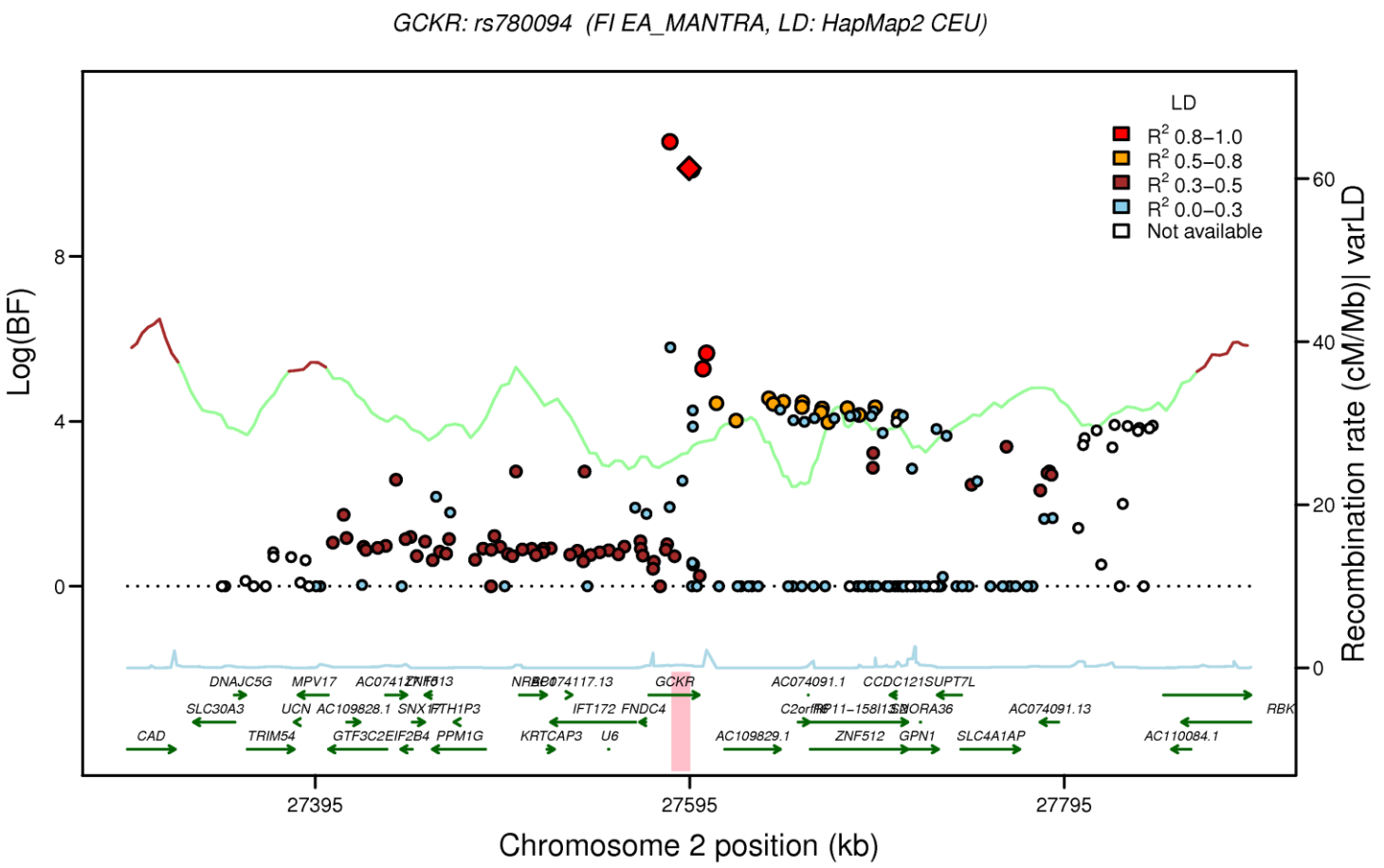
GCKR: rs780094 (FI EA_MANTRA, LD: HapMap2 CEU)
LD
R2 0.8–1.0
R2 0.5–0.8
R2 0.3–0.5
R2 0.0–0.3
Not available
Log(BF)
Recombination rate (cM/Mb)| varLD
27395
27595
27795
Chromosome 2 position (kb)
DNAJC5G MPV17 SLC30A3 UCN AC109828.1 SNX17 FTH1P3 IFT172 FNDC4 GCKR AC074091.1 CCDC121SUPT7L SLCO4A1-AS1 SLCORA36 AC074091.13 RBK
CAD TRIM54 GTF3C2 EIF2B4 PPM1G KRTCAP3 U6 AC109829.1 ZNF512 GPN1 SLC4A1AP AC110084.1

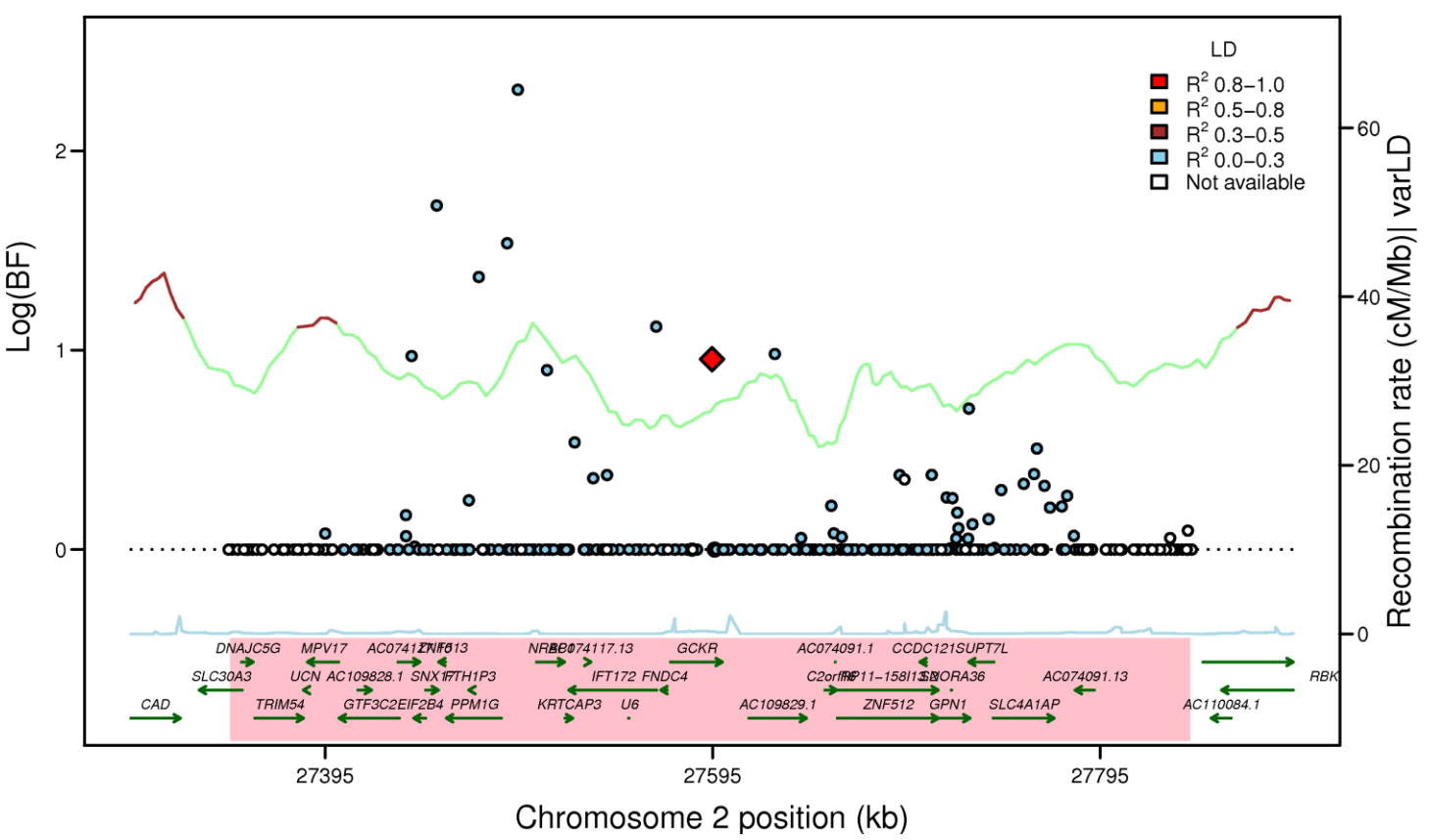
GCKR: rs780094 (FI AA_MANTRA, LD: HapMap2 YRI)
LD
R2 0.8–1.0
R2 0.5–0.8
R2 0.3–0.5
R2 0.0–0.3
Not available
Log(BF)
Recombination rate (cM/Mb)| varLD
27395
27595
27795
Chromosome 2 position (kb)
DNAJC5G MPV17 SLC30A3 UCN AC109828.1 SNX17 FTH1P3 IFT172 FNDC4 GCKR AC074091.1 CCDC121SUPT7L SLCO4A1-AS1 SLCORA36 AC074091.13 RBK
CAD TRIM54 GTF3C2 EIF2B4 PPM1G KRTCAP3 U6 AC109829.1 ZNF512 GPN1 SLC4A1AP AC110084.1

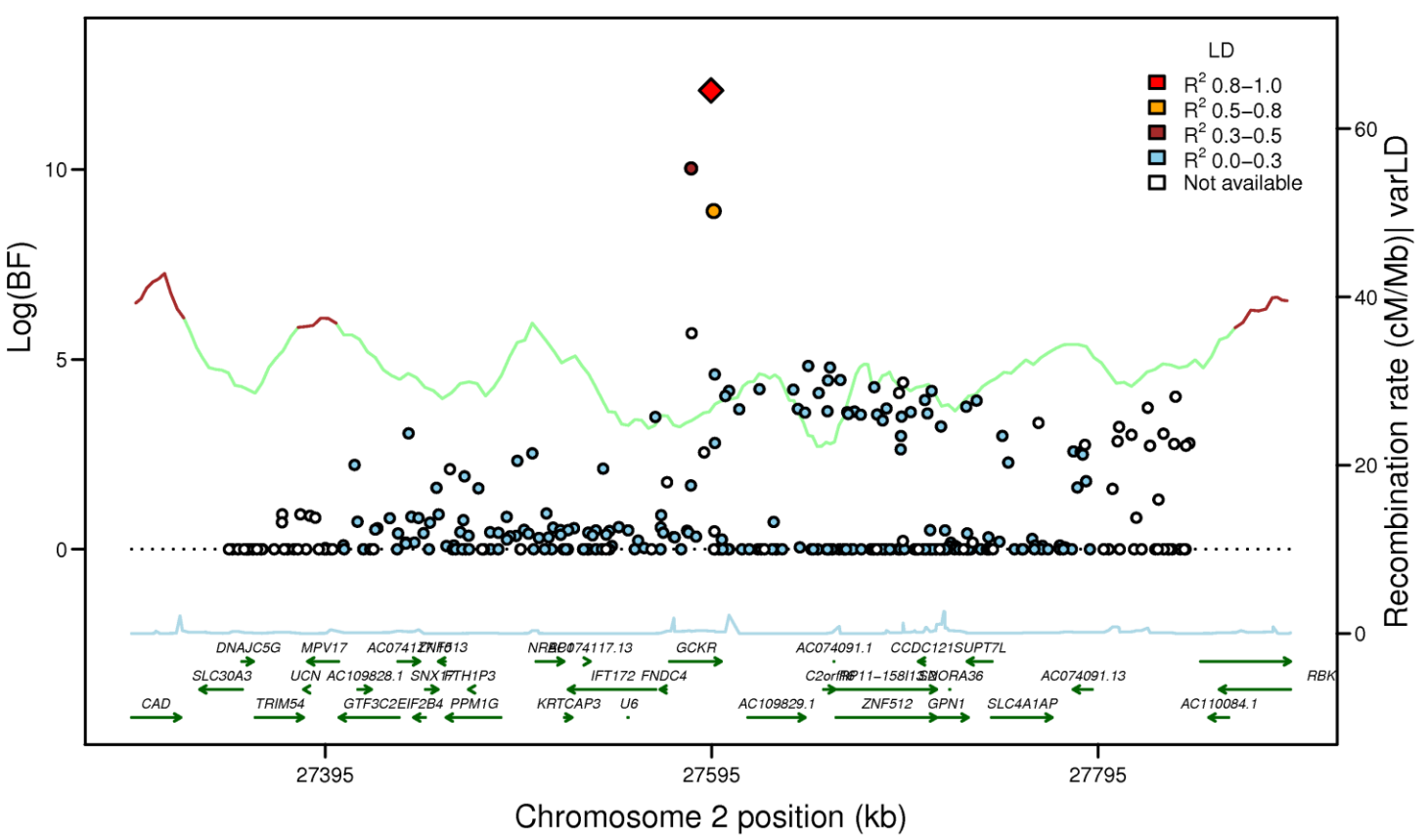
GCKR: rs780094 (FI TE_MANTRA, LD: HapMap2 YRI)
LD
R2 0.8–1.0
R2 0.5–0.8
R2 0.3–0.5
R2 0.0–0.3
Not available
Log(BF)
Recombination rate (cM/Mb)| varLD
27395
27595
27795
Chromosome 2 position (kb)
DNAJC5G MPV17 SLC30A3 UCN AC109828.1 SNX17 FTH1P3 IFT172 FNDC4 GCKR AC074091.1 CCDC121SUPT7L SLCO4A1-AS1 SLCORA36 AC074091.13 RBK
CAD TRIM54 GTF3C2 EIF2B4 PPM1G KRTCAP3 U6 AC109829.1 ZNF512 GPN1 SLC4A1AP AC110084.1

Figure S3T

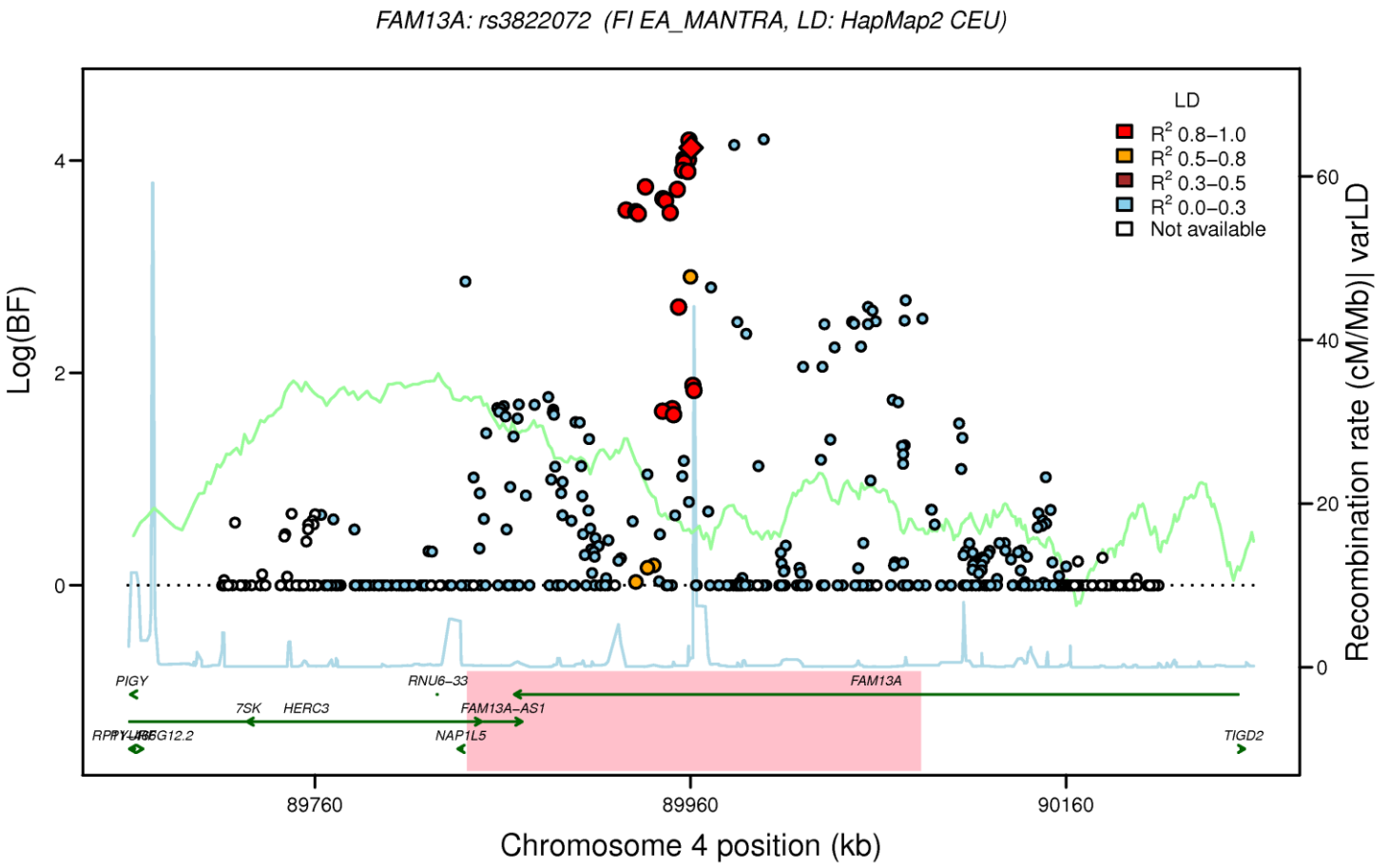
FAM13A: rs3822072 (FI EA_MANTRA, LD: HapMap2 CEU)
LD
R2 0.8–1.0
R2 0.5–0.8
R2 0.3–0.5
R2 0.0–0.3
Not available
Log(BF)
Recombination rate (cM/Mb)| varLD
PIGY
RNU6–33
FAM13A
7SK
HERC3
FAM13A–AS1
NAP1L5
TIGD2
89760
89960
90160
Chromosome 4 position (kb)

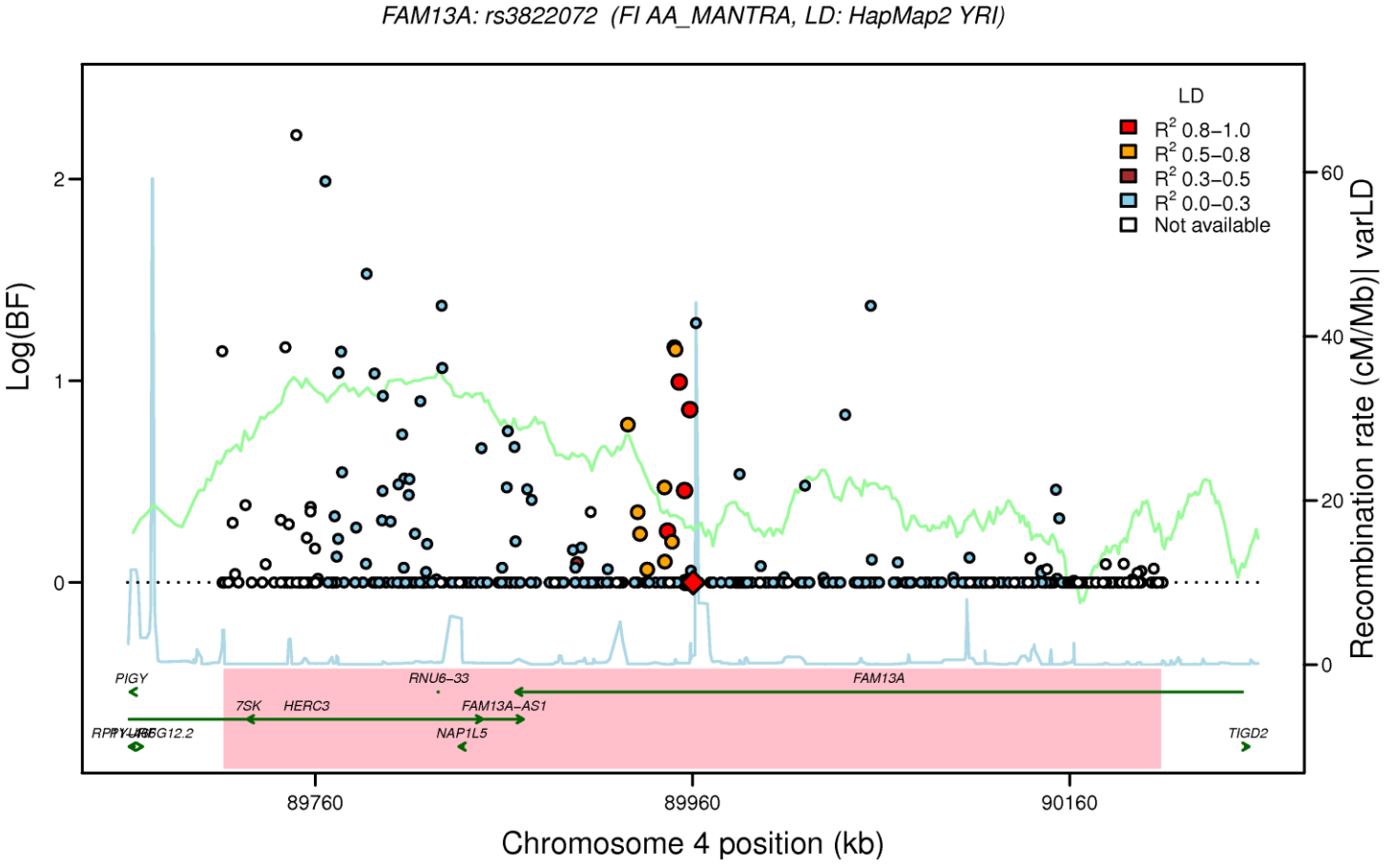
FAM13A: rs3822072 (FI AA_MANTRA, LD: HapMap2 YRI)
LD
R2 0.8–1.0
R2 0.5–0.8
R2 0.3–0.5
R2 0.0–0.3
Not available
Log(BF)
Recombination rate (cM/Mb)| varLD
PIGY
RNU6–33
FAM13A
7SK
HERC3
FAM13A–AS1
NAP1L5
TIGD2
89760
89960
90160
Chromosome 4 position (kb)

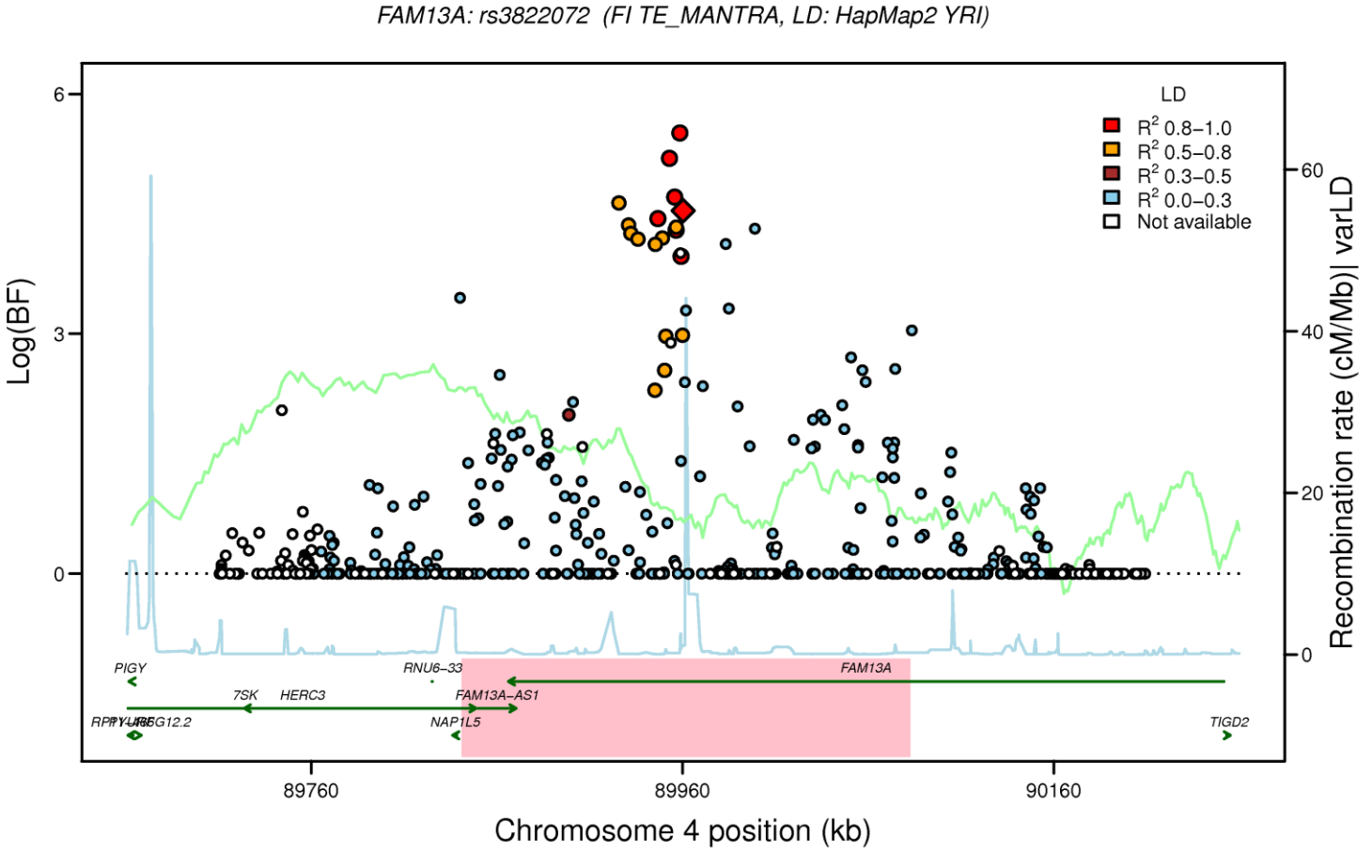
FAM13A: rs3822072 (FI TE_MANTRA, LD: HapMap2 YRI)
LD
R2 0.8–1.0
R2 0.5–0.8
R2 0.3–0.5
R2 0.0–0.3
Not available
Log(BF)
Recombination rate (cM/Mb)| varLD
PIGY
RNU6–33
FAM13A
7SK
HERC3
FAM13A–AS1
NAP1L5
TIGD2
89760
89960
90160
Chromosome 4 position (kb)

Figure S3U

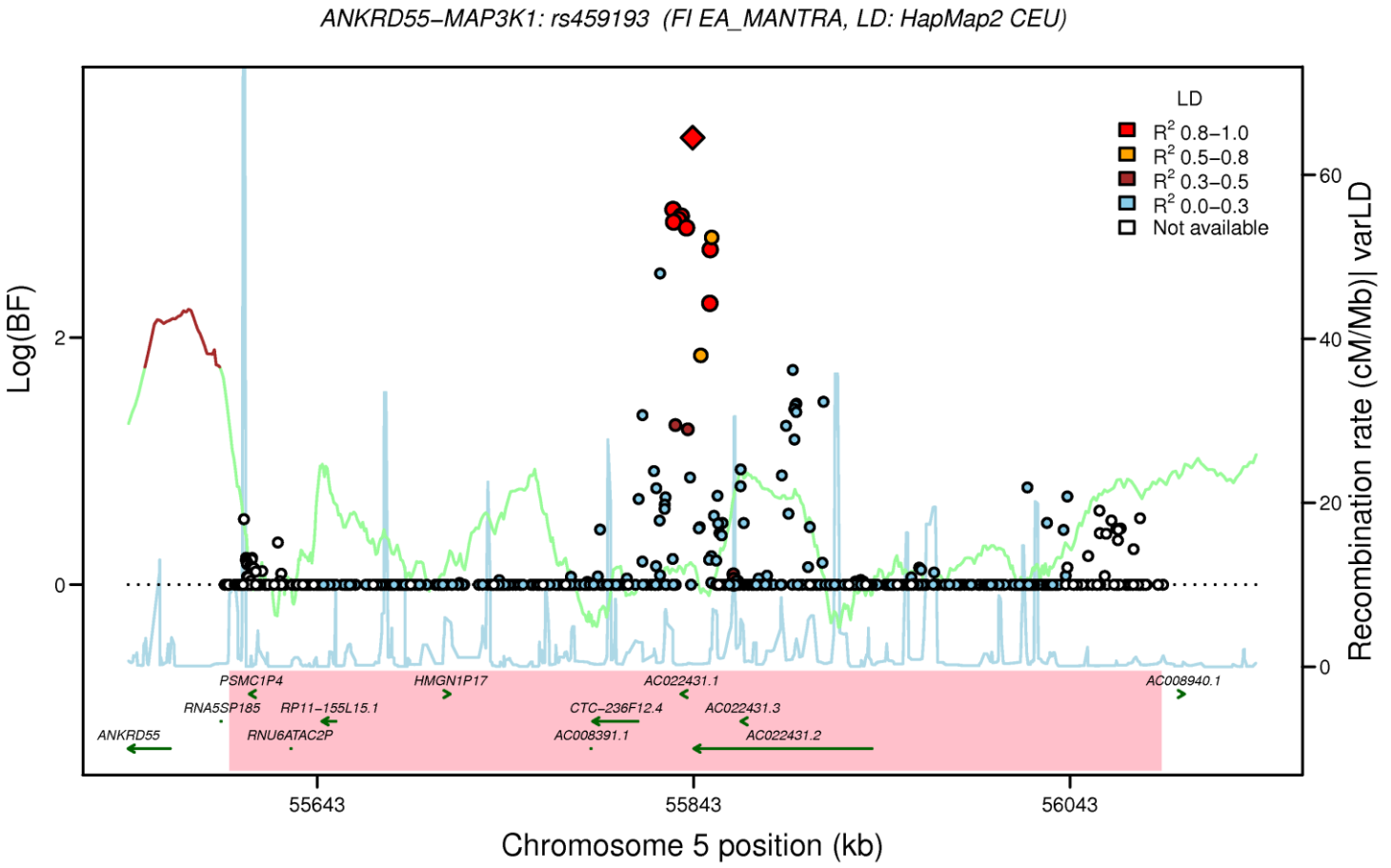
ANKRD55–MAP3K1: rs459193 (FI EA_MANTRA, LD: HapMap2 CEU)
LD
R2 0.8–1.0
R2 0.5–0.8
R2 0.3–0.5
R2 0.0–0.3
Not available
Log(BF)
Recombination rate (cM/Mb)| varLD
PSMC1P4
HMGN1P17
AC022431.1
AC008940.1
RNA5SP185
RP11–155L15.1
CTC–236F12.4
AC022431.3
ANKRD55
RNU6ATAC2P
AC008391.1
AC022431.2
55643
55843
56043
Chromosome 5 position (kb)

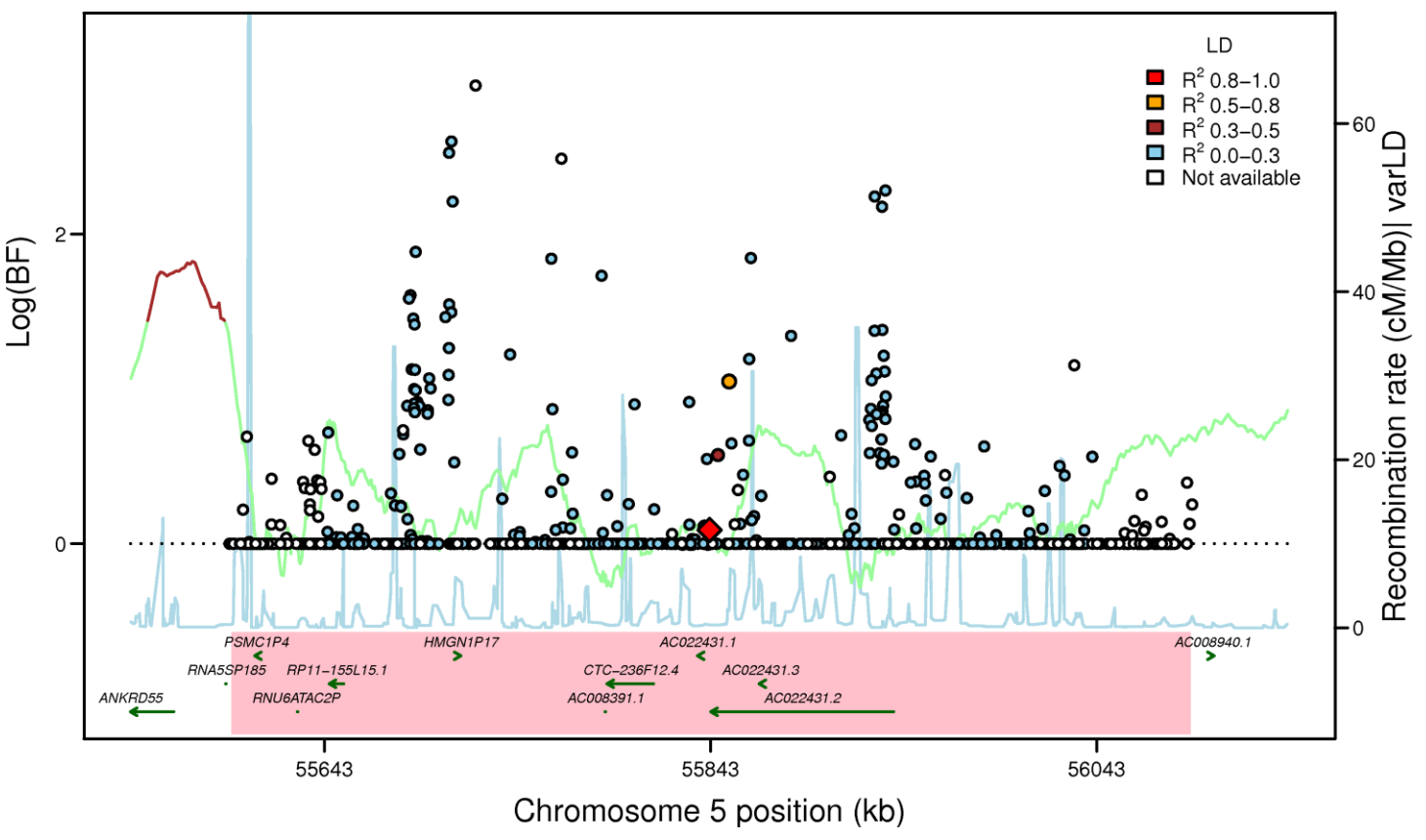
ANKRD55–MAP3K1: rs459193 (FI AA_MANTRA, LD: HapMap2 YRI)
LD
R2 0.8–1.0
R2 0.5–0.8
R2 0.3–0.5
R2 0.0–0.3
Not available
Log(BF)
Recombination rate (cM/Mb)| varLD
PSMC1P4
HMGN1P17
AC022431.1
AC008940.1
RNA5SP185
RP11–155L15.1
CTC–236F12.4
AC022431.3
ANKRD55
RNU6ATAC2P
AC008391.1
AC022431.2
55643
55843
56043
Chromosome 5 position (kb)

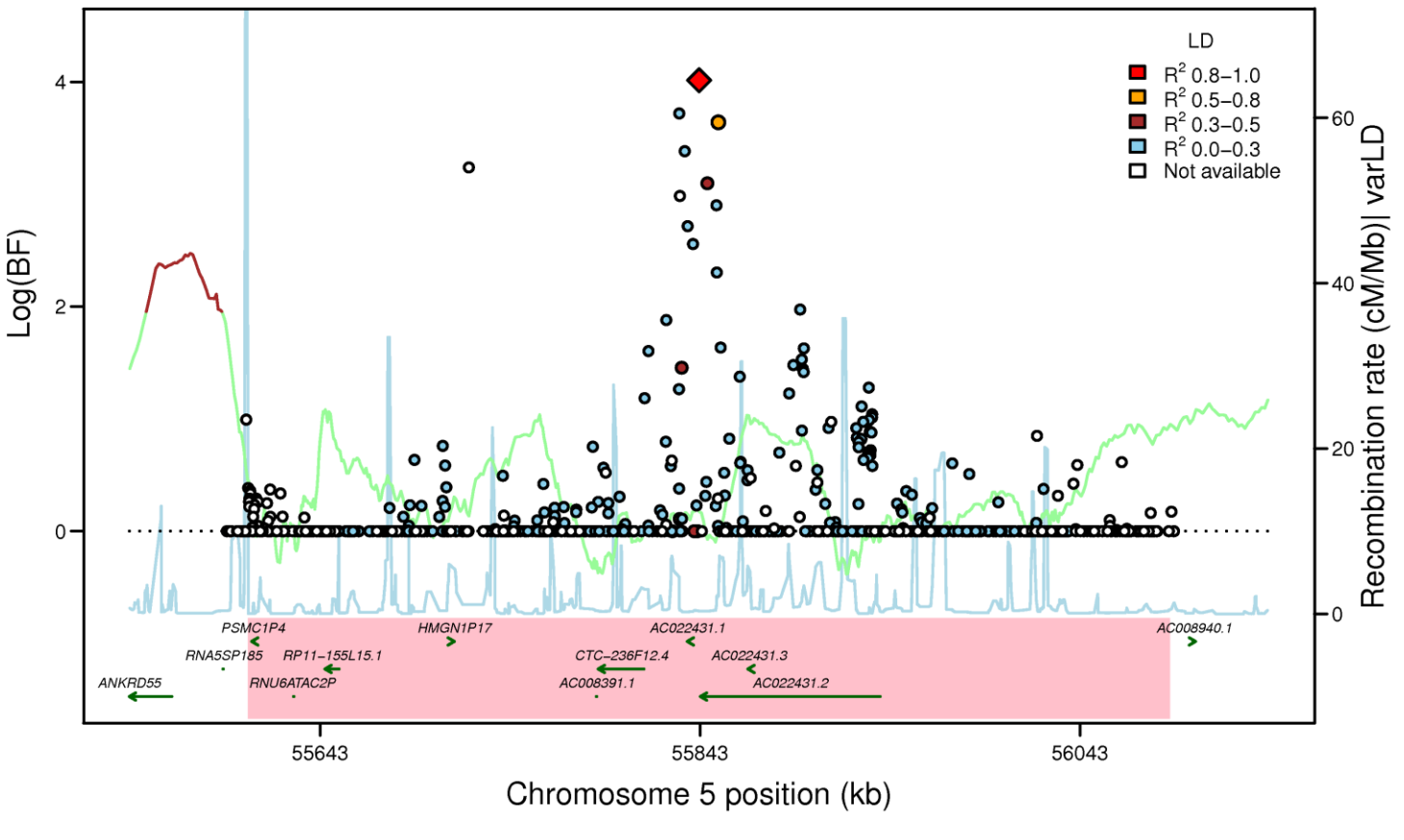
ANKRD55–MAP3K1: rs459193 (FI TE_MANTRA, LD: HapMap2 YRI)
LD
R2 0.8–1.0
R2 0.5–0.8
R2 0.3–0.5
R2 0.0–0.3
Not available
Log(BF)
Recombination rate (cM/Mb)| varLD
PSMC1P4
HMGN1P17
AC022431.1
AC008940.1
RNA5SP185
RP11–155L15.1
CTC–236F12.4
AC022431.3
ANKRD55
RNU6ATAC2P
AC008391.1
AC022431.2
55643
55843
56043
Chromosome 5 position (kb)

Figure S3V

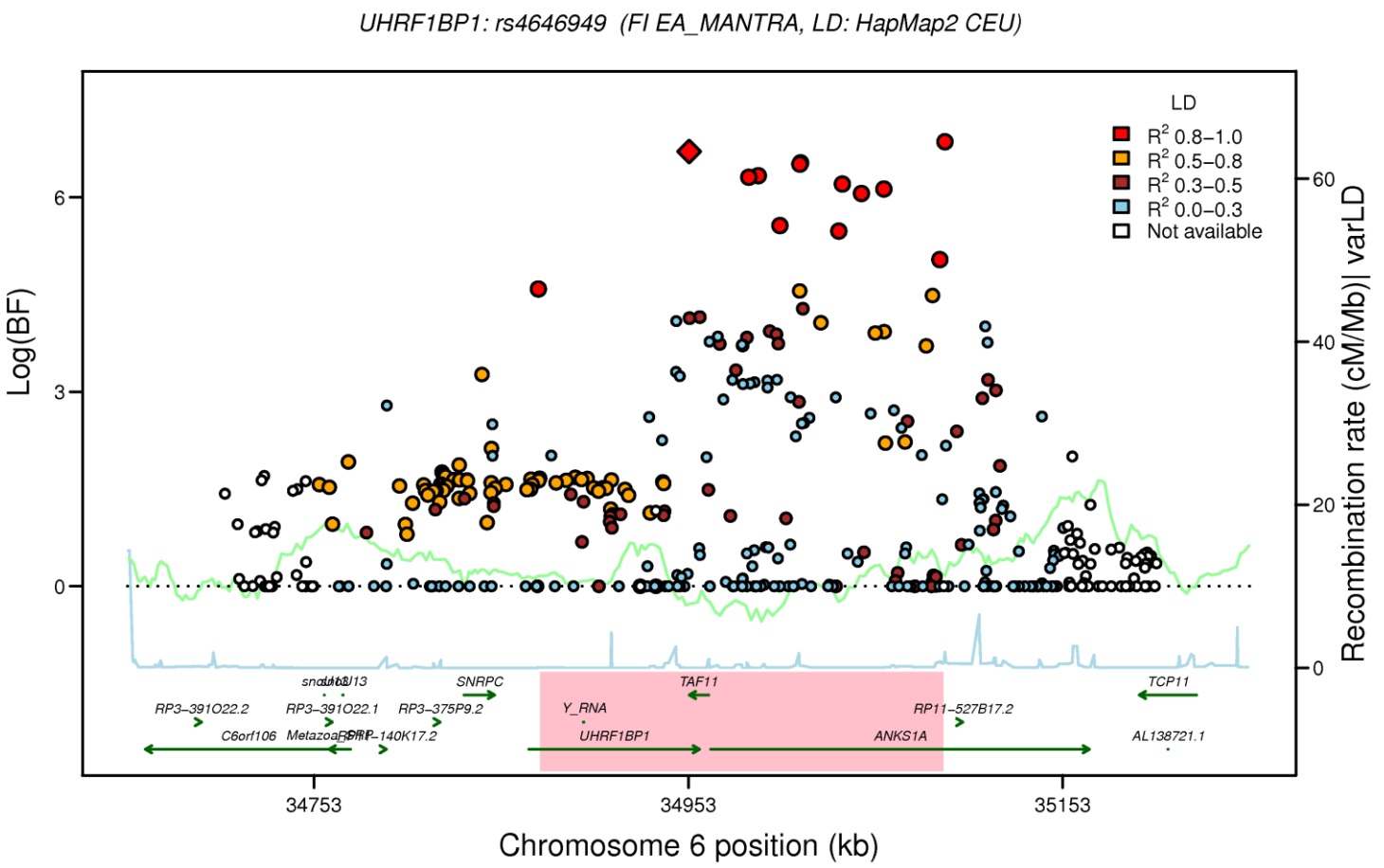
UHRF1BP1: rs4646949 (FI EA_MANTRA, LD: HapMap2 CEU)
LD
R2 0.8–1.0
R2 0.5–0.8
R2 0.3–0.5
R2 0.0–0.3
Not available
Log(BF)
Recombination rate (cM/Mb)| varLD
RP3–391O22.2
RP3–391O22.1
RP3–375P9.2
SNRPC
TAF11
TCP11
Y_RNA
RP11–527B17.2
C6orf106
UHRF1BP1
ANKS1A
AL138721.1
34753
34953
35153
Chromosome 6 position (kb)

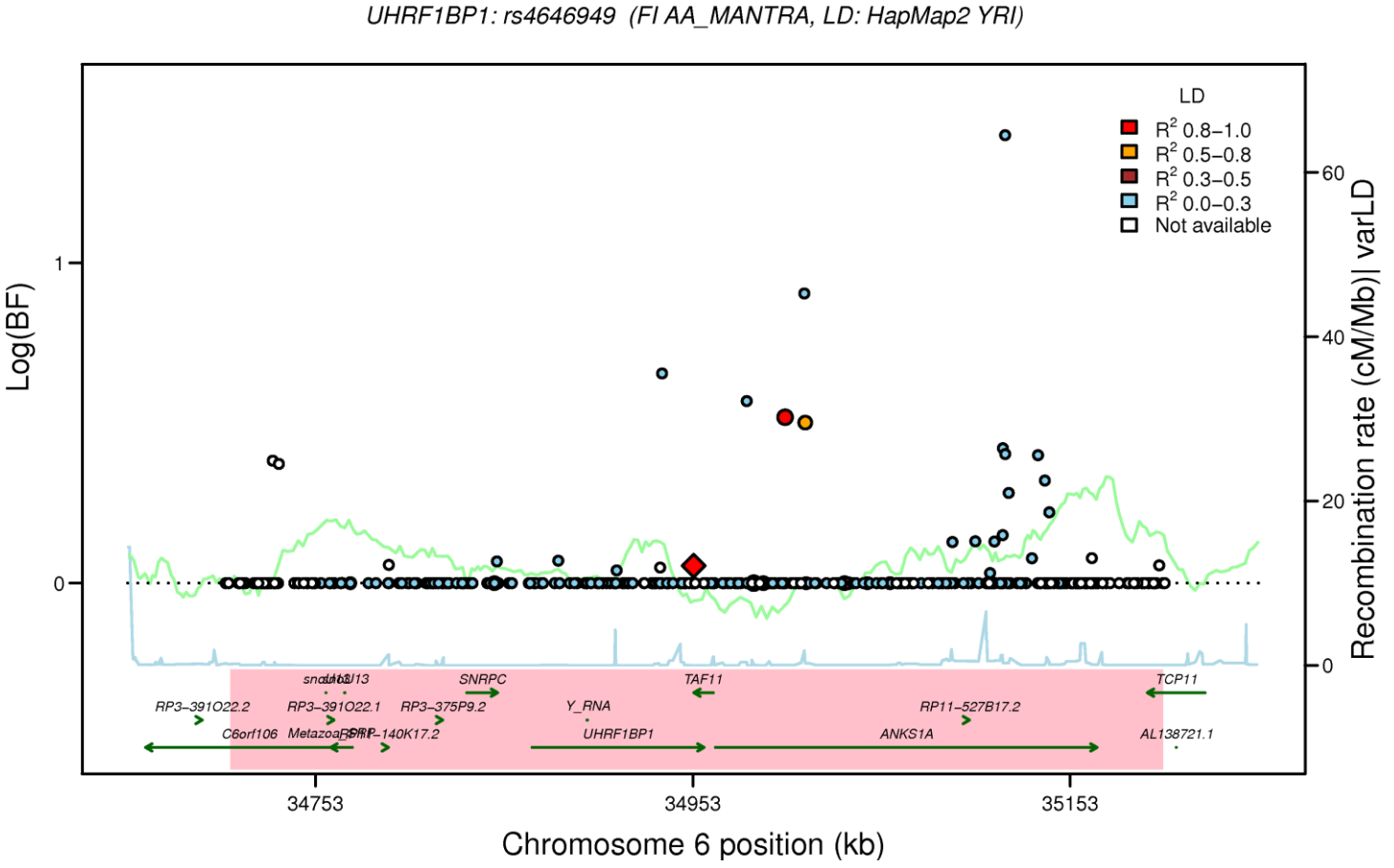
UHRF1BP1: rs4646949 (FI AA_MANTRA, LD: HapMap2 YRI)
LD
R2 0.8–1.0
R2 0.5–0.8
R2 0.3–0.5
R2 0.0–0.3
Not available
Log(BF)
Recombination rate (cM/Mb)| varLD
RP3–391O22.2
RP3–391O22.1
RP3–375P9.2
SNRPC
TAF11
TCP11
Y_RNA
RP11–527B17.2
C6orf106
UHRF1BP1
ANKS1A
AL138721.1
34753
34953
35153
Chromosome 6 position (kb)

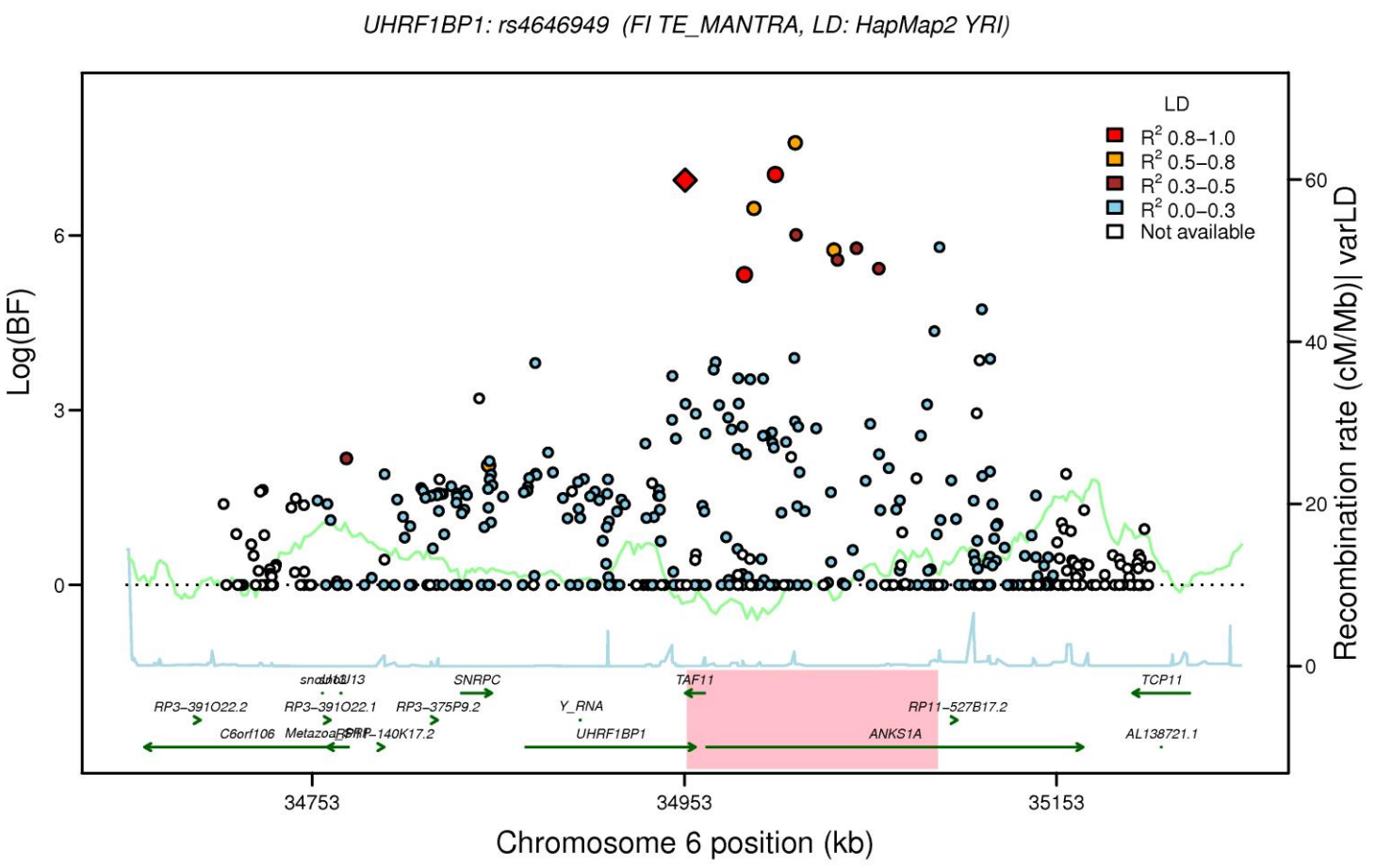
UHRF1BP1: rs4646949 (FI TE_MANTRA, LD: HapMap2 YRI)
LD
R2 0.8–1.0
R2 0.5–0.8
R2 0.3–0.5
R2 0.0–0.3
Not available
Log(BF)
Recombination rate (cM/Mb)| varLD
RP3–391O22.2
RP3–391O22.1
RP3–375P9.2
SNRPC
TAF11
TCP11
Y_RNA
RP11–527B17.2
C6orf106
UHRF1BP1
ANKS1A
AL138721.1
34753
34953
35153
Chromosome 6 position (kb)

Figure S3W

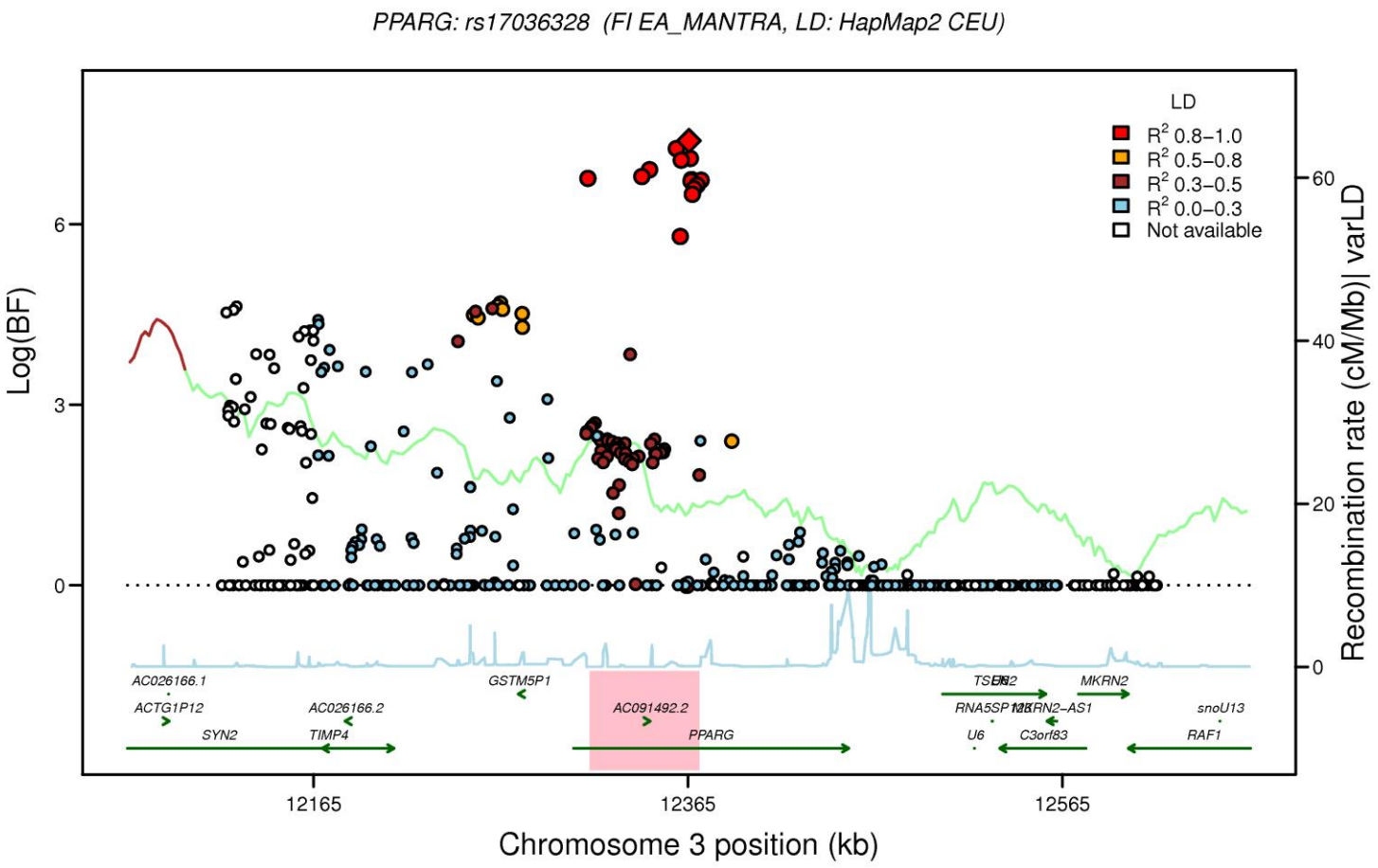
PPARG: rs17036328 (FI EA_MANTRA, LD: HapMap2 CEU)
LD
R² 0.8–1.0
R² 0.5–0.8
R² 0.3–0.5
R² 0.0–0.3
Not available
Log(BF)
Recombination rate (cM/Mb)| varLD
AC026166.1
ACTG1P12
SYN2
AC026166.2
TIMP4
GSTM5P1
AC091492.2
PPARG
MKRN2
snoU13
U6
C3orf83
RAF1
12165
12365
12565
Chromosome 3 position (kb)

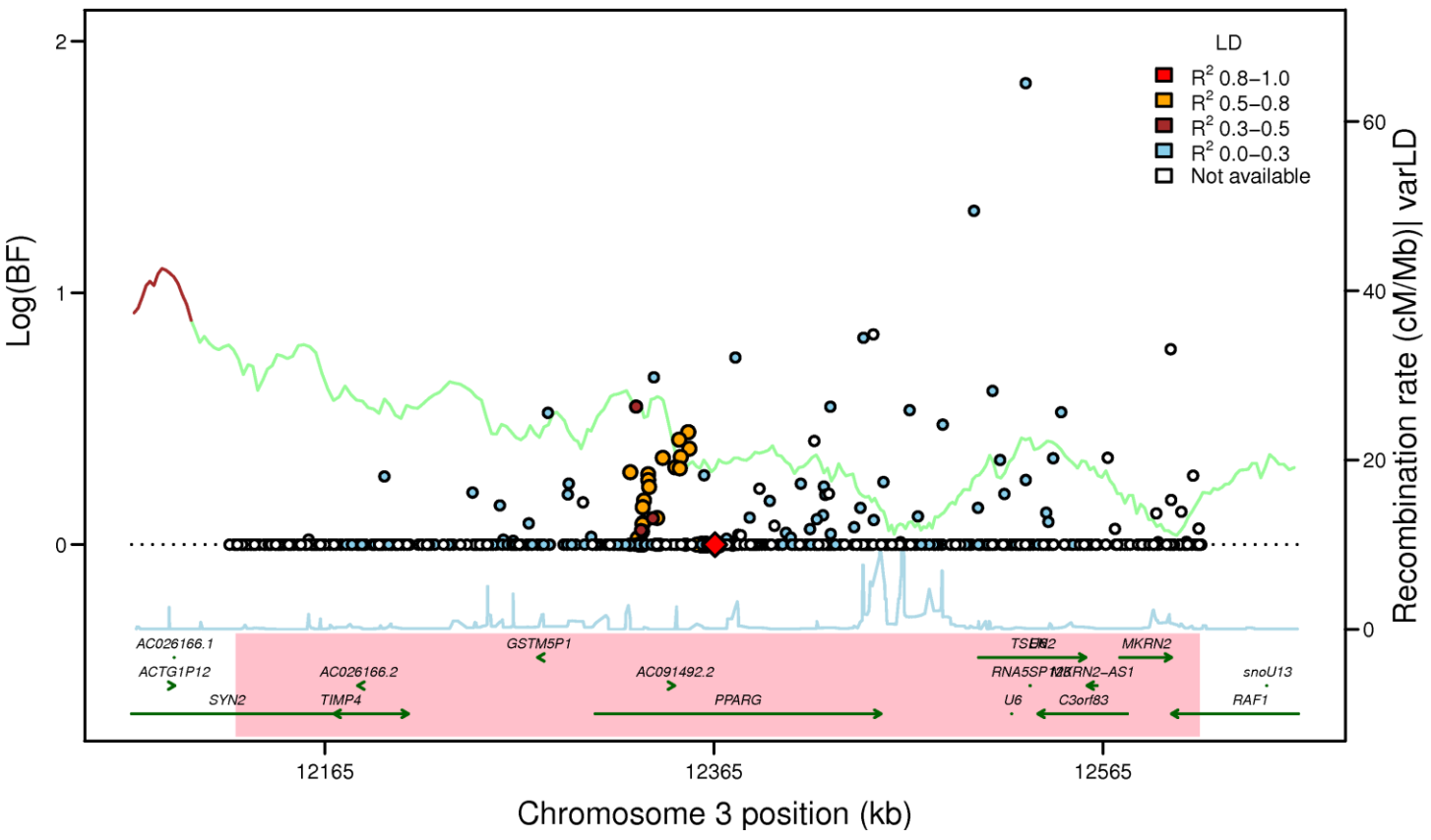
PPARG: rs17036328 (FI AA_MANTRA, LD: HapMap2 YRI)
LD
R² 0.8–1.0
R² 0.5–0.8
R² 0.3–0.5
R² 0.0–0.3
Not available
Log(BF)
Recombination rate (cM/Mb)| varLD
AC026166.1
ACTG1P12
SYN2
AC026166.2
TIMP4
GSTM5P1
AC091492.2
PPARG
MKRN2
snoU13
U6
C3orf83
RAF1
12165
12365
12565
Chromosome 3 position (kb)

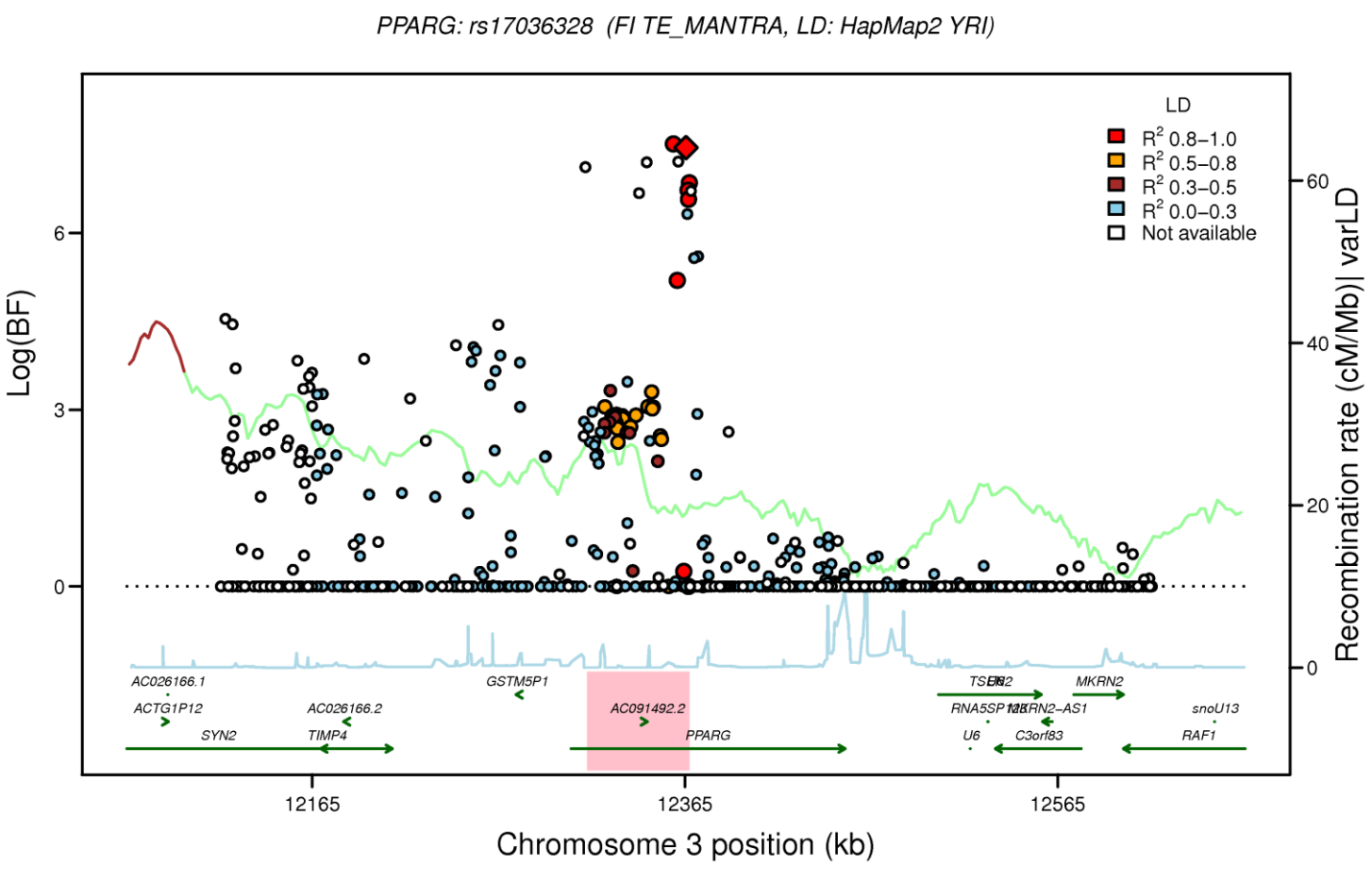
PPARG: rs17036328 (FI TE_MANTRA, LD: HapMap2 YRI)
LD
R² 0.8–1.0
R² 0.5–0.8
R² 0.3–0.5
R² 0.0–0.3
Not available
Log(BF)
Recombination rate (cM/Mb)| varLD
AC026166.1
ACTG1P12
SYN2
AC026166.2
TIMP4
GSTM5P1
AC091492.2
PPARG
MKRN2
snoU13
U6
C3orf83
RAF1
12165
12365
12565
Chromosome 3 position (kb)

Figure S4. Regional association plots merged with data from RegulomeDB and Islet Regulome Browser at 14 FG and 9 FI loci with substantially narrowed credible sets after trans-ethnic analysis.

FG Loci. Islet Regulome legend:

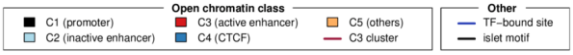

TCF7L2

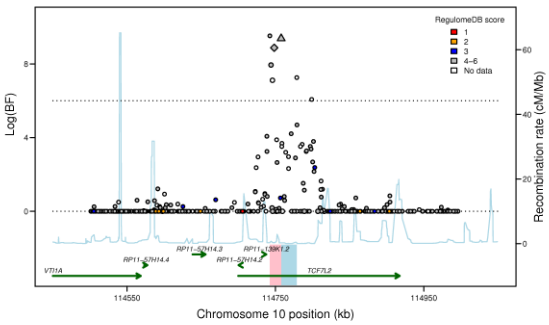

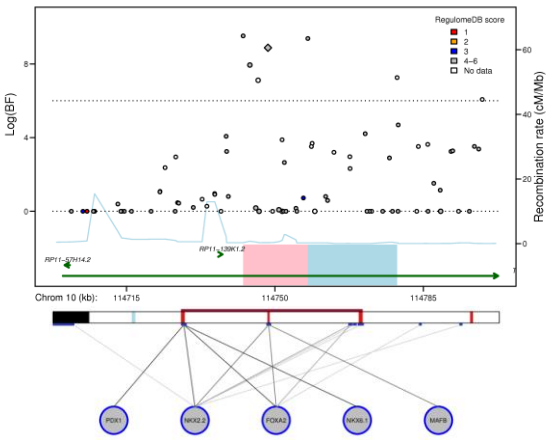

ADRA2

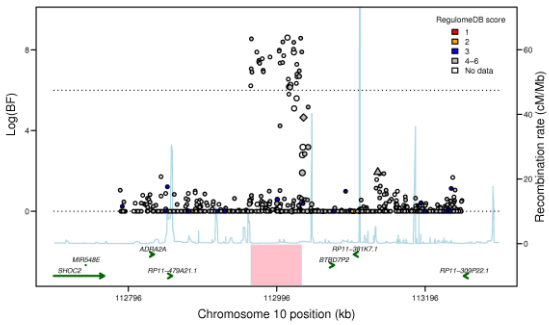

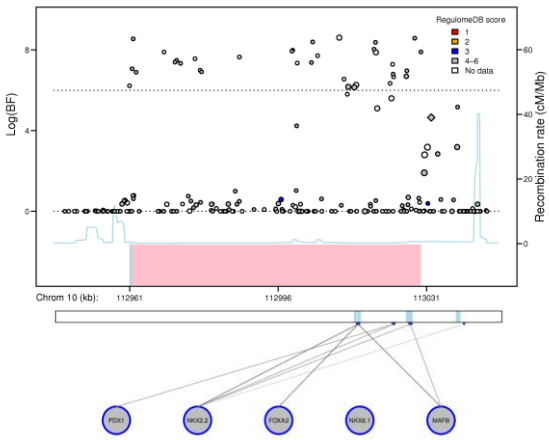

DGKB-TMEM195

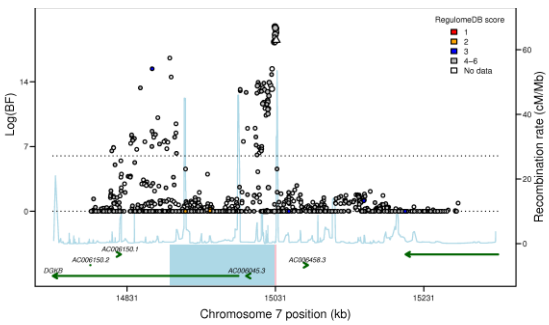

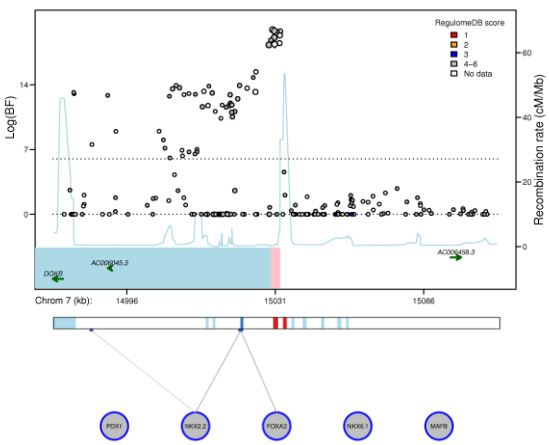

FADS1

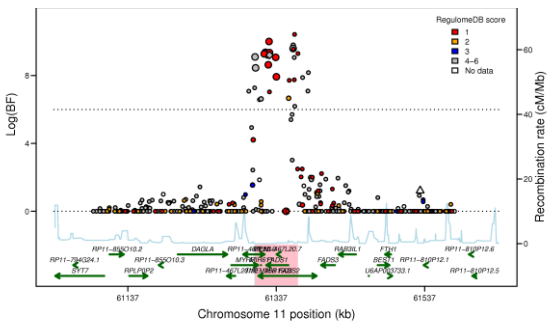

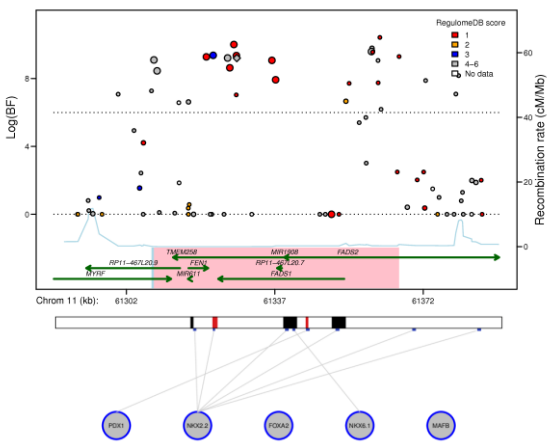

Figure S4, FG Loci continued.

Islet Regulome legend:

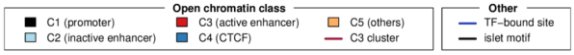

PROX1

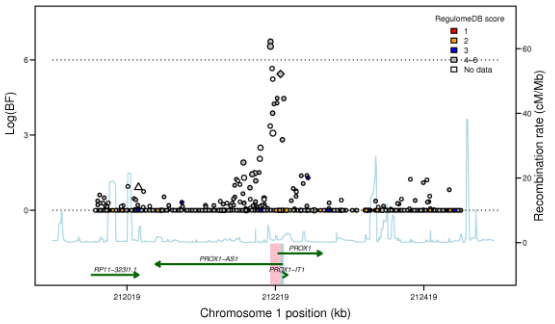

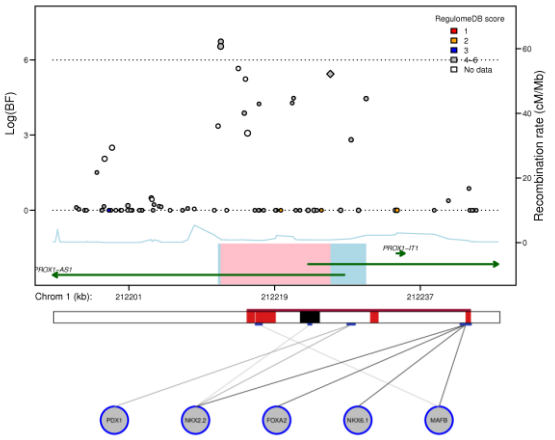

GCK

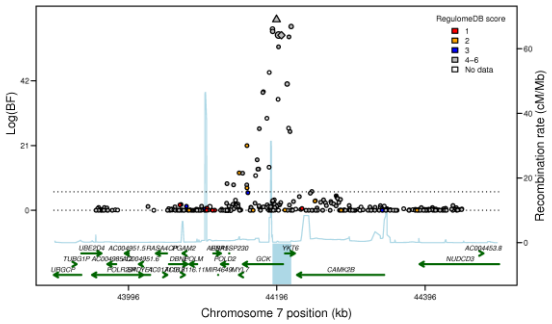

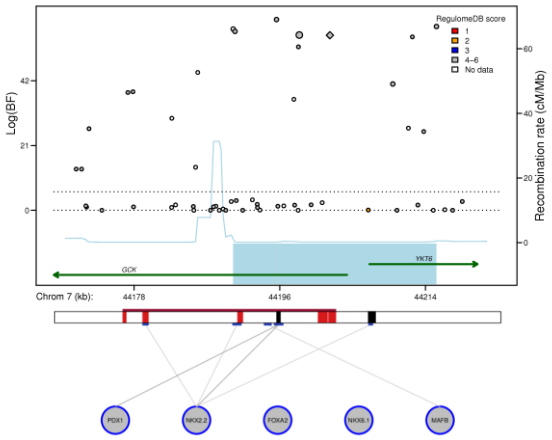

ADCY5

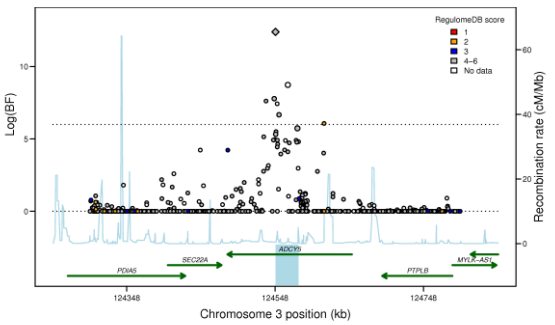

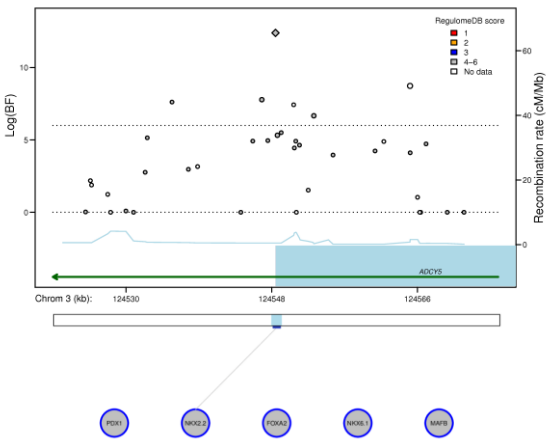

GCKR

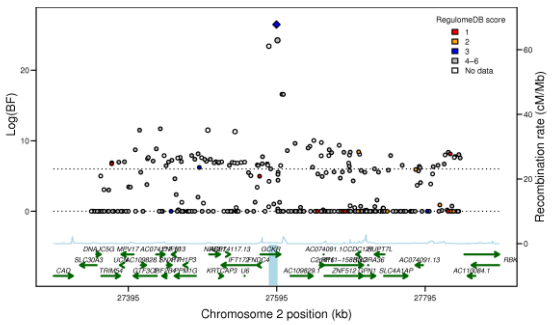

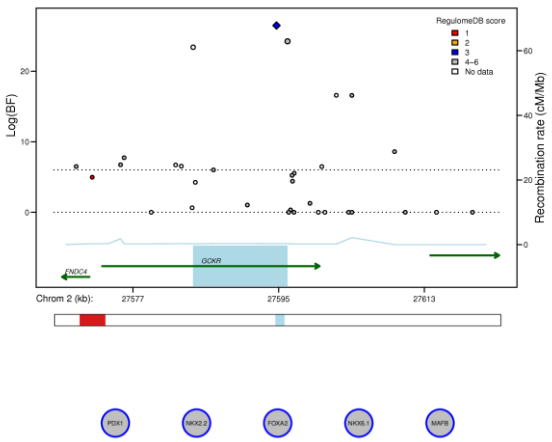

Figure S4, FG Loci continued.

Islet Regulome legend:

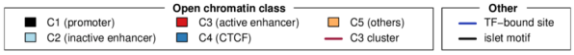

CDKN2B

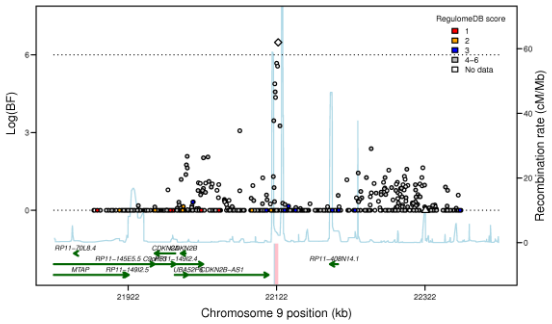

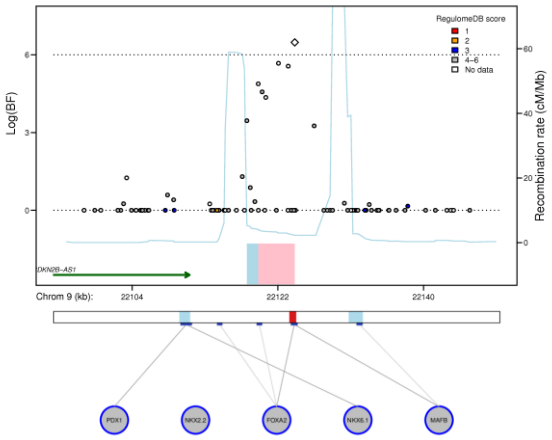

FOXA2

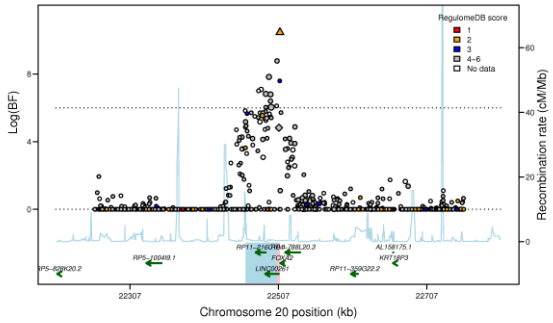

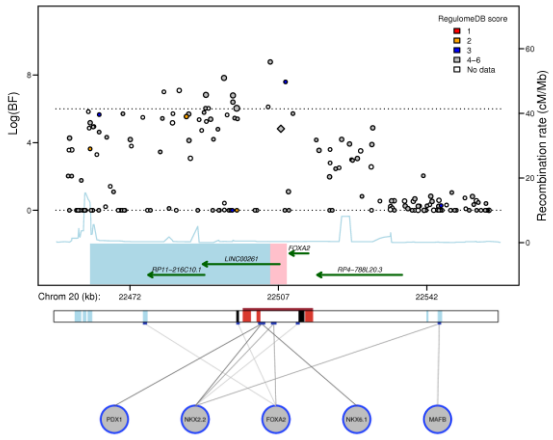

CRY2

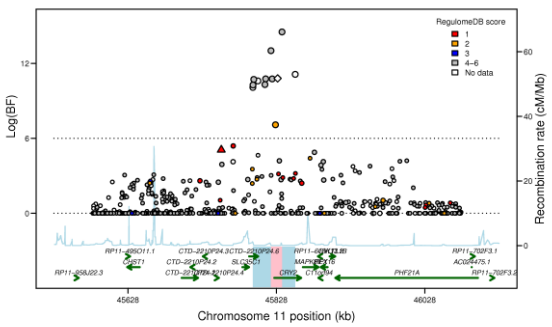

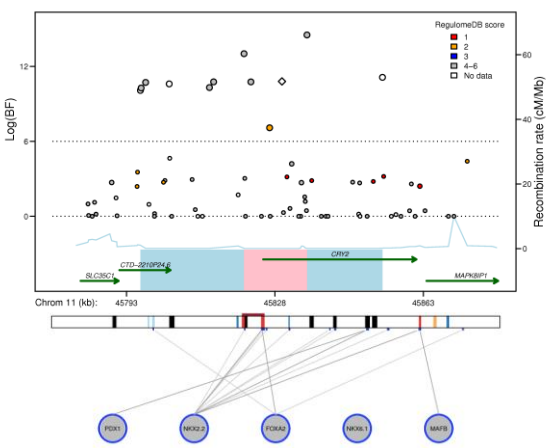

Supplemental Figure 4, FG Loci continued.

Islet Regulome legend:

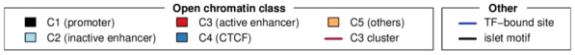

DPYSL5

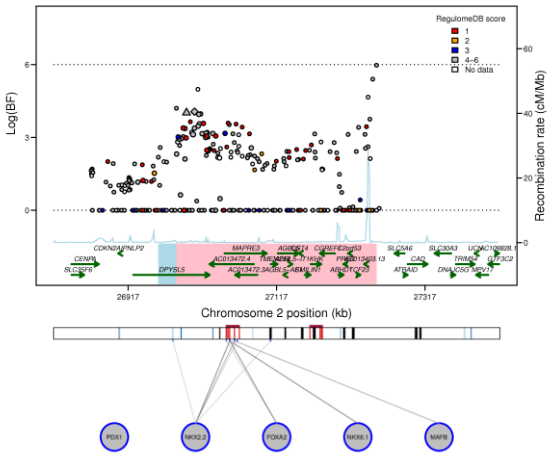

IGF2BP2

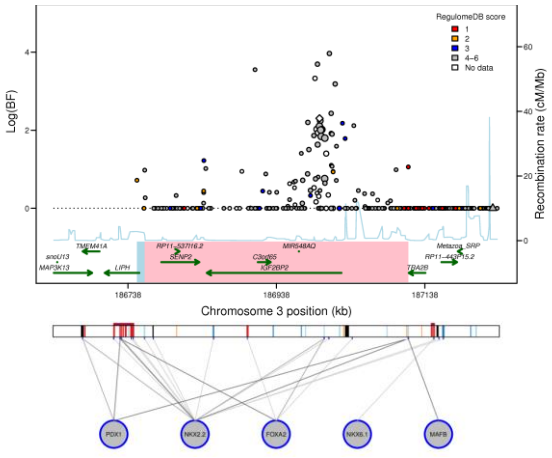

KL

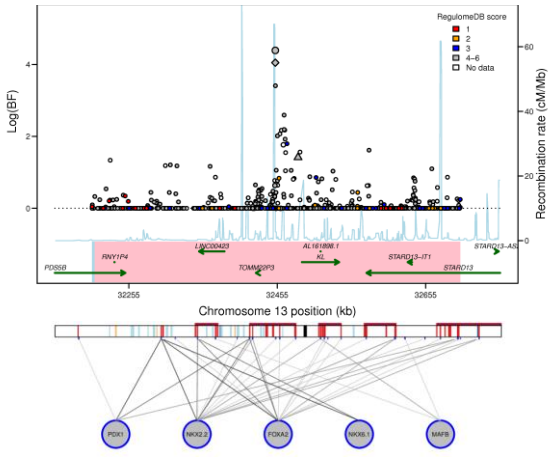

Supplemental Figure 4, FI Loci.

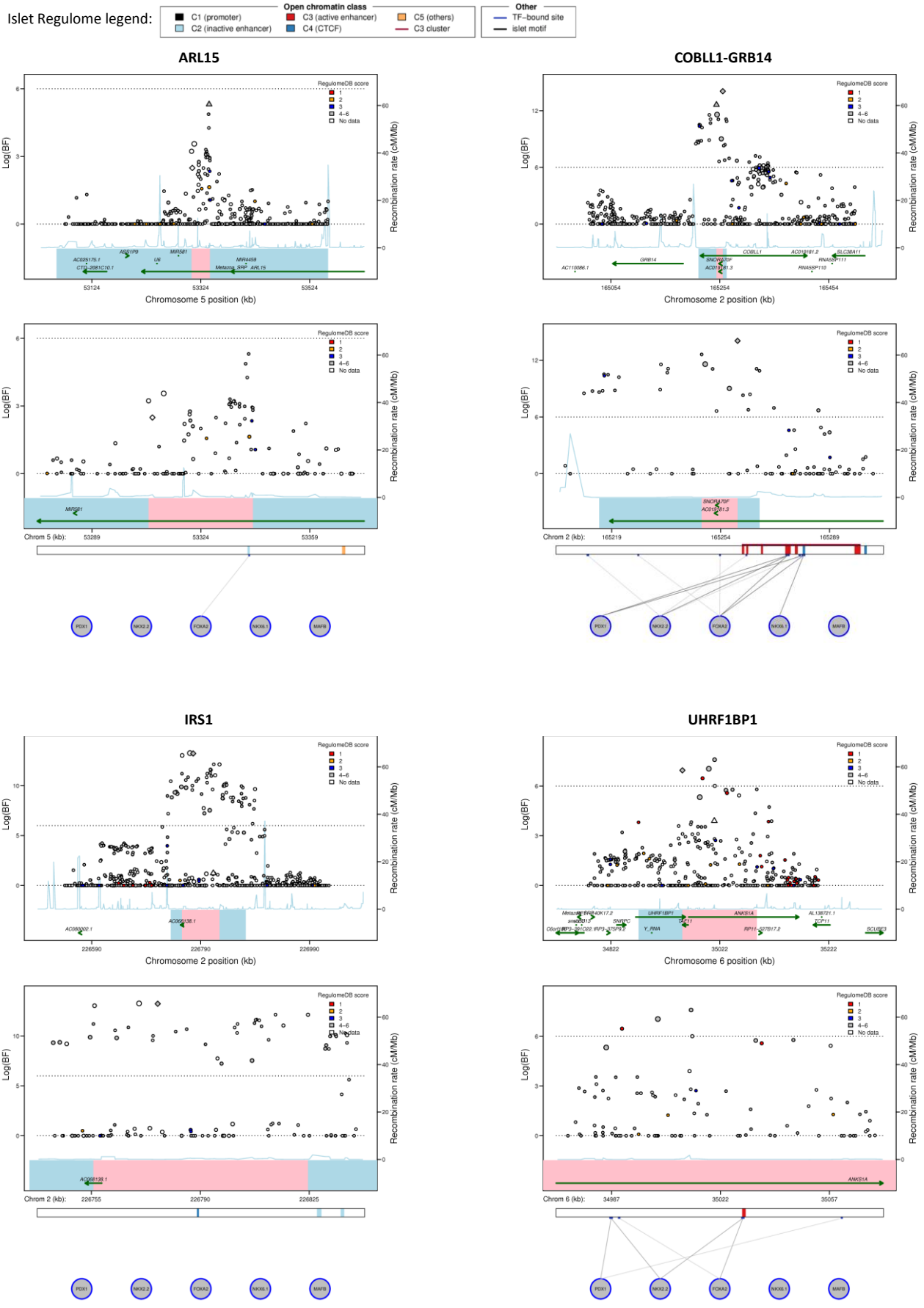

Supplemental Figure 4, FI Loci continued.

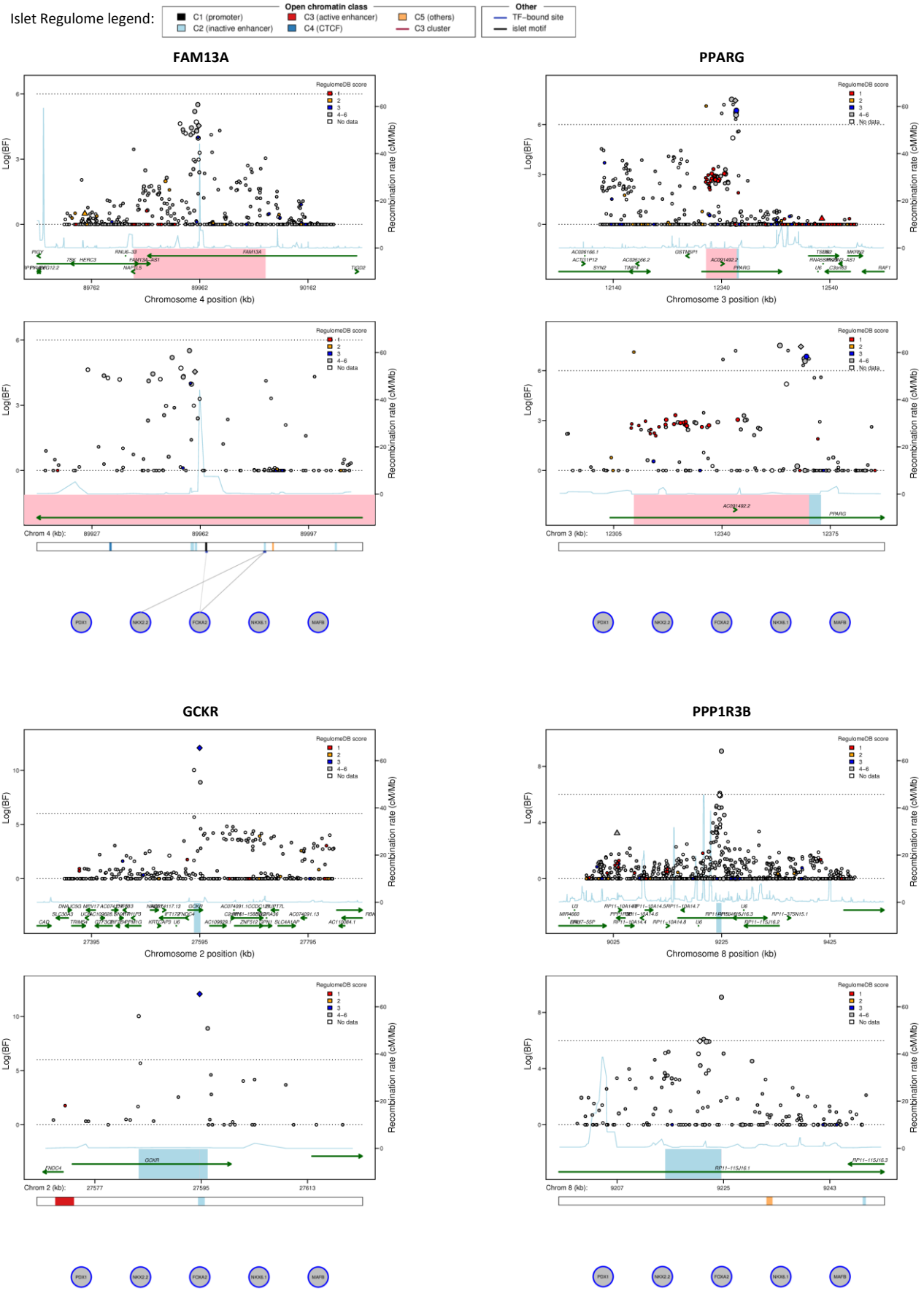

Supplemental Figure 4, FI Loci continued.

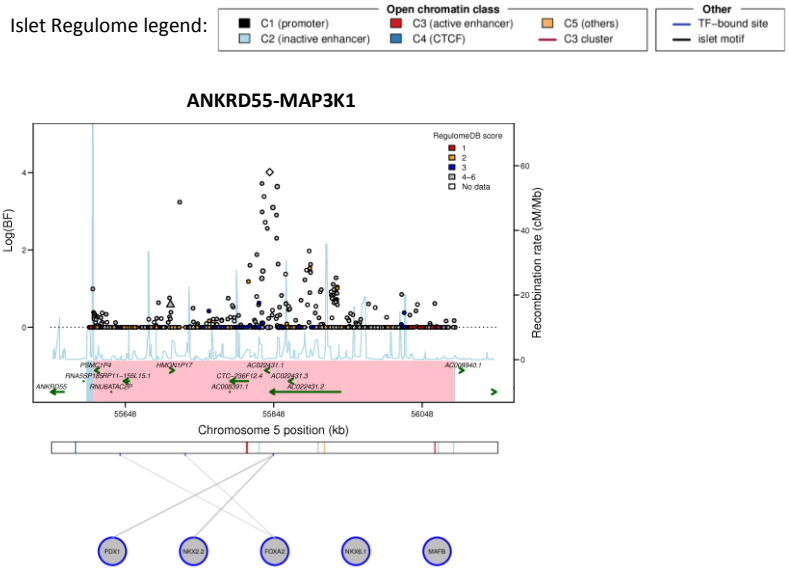

Figure S5

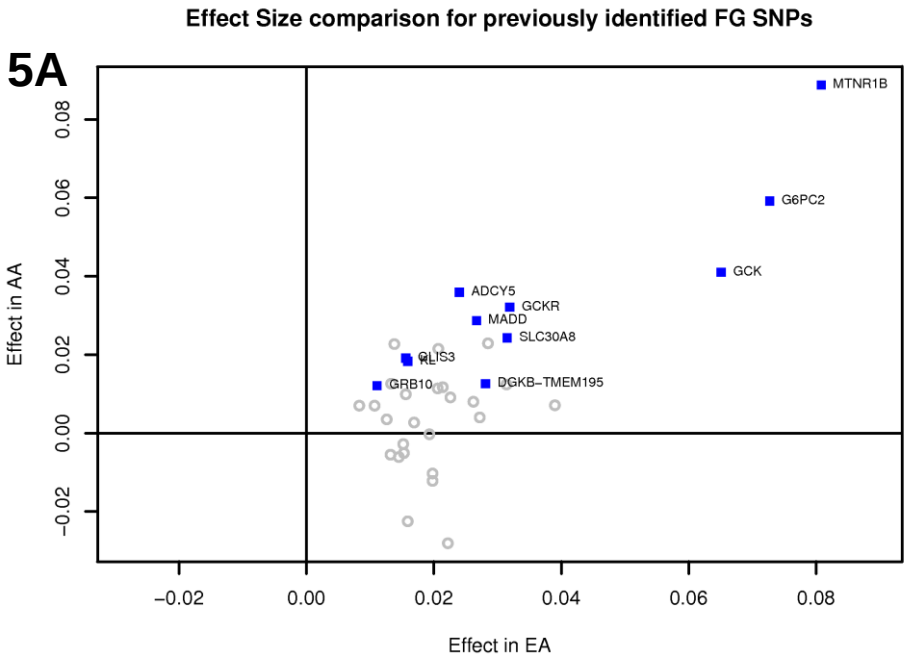

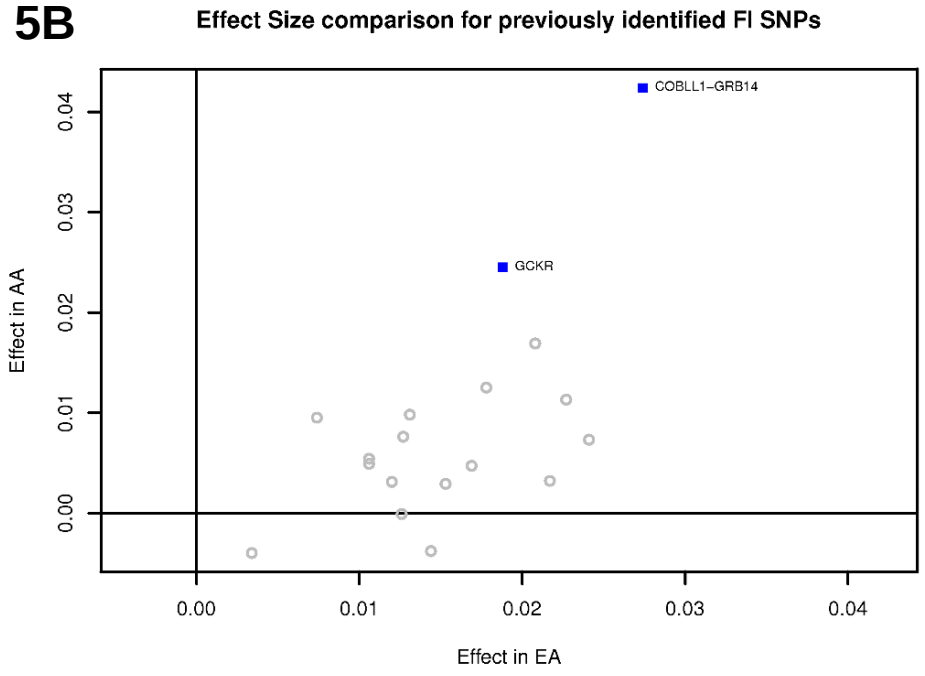

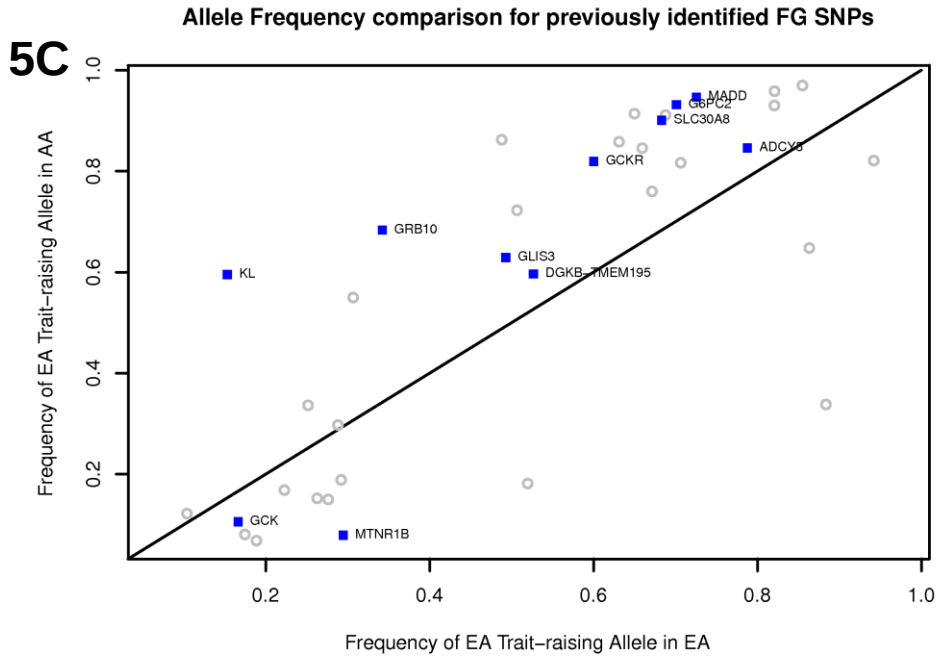

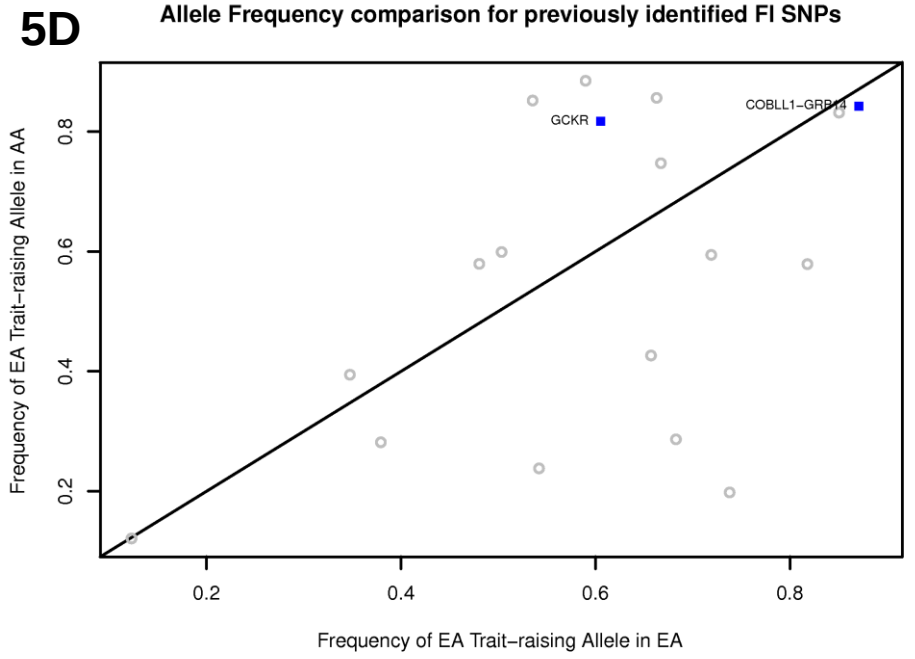

Previously identified EA snp with transferability from EA to AA, i.e P<0.05 in AA and share the same trait-raising allele

Previously identified EA snp without evidence of transferability from EA to AA

Figure S6A

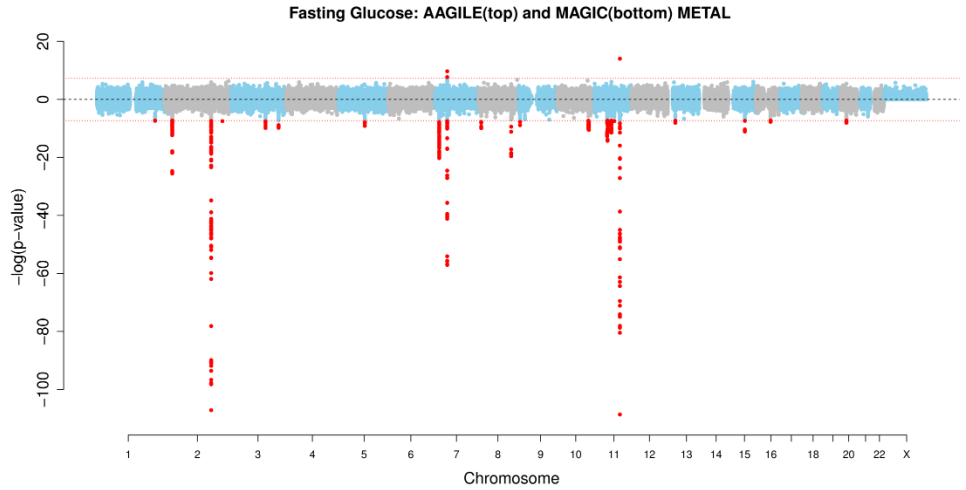

Figure S6B

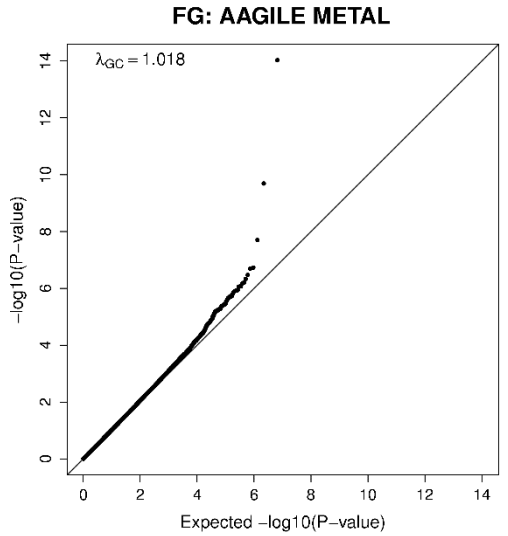

Figure S6C

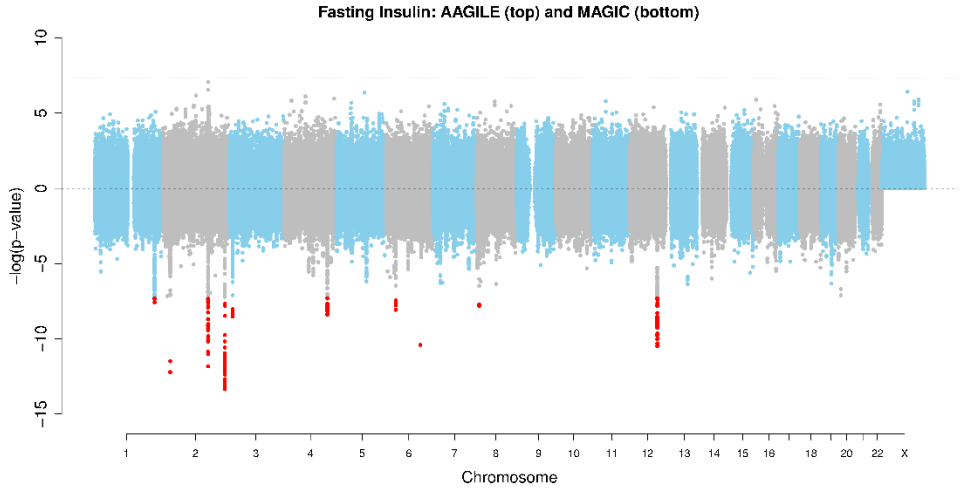

Figure S6D

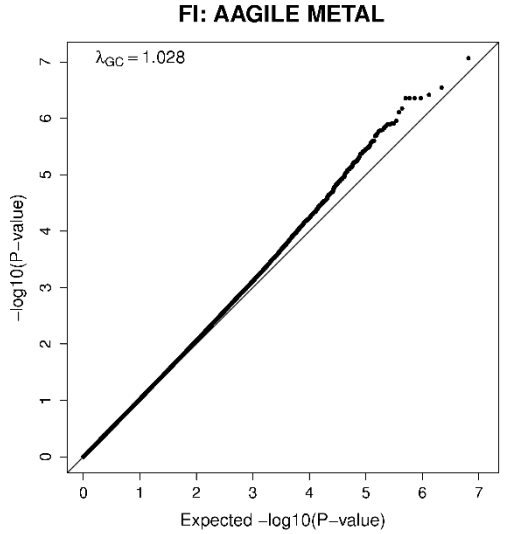

Figure S6E

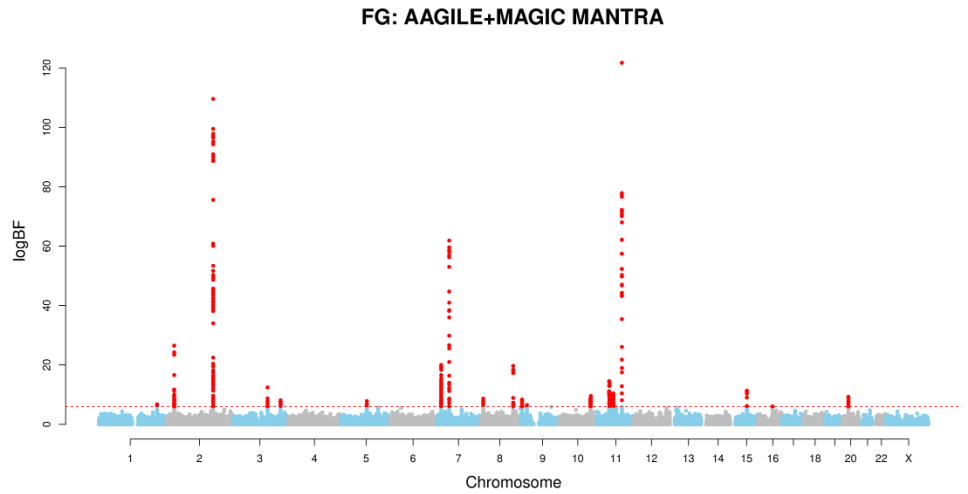

Figure S6F

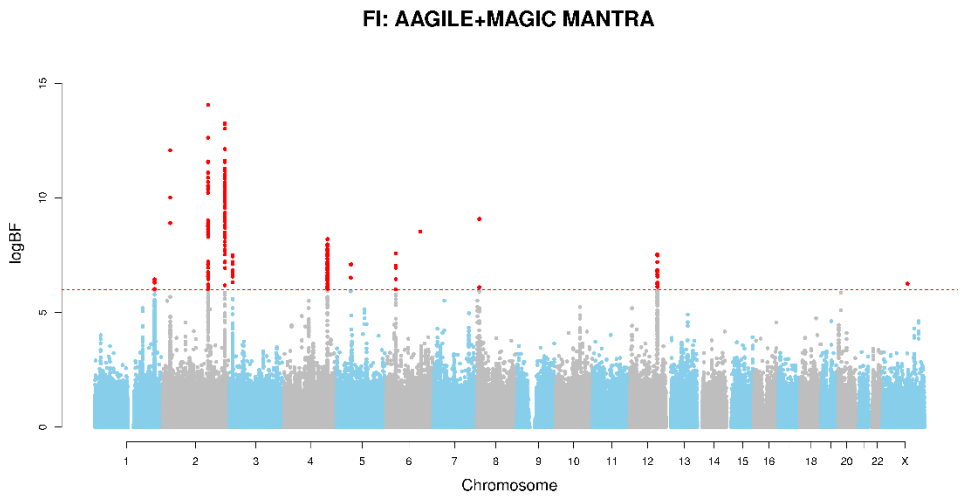

Figure S7

Figure S7A

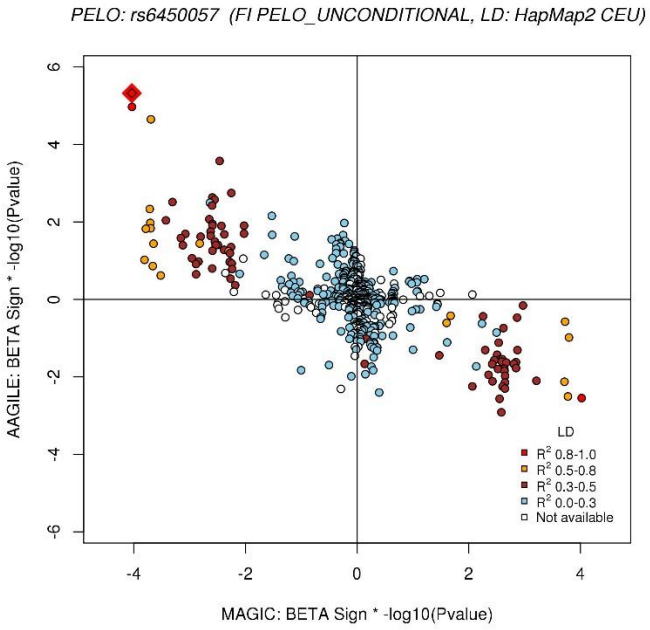

Figure S7B

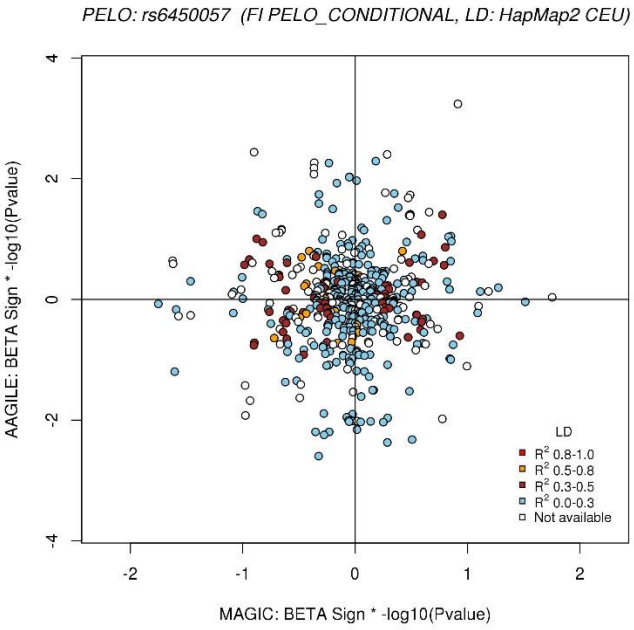

Figure S7C

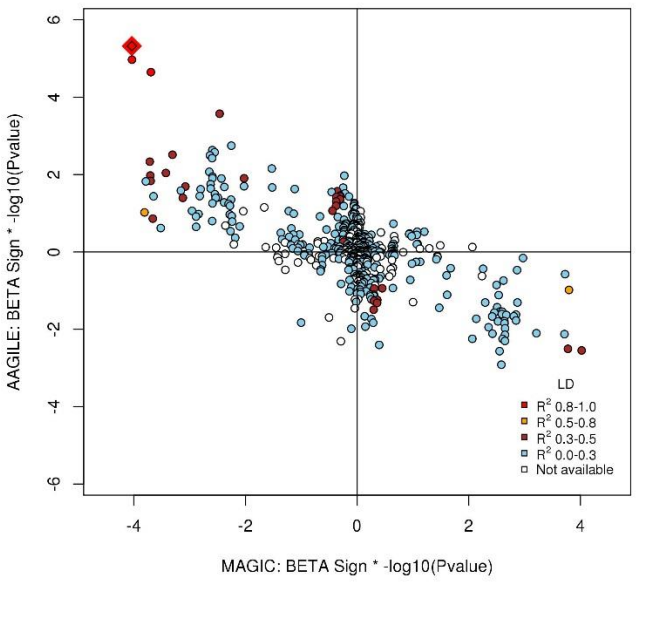

Figure S7D

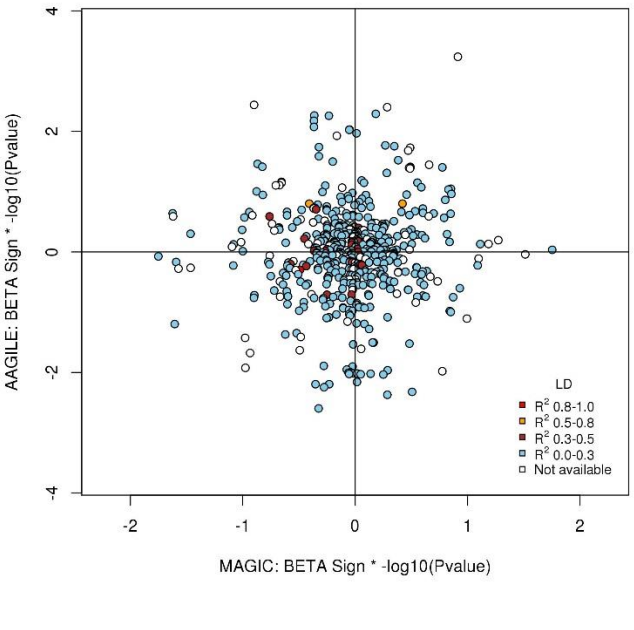

Legend of Supplemental Figures

Figure S1. **Schematic study diagram.**36 fasting glucose (FG) loci, 16 fasting insulin (FI) loci, and 2 loci associated with both FG and FI previously identified in European ancestry (EA) samples were fine-mapped by combining association statistics from EA and African ancestry (AA) samples using Meta-ANalysis of TRans-ethnic Association studies (MANTRA) software. Substantially reduced trans-ethnic credible sets were further examined for evidence of regulatory annotation or enrichment of regulatory marks. Known loci from EA samples were also analysed for transferability to AA samples, for evidence of independent signals in AA populations, and for evidence of selection. Novel FG- and FI-associated loci were identified in fixed effects GWAS meta-analysis in AA samples alone and in trans-ethnic analyses combining EA and AA samples. Two novel loci associated with FI and 24 loci known from EA samples were examined for association with other cardiometabolic traits.

Figure S2. **Venn diagram of trans-ethnic analysis and transferability results.** Venn diagram showing loci exhibiting transferability between EA and AA in brown, loci at which 99% credible set was reduced by at least 20% shown in blue, and overlapping loci in the central area.

Figure S3. **Trans-ethnic fine-mapping of 22 loci (13 FG, 8 FI, and 1 both FG and FI) with greater than 20% reduction in the 99% credible set**. Trans-ethnic analysis of glycemic quantitative loci provides narrowed intervals spanned by the 99% credible set. 500 kb regional association plots centered at the index SNP identified from EA samples at each locus. The X-axis denotes genomic position and the Y-axis denotes the log (Bayes factor), recombination rate and varLD information. The red diamond data point represents the index SNP within the region previously reported from the EA sample. The color of each data point indicates its LD value (r^2) with the index SNP based on HapMap 2 (YRI for AA results and CEU for EA results): white, r^2 not available*;* blue, r^2=0.0-0.2; brown, r^2=0.2-0.5; orange, r^2=0.5-0.8; red, r^2=0.8-1.0. The blue line represents the recombination rate. The green line shows the varLD score at each SNP and is highlighted with dark brown if the varLD score is > 95th percentile of the genome-wide varLD score, comparing LD information between YRI and CEU HapMap2 samples[52]. The interval spanned by the 99% credible set is highlighted in pink. For each locus, three figures were provided. **Panel A. Association results using EA samples. Panel B. Association results using AA samples. Panel C. Association results using both EA and AA samples.**

Figure S4. **Overlay of regional association plots with regulatory annotation at 22 loci (13 FG, 8 FI, and 1 both FG and FI) with greater than 20% reduction in the 99% credible set**. **Top panel:** 500 Kb genomic span showing the top SNP in EA (MAGIC) with a diamond, the top SNP in AA (AAGILE) with a triangle, the EA-only 99% credible set bounded by the blue and pink boxes, and the narrowed trans-ethnic 99% credible set indicated by the pink boxes. SNPs are colored according to score assigned in RegulomeDB with lower score corresponding to stronger level of evidence supporting regulatory function. **Lower panel (where shown):** A zoomed in region of the locus, showing either a 100 Kb or a 50 Kb genomic span. Again, the top SNP in EA (MAGIC) is represented by a diamond, SNPs are colored according to score assigned in RegulomeDB with lower score corresponding to stronger level of evidence supporting regulatory function, and the blue box indicates the span of the EA-only 99% credible set while the pink box indicates the narrowed trans-ethnic 99% credible set. Data from the Islet Regulome Browser for the genomic interval are shown below the regional association plots.

Figure S5. Concordance of effect size and Comparison of EA trait-raising allele Frequency in EA and AA. We show the concordance of effect (**Figures S5A and S5B**) and comparison of

frequency (**Figures S5C and S5D**) for each EA trait-raising allele between EA and AA samples. The blue rectangles represent the SNPs meeting SNP transferability criteria from EA to AA, i.e. association P < 0.05 in AA and sharing the trait-raising allele in EA and AA. Grey circles represent SNPs without evidence of SNP transferability. In **Figures S5A** and S**5B**, X-axis is the effect size in EA and Y-axis is the effect size in AA for the EA trait-raising allele. There is evidence of excess concordance of effect between EA and AA. Specifically, of 36 EA FG index SNPs, 28 SNPs share the same direction in AA (binomial test P of 5.96×10^{-4}), (**Figure S5A**); of 18 EA FI index SNPs, 14 SNPs share the same direction in AA (binomial test P of 1.544E-2), (**Figure S5B**). Also, for both traits, SNPs that meet the transferability criteria tended to have larger effect size of similar magnitudes in both the EA and AA samples than those not meeting criteria. In **Figures S5C** and **S5D,** X-axis is the frequency in EA and Y-axis is the frequency in AA for the EA trait-raising allele. There is wide variation in the frequency of the EA trait-raising allele between EA and AA; the majority of SNPs with locus transferability from EA to AA exhibit higher frequency of the EA trait-raising allele in AA than in EA.

Figure S6. Genome-wide association plots and quantile-quantile (QQ) plots for FG and FI. **Figures S6A** and S**6C** display the Miami plots of association, which mirror the results of AA (on the top) and EA (on the bottom). The X-axis is the chromosome and position and the Y-axis is the –log-scale of association *P*. **Figures S6B** and S**6D** are the QQ plots for FG and FI, respectively. Both associations of FG and FI are minimally inflated with lambda of 1.018 and 1.028, respectively. **Figures S6E** and S**6F** are the genome-wide association plots of trans-ethnic meta-analysis results for FG and FI, respectively. The X-axis is the chromosome and position and the Y-axis is the –log-scale of association *P*.

Figure S7. Conditional analysis at *PELO*/rs6450057. The product of the sign of the beta-coefficient for FI level and –log(*P*-value) for each SNP residing ±250kb of the top SNP, rs6450057, at the locus in EA samples (MAGIC) and in AA samples (AAGILE) plotted on the X- and Y-axis, respectively. **Figures S7A** and **7C** show the comparison for unconditional association results with HapMap 2 CEU and YRI LD information, respectively. **Figures S7B** and **S7D** show the comparison for conditional association results with HapMap 2 CEU and YRI LD information, respectively. There is a clear pattern in the discordant directions of effect between EA and AA. However, after conditional analysis on the top SNP, this discordant pattern disappears, implying that the top SNP rs6450057 drives the original association signal.

Supplemental Tables

Table of Contents (All Tables are available in a separate file.)

References

1. Manning, A.K. *et al.* A genome-wide approach accounting for body mass index identifies genetic variants influencing fasting glycemic traits and insulin resistance. *Nature genetics* **44**, 659-69 (2012).
2. Wang, Y.J. *et al.* The association of the vanin-1 N131S variant with blood pressure is mediated by endoplasmic reticulum-associated degradation and loss of function. *Plos Genetics* **10**, e1004641 (2014).
3. McCarty, C.A. *et al.* The eMERGE Network: a consortium of biorepositories linked to electronic medical records data for conducting genomic studies. *BMC medical genomics* **4**, 13 (2011).
4. Lettre, G. *et al.* Genome-wide association study of coronary heart disease and its risk factors in 8,090 African Americans: the NHLBI CARe Project. *Plos Genetics* **7**, e1001300 (2011).
5. Ng, M.C. *et al.* Meta-analysis of genome-wide association studies in African Americans provides insights into the genetic architecture of type 2 diabetes. *Plos Genetics* **10**, e1004517 (2014).
6. Monda, K.L. *et al.* A meta-analysis identifies new loci associated with body mass index in individuals of African ancestry. *Nature genetics* **45**, 690-6 (2013).
7. Liu, C.T. *et al.* Genome-wide association of body fat distribution in African ancestry populations suggests new loci. *Plos Genetics* **9**, e1003681 (2013).
8. Ward, L.D. & Kellis, M. HaploReg: a resource for exploring chromatin states, conservation, and regulatory motif alterations within sets of genetically linked variants. *Nucleic acids research* **40**, D930-4 (2012).